BATCH ADSORPTION STUDY FOR THE REMOVAL OF TEXTILE DYES FROM AQUEOUS SOLUTIONS USING *Pandanus Amaryllifolius* (RAMPE) LEAVES.

Sasiri Lakshitha Gamage Haththotuwa

(169158R)

Degree of Master of Science

Department of Civil Engineering

University of Moratuwa

Sri Lanka

April 2022

BATCH ADSORPTION STUDY FOR THE REMOVAL OF TEXTILE DYES FROM AQUEOUS SOLUTIONS USING *Pandanus Amaryllifolius* (RAMPE) LEAVES.

Sasiri Lakshitha Gamage Haththotuwa

(169158R)

Thesis Submitted in Partial Fulfilment of The Requirements for The Degree Master of Science in Environmental Engineering and Management

Department of Civil Engineering

University of Moratuwa

Sri Lanka

April 2022

DECLARATION

"I declare that this is my own work, and this thesis does not incorporate without acknowledgement any material previously submitted for a Degree or Diploma in any other University or institute of higher learning and to the best of my knowledge and belief, it does not contain any material previously published or written by another person except where the acknowledgement is made in the text.

Also, I hereby grant to University of Moratuwa the non-exclusive right to reproduce and distribute my thesis, in whole or in part in print, electronic or other medium. I retain the right to use this content in whole or part in future works (such as articles or books)."

Signature: Date:

The above candidate has carried out research for the Masters under my supervision.

Name of the supervisor : Prof. B. M. W. P. K. Amarasinghe

Signature of the supervisor : Date:

DEDICATION

This thesis is dedicated to my loving parents, who were the strength to carry on this research experiment from beginning to end by supporting me in every way possible.

ACKNOWLEDGEMENTS

I like to extend my heartfelt gratitude to my supervisor Prof. B. M. W. P. K. Amarasinghe, Senior professor Department of Chemical and Process Engineering, for allowing me to complete the research. Madam, your guide, and encouragement helped me to achieve this success. Your support was immense, and it was fortunate to designate you as my supervisor.

I express my heartiest gratitude to my course coordinator Prof. Jagath Manatunge for encouraging me to complete the research component by obtaining time extensions due to Covid 19 pandemic situation. Sir' Your support is immense and if not, I'll not able to complete this research. I would thank Prof. M. Jayaweera and Prof. B. Gunawardana for directing me to choose the proper research area with practical feasibility.

I would thank Prof. S. Walpalage, Head of the Department of Chemical and Process Engineering for the permission to access laboratories during the Covid pandemic movement restriction situation.

I wish to express my sincere thanks to Mr H. P. Mahendra Technical officer and Mr V. Somarathna Lab attendant of Transport Phenomena Laboratory, Ms D. Rodrigo Technical officer of Environmental Engineering Laboratory, Mr J. D. Wijegunarathna Technical officer of the Instrument Centre and Ms W. S. M. Silva Technical officer of Latex Technology Laboratory of Department of Chemical and Process Engineering, Mr M. Jayaweera Technical officer Analytical laboratory, Mr P. Gunawardana Technical officer Polymer laboratory of Department of Material Science and Engineering University of Moratuwa for their invaluable support to experiments.

I appreciate Mr K. Keerthirathna, Assistant General Manager Manufacturing, and Mr Palitha Indrajith, Factory Manager of Royal Ceramics Lanka PLC for supporting my

research experiment by arranging my work accordingly. I would be grateful to my parents and wife for giving their unconditional love and support to fulfil my aims.

Abstract

With the development of the manufacturing industry in recent days, there are obvious advantages and some disadvantages to human beings. One of the leading disadvantages is environmental pollution. Water pollution continues due to the continual uncontrolled largescale release of dyes to water bodies mainly from the textile industry effluents. These dyes can threaten directly and indirectly human, plant and animal life.

This research is focused on removal of selected textile dyes methylene blue, crystal violet, congo red, reactive red and reactive black B via adsorption. The adsorbent was dried leaf powder of flavouring plant *Pandanus amaryllifolius*, widely famous as *'rampe'*. Rampe leaves powder was chosen as the adsorbent due to its wide availability, simplicity in preparation and mainly due to its ability to remove poisonous substances.

Batch adsorption experiments were carried out at room temperature to investigate the adsorption capacity, kinetics of adsorption and equilibrium data. The analytical instrument UV-Visible Spectrophotometer was used to determine the dye concentrations.

Batch test results showed that the adsorbent removes Methylene blue, Crystal violet, Congo red up to 95%, 90%, and 81%. However, reactive red and reactive black B dyes did not show significant removal. Kinetic studies showed that the adsorption followed the pseudo-second order kinetic model. According to the intraparticle diffusion model, adsorption happened with two steps for all three dyes. The equilibrium data comply with Langmuir isotherm with maximum adsorption capacities of 38.46, and 20.33 mg g^{-1} for methylene blue and crystal violet respectively. Congo red complied with Temkin isotherm. FTIR and SEM analysis of the adsorbent before and after adsorption revealed MB, CV, and CR were adsorbed to PALP with chemisorption by creating hydrogen bonds and significant amount of the mass transfer were happened through papillose cells on the leave surface.

Keywords: Batch adsorption; *Pandanus amaryllifolius* leaves; Textile dye

TABLE OF CONTENT

LIST OF FIGURES

LIST OF TABLES

LIST OF ABBREVIATIONS

Abbreviation	Description
AC	Activated Carbon
AFO	Avrami factionary Order
ATR	Attenuated Total Reflection
BET	Brunauer Emmett Teller
BOD	Biochemical Oxygen Demand
CL_{50}	Limited Concentration
COD	Chemical Oxygen Demand
CR	Congo Red
CV	Crystal Violet
EDTR	Endothermic Reaction
ELM	Elovich Model
EXTR	Exothermic Reaction
FIM	Freundlich Isotherm Model
FSIM	Fritz Schlunder Isotherm Model
FTIR	Fourier Transform Infrared
HIM	Hill Isotherm Model
IMR	Impregnation Ratio
IR	Infra-Red
KCIM	Koble-Corrigan Isotherm Model
LC_{50}	Lethal Concentration for kill 50% of population
LIM	Langmuir Isotherm Model
MB	Methylene Blue
MBR	Membrane Bio Reactor
MWCNT	Multi Walled Carbon Nanotubes
NSP	Non-Spontaneous Process
PALP	Pandanus Amaryllifolius Leaves Powder
PFO	Pseudo First Order

PSO	Pseudo Second Order
PTFE	Poly Tetrafluoroethylene
RBB	Reactive Black B
RPIM	Redlich Peterson Isotherm Model
RPM	Rounds Per Minute
RR	Reactive Red
SEM	Scanning Electron Microscope
SIM	Sips Isotherm Model
SP	Spontaneous Process
TIM	Temkin Isotherm Model
TOC	Total Organic Carbon
TSS	Total Suspended Solids
UV	Ultraviolet

LIST OF APPENDICES

1. INTRODUCTION

Due to the development of the textile industry, the process of dyeing also developed and currently many dyeing agents are produced with different colours. There are about twelve classes of dyes in the group (Gita, et al., 2017).

There are more than 100,000 types of dyes available in market with bulk production of 700,000 MT annually for industrial use (Berradi, et al., 2019). Most occasions those dyes discharge into water bodes due to not having proper treatment for the effluent water. The problem arises when recovering polluted water bodies due to higher operational costs. Therefore, the best thing is the prevention of natural water body contamination from dye effluents (Bouras, et al., 2017).

Contamination of textile dye into water bodies can seriously damage the aquatic system. That can result in the reduction of the aesthetic quality of natural water resources, increase of chemical oxygen demand, increase of biochemical oxygen demand, create toxic for aquatic life, create carcinogenicity, multiagency, bioaccumulation and disturbed photosynthesis (Gita, et al., 2017).

Several techniques are available to remove dyes from contaminated wastewater; namely chemical, physical, and biological treatments. Ozon oxidation, oxidation, enton oxidation, photochemical and Ultraviolet (UV) irradiation are some chemical treatment methods available for dye removal. Chemical treatments, catalytic oxidation, and electrochemical treatments are not famous in the industry due to their high operating cost and complex operation. Due to the complex structure of many dyes, it is hard to remove them completely using conventional biodegradation methods. Aerobic and anaerobic treatments are conventional biological dye removal methods. There are novel biological techniques available such as degradation using cultures of fungi and microbes, and the use of algae and enzymes (Katheresan, et al., 2018). Biosorption is one of the best methods for removal due to its low cost and higher effectiveness. There are hundreds of biomaterials such as bacteria, algae, fungi, seaweeds, plant leaves, and roots that are tested and evaluated for different

dyes (Bouras, et al., 2017). The available physical removal techniques are reverse osmosis, nano, and ultra-filtration (Katheresan, et al., 2018).

In this study adsorption of five textile dyes that are toxic in the natural environment were tested. *Pandanus amaryllifolius* (Rampe) leaves powder was used as the adsorbent. The objectives of research are;

- To determine the adsorption capacity of *Pandanus amaryllifolius* (Rampe) leaves powder for the five dyes types selected.
- Conduct batch adsorption experiments to determine the adsorption kinetics and equilibrium data for the selected dye types.
- Characterize the adsorbent and determine the physical and surface properties

2. LITERATURE REVIEW

2.1. Sources of Dyes in Past

In the past, different colours of pigments had been extracted from different plant and animal sources. Indigo dyes had been extracted from Indigofera species and woad. Purple dyes such as Shellfish purple had been extracted via molluscs and lichen dyes had been extracted from the fermentation of lichens. Red dyes had been extracted from Coccidia family parasites and Kermes. Plant anthraquinone reds from plant roots, family Rubiaceae and redwoods such as brazilwood, peach wood and sappanwood. Flavonoids had been used as yellow dyes extracted from materials like bog myrtle plant leaves, quercitron bark, Persian berries, saw-wort, and dyer's greenweed. Saffron plucked from the stigmata of flower Crocus sativus. Turmeric had been popular in India and the dye extracted from the root of the plant Curcuma domestica. Brown and the black dye had been obtained from tannins and the main source was oak galls (Hulme, et al., 2004).

2.2. Natural Dyes

Natural dyes have been extracted from plants and animals. When colouring cotton, sun bleaching is the most environmentally friendly process, but overexposing to the sun will lead aged appearance. Natural dye production decreased due to cheaper, faster, and more efficient production processes available for synthetic dyes. Still, natural dyes are an alternative because of having a wide array of bold and fade resistance properties. Natural dyes are environmentally friendly, but have minus points when considering the requirement of synthetic chemicals for bound to fibre, requirement of a high amount of water, high investment due to land, raw material requirement and time-consuming to achieve full potential. Cotton can dye with berberine, which gives strong yellow and natural colour with antimicrobial activity. It gives a higher affinity to protein-based fibres and a low affinity to cellulose fibres (Khattab, et al., 2020).

2.3. Dye Classification

The purpose of dyes is to colourise the fabrics, leather, paints, cosmetics, biological markers etc. Synthetic dye replaced natural dye end of the nineteenth century (Nikfar & Jaberidoost, 2014). Those dyes consist of organic nature. But those molecules have adverse effects on the environment when contacted with natural water bodies due to their water solubility and persistency. Usually, 10 % to 15 % of the initial concentration remain in the wastewater. It produces visible colour even in low concentrations. According to the performance and process of wastewater treatment plant, the removal will depend on (Pal, 2017). There are a few classifications for dyes. Based on nuclear structure (cationic or anionic), chemical structure (nitroso, nitro, monoazo, diazo, stilbene, diarylmethane, triarylmethane, xanthene, acridine, quinoline, methine, thiazole, indamine, indophenol, azine, oxazine, thiazine, aminoketone, anthraquinone, indigoid, phthalocyanine, and inorganic pigments), Source (natural, synthetic) and Industrial Application (Nikfar & Jaberidoost, 2014). There are many types of dyes in the textile industry. For example, acid dyes, direct dyes, azo dyes, disperse dyes, sulfur dyes, fibre reactive dyes, basic dyes, oxidation dyes, mordant dyes, developed dyes vat dyes, pigments, optical/fluorescent brighteners, and solvent dyes (Gita, et al., 2017).

There are some similarities between dye chemical structures present in the same chemical class as acid, direct and reactive dyes. Disperse, mordant and vat dye are structurally similar in compounds of the same family and do not correlate with the same colour (Croce, et al., 2017).

I. Acid dyes

Due to the dying process is being carried out in the acidic phase, these dyes known as acid dyes. In solution, these dies are anionic. With fibres that contain cationic sites, acid dyes are well reacting. There are four types of acid dyes available according to dying characteristics. Level dyeing or equalising dyes, fast acid dyes, milling acid

dyes and super-milling acid dyes (Sekar, 2011). Acid dyes, colour, silk, wool, and animal fibres (Nikfar & Jaberidoost, 2014).

II. Direct dyes

Dying of cellulose fibres can be performed using direct dyes without applying mordants. These dyes have low fastness to washing and do not bring bright shades. It can categorize as anionic dyes due to its application with an electrolyte bath (Pal, 2017). Cotton, wool, flax, and leather can be coloured using direct dyes (Nikfar & Jaberidoost, 2014).

III. Azoic dyes

About 66% of all types of colourant dies are consistent with azo dyes. Those are categorised under the azo category due to the presence of an azo group (Pal, 2017).

IV. Disperse dye

Disperse dyes have partial solubility with water. Polyester, acrylic, acetate, and nylon fibre are coloured using dispersed type dye. Generally, these dyes do not use for natural fibres (Nikfar & Jaberidoost, 2014).

V. Sulfur dye

Sulfur dyes are used for colour cotton due to their inexpensiveness, high wash fastness, and easiness at application. These dyes can generate by reacting several organic compounds with sodium sulfides and sulfur. Those are water-insoluble and can dissolve in alkaline sodium sulfide solution (Nikfar & Jaberidoost, 2014).

VI. Reactive dyes

Reactive dyes came into the picture in the 1950s. This dye molecule is consistent with two parts. The first moiety can be anthraquinone, phthalocyanine or azo with the chromophore. The other moiety relates to the second reactive group, which can make covalent bonds with amine or sulfhydryl groups (Nikfar & Jaberidoost, 2014).

Reactive dye turns to a new molecule after it contacts the fibre molecule. Application of reactive dye requires high pH solutions or neutral solutions. Applying heat to dry textiles can generate different shades using reactive dyes. When taking 95% of these dyes are azo dyes (Pal, 2017).

VII. Basic dyes

Basic dyes use to dye silk, wool, nylon, polyester and modacrylic materials (Nikfar & Jaberidoost, 2014).

VIII. Mordant Dyes

As the name says, mordant dye requires mordant material to generate a colour. Such mordant examples are tannic acid, sumac, gall nuts, oleic acid, stearic acid and metallic mordants such as soluble salts, aluminium, copper, tin etc. Usually, metallic mordants are used more than acid mordants (Nikfar & Jaberidoost, 2014).

IX. Vat dyes

These types of dye cannot apply to fabric with water because these dyes are not soluble in water. So, these dyes need alkaline treatment after applying to the fabric material. These dyes can oxidise in an open atmosphere. Vat dyes fastest easily for cotton, linen and rayon fabrics (Pal, 2017).

2.4. Impacts of Textile Dye in Wastewater

2.4.1. Environmental impacts

With industrial development lot of textile industries are operating. Some of them release the textile effluents to natural water bodies. In a natural environment, it is difficult to neutralize the effects done by pollution load under normal ecological conditions. As a result, it can create several consequences for the aquatic environment. Due to the reduction of light penetration through the water, photosynthesis can reduce and trigger eutrophication. The presence of dye in water

can result in pH variations, Biological Oxygen Demand (BOD) levels increase, Chemical Oxygen Demand (COD) levels increase, and Total Organic Carbon (TOC) and Total Suspended Solids (TSS) increase. High mineral content and low consumption by aquatic plants create an uncontrolled proliferation and lead to depletion of soluble oxygen. High amounts of organic matter tend to have bad taste, colour, and odour. Generally, 7-8 mg of organic matter can be degraded by microorganisms consuming oxygen in 1.0 L of water. Dye molecules have slow degradation and retain with water if released into the environment. This phenomenon is called persistence. The persistency of a molecule has a relationship with its chemical reactivity. Saturated ones have more persistency than unsaturated ones. If molecule is aromatic, it can increase persistency according to the number of substitutes connected. If the dye-containing alkyl group and the substitute is halogen, it can also increase the potential of persistency of molecule in water. When the dye concentrations get higher and higher in the water bodies, it can cause biomagnification. This means the species located end of the food chain can accumulate a higher concentration of toxic compounds than the leading species and maybe the end of the food chain could be human. According to Ecological and Toxicological Association of Dyes and Organic Pigments Manufacturers, 98 % of dyes have Limited Concentration (CL_{50}) above 1.00 mg L^{-1} and 59% have Lethal Concentration for kill 50% of population (LC_{50}) above 100 mg L^{-1} for the toxicity of fish (Berradi, et al., 2019).

About 15-50 % azo dyes are released as waste during the dying process without binding to the fabric. Soil porosity can reduce by clogging the soil pores. As a result, soil productivity can be reduced (Khattab, et al., 2020). Some developed countries use that water for agricultural purposes. Globally, where the labour costs are low and have relatively high demand, small scale factories are present and such factories release those toxic dye wastes directly into water bodies (Lellis, et al., 2019). Due to the possibility of altering soil properties chemically and physically, azo dyes are harmful to flora and fauna. Due to toxicity, it can kill soil microorganisms and can reduce agricultural productivity (Hassaan & Nemr, 2017). From algae, fish, bacteria, and daphnids, algae are the most sensitive type for toxicity and the ranking for the

toxicity less than 100.00 mg L^{-1} concentration of dye can be given as mordant>basic/acid/disperse>direct>reactive (Croce, et al., 2017). Dyestuff can influence the growth protein amount, pigment content, and nutrient amount in the algae. Ramazol red brilliant and indigo dye inhibit algae growth (Gita, et al., 2017).

2.4.2. Health impacts

Dye contamination can create health problems due to changing water quality and initiating toxicity. Most of those toxic substances are azo dyes and can be diazo and cationic dyes. As a result of prolonged exposure to those substances, it can cause allergies, dermatitis, skin irritations, cancers, and mutation. Sometimes cause damage to the immune system and reproductive systems in human beings. It should note that 60-70 % of azo dyes are toxic and identified as carcinogens (Berradi, et al., 2019).

Textile wastewater contains inorganic and organic pollutants. An analysis done by a set of biological tests shows that these pollutants are mutagenic and genotoxic. In the experiment, those wastes were able to increase the revertant count of ames in salmonella genetic strains and make mutations to bacteria deoxyribonucleic acid (Khan, et al., 2019).

Azo dyes are a frequent component in the textile industry, and about 60-70 % of the stuff are azo dyes. Aromatic amines are produced by dermal, systematic and biotransformation of dye by bacteria. The Ames test with S. Typhimurium strains shows about 40 different aromatic amines from about 180 azo dyes used in the textile industry being mutagenic (Merlot & Bruschweiler, 2017). About 100 dyes have the potential to form carcinogenic amines among 4000 investigated dyes. But also, those are prohibited, available in the market (Lellis, et al., 2019). Aromatic amines can be absorbed by the skin and other exposed organs. Those compounds can be mobilised by water. The fastest way of absorbing is ingestion. Those dyes become dangerous when metabolized by liver enzymes (Hassaan & Nemr, 2017).

Water treatment processes such as coagulation, flocculation, chlorination, and floatation cannot remove the dye. Therefore, it is necessary to stop contamination of freshwater bodies from effluent like dye to prevent mutagenic activities (Carneiro, et al., 2010).

2.5. Physical Remediation Techniques for Textile Dye in Wastewater

2.5.1. Adsorption

Adsorption is a simple and effective process with many materials available. Because of its low investment, simple operation and design, no toxic compound generation and safe recovery of adsorbent it is a popular method for dye removal in wastewater. There are many adsorbent materials available. Some examples are, tamarind wood, agricultural waste biomass, gypsum, and sludge (Mittal, et al., 2009). Some low-cost adsorbents are researched for removal of anionic dyes are cattail root, pine cones, coir pitch, jujube seeds, pinon seeds, banana peels, myrtus communis and pomegranate, fungi, neem leaves, parthenium bagasse fly ash, calcium-rich fly ash, red mud, chitosan, kaolin, bentonite, montmorillonite, mesoporous activated carbon, and aniline-propyl silica xerogel (Dahr, et al., 2014). To remove dye most frequently using adsorbent material is activated carbon. But there are some limitations along with activated carbon. Such as high cost and problems of disposal of saturated activated carbon because of difficulty in regenerating (Dahr, et al., 2014). Therefore, research on bio sorbents is the most concerned topic nowadays. Some examples are cellulose, chitosan, sawdust, sugar cane, Brazilian pine-fruit shell, and other agricultural residues (Raymundo, et al., 2010). Some modifications are conducted to the adsorbents to increase adsorbent capacity by increasing the fraction of surface-active sites such as OH^-, SO_4^{2-}, PO_4^{3-}, $RCOO^-$, amide and amino groups on the adsorbents. There are some modified adsorbents prepared from agricultural by-products are peanut husk, coir pith, wheat straw, barley straw, palm ash, straw, sugarcane bagasse, banana peel, sawdust, aminated pumpkin seed powder, cationic modified orange peel powder (Munagapati & Kim, 2016).

2.5.2. Filtration

Microfiltration can remove macromolecules of dye size between 0.10-1.00 μm. Generally, 90 % of suspended solids and turbidity can also remove with microfiltration. There are different types of membranes available with materials like Poly Tetrafluoroethylene (PTFE). The operating pressure of these membranes is between 20-100 psi. In ultra-filtration 31-76 % removal of dye macromolecules can be achieved. These membranes are also made from materials like Poly Vinyl Chloride and PTFE. Nanofiltration can be removed 70 % of colour and compounds that have low molecular weight, reactive dyes, etc. These membranes are much more vulnerable to fouling. Reverse osmosis can remove most of the ionic compounds and reactive dyes. These membranes are also vulnerable to fouling like nanofiltration membranes (Saini, 2017).

2.5.3. Irradiation

Irradiation can break down dye molecules effectively. This process uses a UV beam as a radiation source and the wavelength is below 253.7 nm. This process needs enough dissolved oxygen to obtain good results.

2.6. Chemical Remediation Techniques for Textile Dye in Wastewater

2.6.1. Oxidation

Oxidation with sodium hypochlorite is done by cleavage azo bond present in the azo dyes. This oxidation process is accelerated by the concentration of chlorite ions and at the same time, it reduces the pH of the solution. This method is generally not popular, and it is not recommended to use for the removal of dispersed dye and aromatic compounds which contains toxic molecules. This process is recommended for the removal of compounds that contains amino groups (Saini, 2017).

Oxidation with hydrogen peroxide can be divided into two application methods. One method is Fenton oxidation which uses iron salts to activate hydrogen peroxide, other than the use of UV radiation or visible light alone. This method can make a more powerful oxidation medium than H_2O_2 and O_3. But the efficiency of treatment will be depending on the parameter such as effluent characteristics and pH. Another method is the heterogeneous systems along with zeolites, clays and semiconductors which may or may not use UV. Those methods have several advantages such as reduction of COD, colour, and toxicity in both soluble and insoluble dyes. The only problem is the separation of photocatalysts used (Saini, 2017).

Ozone oxidation happens with the cleavage of conjugated double bonds present in organic dye molecules and decolouration happens because of the oxidation. This process can generate different types of by-products which can be toxic and prolonged oxidation with ozone can remove those toxic compounds. Ozone gas can be applied to the wastewater directly for oxidation and the disadvantage is the destabilisation due to available salt, pH variations and temperature variations of the media (Saini, 2017).

Photochemical oxidation is the process that uses hydrogen peroxide and visible or UV light which can break down dye molecules to H_2O, CO_2, and other oxides by hydroxyl radicals. Process efficiency will depend on the concentration of H_2O_2, pH and intensity of the radiation (Saini, 2017).

2.6.2. Coagulation and precipitation

Neutralising the charges in the particles and allowing them to form clusters is the operation in the coagulation process. These clusters can settle gravitationally due to their higher density than the single particle in the emulsion. There are different types of coagulant aids such as aluminium salts, ferric salts, and polymers (Saini, 2017).

2.7. Biological Remediation Techniques for Textile Dye in Wastewater

There are several different techniques are available for the treatment of wastewater that comes out via dye stuff processing facilities. Biological treatment with aerobic or anaerobic systems is on the leading of them. For colour removal adsorption techniques are used, but it is effective with low concentration effluent. The most effective method for the removal of colour for higher loads is coagulation and flocculation by chemical introduction. Oxidation via strong oxidants is also popular. But due to high operating costs, its application is also limited (Khattab, et al., 2020). When considering treatment options, has its disadvantages. For incineration, the formation of dioxin and furan via incomplete combustion, for biological treatment takes a long period for removal, for adsorption phase transfer without destroying the compound. In advanced oxidation processes can generate hydroxyl free radicals and destroy many contaminants which do not remove by conventional oxidation processes (Hassaan & Nemr, 2017).

2.7.1. Phytoremediation

Phytoremediation can describe as the whole process of degradation, extraction, transformation, and detoxification of compounds using plant enzymes by plants. Some plants are effective for phytoremediation of textile dye and doing it by employing processes such as rhizofiltration, phytoextraction or phytoaccumulation, phytodegradation and rhizodegradation. Examples of hydroponic systems tabulated in Table 2.1,

Table 2.1 Hydroponic plants for phytoremediation

Plant	**Removing Compound**
Nasturtium officinale (Brassi-caceae)	Basic Red 46
Pennisetum purpureum (Poaceae)	Poly R-478

Plants consist of hairy roots cultures such as *Agrobacterium rhizogenes* may produce secondary metabolites to accumulate or remove contaminants. Such examples are in Table 2.2.

Table 2.2 Root culture plants for phytoremediation

Plant	**Removing Compound**
Tagetespatula (Asteraceae)	Red 198
T. patula	Methyl Orange
	Orange M2RL
	Golden Yellow HER
	Navy Blue HE2R
	Reactive Red M5B
Sesuvium portulacastrum (Aizoaceae)	Reactive Green 19A-HE4BD

Examples of phytoremediation by callus and cell suspension cultures are tabulated in Table 2.3.

Table 2.3 Callus and cell suspension cultures for phytoremediation

Plant	**Removing Compound**
Tecoma Stans (Bignoniaceae)	Malachite Green
Blumeamalcolmii (Asteraceae)	Malachite Green
	Remazol Red
	Red HE8B
	Methyl Orange
	Red Reactive 2
	Red HE 7B
	Golden Yellow HER
	Scarlet GDR

The challenges are there for phytotechnologies such as lab-scale experiments in hairy roots, and cell suspension culture because the systematic behaviour and efficiency are more sensitive to variations in environmental factors. There are some advantages also. Such as the mix of different types of plants, bacteria and fungi can improve the efficiency of biodegradation. Examples of consortia of plants are given in Table 2.4.

Table 2.4 Plant consortia for phytoremediation

Removing Compounds	**Plant consortia**
Brown 5R	*Ipomea hederifolia (Convolvulaceas)*
	Ipomea Aquatica (Convolvulaceas)
Congo Red (CR)	*Typha angustifolia (Typhaceae)*
	Paspalum scrobiculatum (Poaceae)

The phytoremediation technique is more economical and environmentally friendly, but it highly depends on soil properties and the plant's capability for degradation (Lellis, et al., 2019).

2.7.2. Bioremediation by microorganisms

Bioremediation can be done by biostimulation or bioaugmentation. Which is the supply of nutrients to local microorganisms or the introduction of exogenous microorganisms. Bioremediation by microorganism have high percentage removal and is comparatively economically viable and generate less sludge mass. Those treatments need good care with monitoring oxygen level, pH level, agitation and mixing, effluent concentration, temperature etc. There are ex-situ bioremediation techniques such as composting and land farming, use for bioreactor facilities and species of plants and crops that have been genetically modified. The main idea of biodegradation is converting/decomposing the effluent into carbon dioxide, water and inorganic final product which is called mineralization. To increase the biodegradation capacity of native microorganisms it is possible to extract microorganisms which able to encode degradative enzymes and clone those microorganisms' genes and introduce them to native species. These can call super degrading bacteria which consist of engineered or hybrid strains. Examples of the engineered bacteria are listed in Table 2.5.

Table 2.5 Engineered bacteria to remove dye pollutants

Wild bacteria	**Gene encodes receiving bacteria**	**Gene enzyme**	**Removing compound**
Pseudomonas luteola	*Escherichia coli*	Azoredutase	Azo textile dyes
Bacillus subtilis	*Escherichia coli*	CotA laccase	Azo and anthraquinone dyes

Some enzymes supporting biodegradation such as peroxidase, laccase, and tyrosinase. Dyes consumed by microorganisms to get nitrogen and carbon. These dyes can metabolise under aerobic or anaerobic conditions. The disadvantages to bacterial biosorption are pre-treatment and dye effluents characteristics and disposal of bacterial biomass. Operating cost is less and operate with an adsorption system to achieve higher removal efficiencies. Pure cultures of bacteria can do the biodegradation of textile dyes such as bioaugmentation of activated sludge. Examples of bioaugmentation of activated sludge are tabulated in Table 2.6.

Table 2.6 Biodegradation by bioaugmentation of activated sludge

Bacteria	**Removing compound**
Aeromonas punctata	Acid Red88 Reactive Black 5 Direct Red 81 Disperse Orange3
Shewanella putrefaciens	

Examples for biostimulation tabulated in Table 2.7.

Table 2.7 Biodegradation by biostimulation

Bacteria	**Substrate**	**Method**	**Removing compound**
Pseudomonas aeruginosa	Glucose	Aerobic	Navitan Fast Blue S5R
Aeromonas hydrophila	Sucrose and yeast Extract	Lignin peroxidase enzyme, laccase enzyme	Crystal Violet (CV)
Acinetobacter sp. SW30	Sodium Borohydride	gold nanoparticles	Direct Black 22, Reactive Yellow 186

Examples for co-culture bacteria tabulated in Table 2.8.

Table 2.8 Co-culture bacteria for biodegradation

Removing compound	**Bacteria co-culture**
Green HE4BD	*Proteus Vulgaris*
	Micrococcus glutamicus
Red violet	*Ochrobactrum sp.*
	Pseudomonas aeruginosa
	Providencia vermicola

In high dynamic process conditions like pH, temperature, toxicity, and salinity extremophiles and extremozymes work well. A high salinity level can create many problematic situations in textile wastewater treatment, but there are some examples of better degradation combinations given in Table 2.9.

Table 2.9 Bacteria works in saline water

Bacteria	**Metallic cation**	**Removing compound**
Bacillus	NaCl	Brilliant Red X-3B
Shewanella aquimarina	NaCl	Acid Red 27
Scheffersomyces spartinae	High salinity	Acid Scarlet 3R
Pichia occidentalis	High salinity	Acid Red B

(Lellis, et al., 2019).

Mycoremediation is done by fungi degrading pollutants with extracellular enzymes by using biosorption, bioaccumulation, and biodegradation as the mechanisms.

Biosorption can have done by live or dead cells of fungi. Biodegradation of dye done by fungi using enzymes. The examples of biosorption fungi are given in Table 2.10.

Table 2.10 Sorption fungi for degrading pollutants

Fungi	**Pollutant**
Aspergillus Niger	Orange G
	Direct Blue 199
Trichoderma sp.	Orange G
Aspergillus flavus	Methyl Orange
Aspergillus fumigatus	Methylene Blue (MB)

(Lellis, et al., 2019).

2.7.3. Bioremediation by enzymes

Enzymes are a good alternative when compare with conventional methods. Which can generate reactive free radicals and manage highly diluted unmanageable pollutants. To generate bulk amounts of those enzymes at low cost the advanced genetic engineering approaches can help to modify gene sequences of the host bacteria. The nanostructures like carbon nanotubes with have a large specific surface area, good chemical and mechanical stability can be facilitated for immobilization of enzymes with increased stability. The main disadvantage of the use of enzymes is it is much more sensitive to inhibitors present in the effluent and can inactivate the enzyme. Azoredutase, and laccase are some examples of enzymes that can use to degrade textile dye. Azoreductase does the reaction by reductive cleavage of azo bonds with the support of coenzymes and producing aromatic amines which convert into carbon dioxide and water. Laccase enzymes oxidize the dye compounds to organic molecules such as ether, aromatic amines, and non-phenolic compounds. Therefore, the laccase enzyme can use for the detoxification of textile wastewater with less harm than the parent molecule (Lellis, et al., 2019).

2.8. Adsorption Isotherm Studies

The amount of dye adsorbed at contact time t was calculated using Equation 1 and percentage adsorption was calculated using Equation 2.

$$q_t = \frac{c_0 - c_t}{w} v \quad (1)$$

$$Percentage\ removal = \frac{(c_0 - c_t)}{c_0} \times 100\% \quad (2)$$

Where, t contact time (min) q_t (mg g^{-1}) is the amount of dye adsorbed at contact time t, c_0 initial dye concentration in solution (mg L^{-1}), c_t solution dye concentration at equilibrium (mg L^{-1}) and w is mass of adsorbent (g) and v is the volume of solution (L) (Pimentel, et al., 2011).

2.8.1. Langmuir isotherm

Langmuir isotherm model (LIM) explains homogeneous adsorption by the finite number of sites located on the adsorbent surface and adsorption happens as monolayer adsorption without having an interaction of adjacent ions adsorbed by the surface of the adsorbent. The Langmuir isotherm model is given by Equation 3.

$$\frac{1}{q_e} = \frac{1}{q_m K_a c_e} + \frac{1}{q_m} \quad (3)$$

Where q_e is the amount of dye adsorbed at equilibrium (mg g^{-1}), c_e is the equilibrium concentration of dye (mg L^{-1}), K_a equilibrium constant known as adsorption energy (Lm g^{-1}) and q_m is the maximum monolayer adsorption capacity of *Pandanus Amaryllifolius* leaves powder (PALP) (mg g^{-1}) (Pimentel, et al., 2011).

2.8.2. Freundlich isotherm

Freundlich isotherm model (FIM) explains heterogeneous adsorption by sites on the adsorbent surface and adsorption happens as multilayer adsorption and it assumes adsorption continues as exponentially due to adsorbed surface acting as an adsorbent repeatedly (Jeyavishnu & Alagesan, 2020). Freundlich isotherm model is given by Equation 4

$$\log q_e = \log K_f + \frac{1}{n} \log c_e \quad (4)$$

Where q_e is the amount of dye adsorbed at equilibrium (mg g^{-1}), c_e is the equilibrium concentration of dye (mg L^{-1}), K_f and n are constants related to adsorption capacity and intensity (Pimentel, et al., 2011).

Here, 1/n is the nonlinearity exponent. Generally, $1/n \leq 1.00$. Solutions of low hydrophobic property can expect nonlinearity. If 1/n = 1 means, for all concentration ranges relative adsorption same and adsorption will follow C-type isotherm. If $1.00 > 1/n > 0.7$, adsorption follows L- type isotherm and which results in an increase of chemical concentration with a reduction of relative adsorption due to saturation of active sites. If $1/n < 0.7$ will result in a highly curved adsorption isotherm. In $1/n > 1$ can observe adsorption for solutions with lower concentrations of polar functional groups. This condition cannot find in generally other than in S-type adsorption isotherm (Technical report 123 Freundlich isotherms, n.d.).

2.8.3. Temkin isotherm

According to the Temkin isotherm model (TIM), it describes heat of adsorption of all adsorbate molecules in layer of adsorbent surface get reduce linearly instead of logarithmically due to the interactions occurred by adsorbate molecules. Temkin isotherm model is given by Equation 5.

$$q_e = B_T \ln A_T + B_T \ln c_e \quad (5)$$

Where q_e is the amount of dye adsorbed at equilibrium (mg g^{-1}), c_e is the equilibrium concentration of dye (mg L^{-1}), B_T are Temkin isotherm constants. A_T is Temkin isotherm equilibrium binding constant related to maximum binding energy (L g^{-1}) (Elkady, et al., 2011).

2.9. Adsorption Kinetic Studies

2.9.1. Lagergren's pseudo-first order equation

Lagergren's pseudo-first order (PFO) equation can explain the rate of adsorption of dye into PALP directly proportional to the difference between adsorbed dye into PALP at considering time and at the equilibrium. It assumes interaction between

adsorbent and adsorbate depends on reaction rate and this describes reversibility of liquid and solid phase adsorption equilibrium. Lagergren's equation is given by equation 6.

$$\log(q_e - q_t) = \log q_e - \left(\frac{K_1}{2.303}\right) t \quad (6)$$

Where q_e is the amount of dye adsorbed at equilibrium (mg g^{-1}), t is contact time (min), q_t is the amount of dye adsorbed at contact time t (mg g^{-1}) and K_1 is the pseudo-first-order rate constant (min^{-1}) (Pimentel, et al., 2011).

2.9.2. Pseudo-second order equation

Pseudo-second order (PSO) equation can explain chemisorption kinetics of adsorbate on the adsorbent. Pseudo-second order equation given by equation 7.

$$\frac{t}{q_t} = \frac{1}{K_2 {q_e}^2} + \frac{1}{q_e} t \quad (7)$$

Where q_e is the amount of dye adsorbed at equilibrium (mg g^{-1}), t is contact time (min), q_t is the amount of dye adsorbed at contact time t (mg g^{-1}) and K_2 is the pseudo-second-order rate constant (g mg^{-1} min^{-1}) (Pimentel, et al., 2011).

2.9.3. Intra-particle diffusion studies

Adsorptions occur by diffusion of dye molecules into the porous interior of the PALP. Morris and Weber's model for intra-particle diffusion is given in Equation 8.

$$q_t = k_d t^{0.5} + \delta \quad (8)$$

Where q_t is dye concentration adsorbed in contact time t (mg g^{-1}), k_d intra-particle diffusion rate constant (mg g^{-1} $min^{-0.5}$), t contact time (min) and δ is boundary layer effect (mg g^{-1}). k_d and δ can be found by plotting q_t vs $t^{0.5}$ (Amarasinghe & Amarasinghe, 2020).

2.10. Further Studies for Evaluate behaviour of Adsorption

There are many other isotherms developed to predict adsorption behaviour. Some of them are Brunauer Emmett Teller (BET) isotherm model, Fritz Schlunder isotherm model (FISM), Sips isotherm model (SIM), Hill isotherm model (HIM), Koble-Corrigan isotherm model (KCIM), and Redlich Peterson isotherm model (RPIM).

There are other kinetic equation models available. Some of them are Avrami factionary order (AFO), and Elovich model (ELM).

To observe adsorption thermodynamic behaviour, there are few calculations available. Those calculations can be conducted to verify the adsorption follows as Endothermic reaction (EDTR), or Exothermic reaction (EXTR), and verify whether the reaction has Spontaneous (SP) or Non-Spontaneous (NSP) nature.

2.11. Congo Red Dye

Congo red dye has a formula of $C_{32}H_{22}N_6Na_2O_6S_2$, and a molecular mass of 696.66 g mol^{-1}. CR is a sodium salt of benzidinediazo-bis-1-naphthylamine-4-sulfonic acid (Patel & Vashi, 2012). It shows higher water-solubility, and it is a diazo dye with a brownish-red colour stable crystal in atmospheric conditions with a solubility of 33.3 mg mL^{-1} (Mittal, et al., 2009). CR is produced via the reaction of tetrazotised benzidine and napthionic acid in 1:2 stoichiometry. CR is a known carcinogen and serious aquatic hazard, and it is very stable in water due to its chemical structure (Munagapati & Kim, 2016). Molecular structure of CR is given in the Figure 2.1.

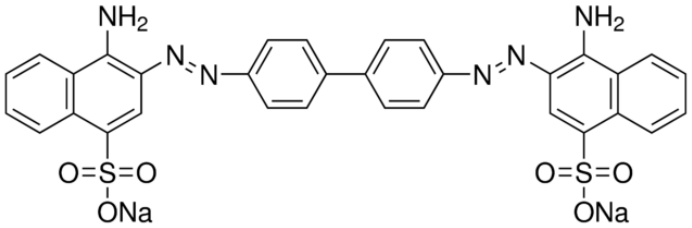

Figure 2.1 Molecular structure of Congo Red

CR is stable thermally, optically and physio chemically which makes it difficult to biodegrade. CR is an anionic diazo dye which prohibited to use in several countries due to its known issues of human carcinogenicity, allergenicity, reducing the potential of serum protein concentration, the possibility of platelet aggregation, cause of thrombocytopenia and disseminated micro embolism (Dahr, et al., 2014). Research has been done to evaluate the toxicity of CR dye using *Ceriodaphnia dubia*. Very low concentrations of CR show toxic effects on the reproduction and survival of *Ceriodaphnia dubia* (Zamora, et al., 2016).

2.11.1. Removal of congo red via adsorption

In column adsorption process with a fixed bed of rice husks can remove aqueous CR. The breakthrough curve can influence by flow rate, initial CR ppm level and bed height. Bed Depth Service Time model can describe the effect of bed height on breakthrough curves. Thomas model can describe experimental setup breakthrough curves and the Adams Bohart model can describe initial column dynamics (Han, et al., 2008). Some adsorbent materials tested to remove congo red are given in the Table 2.11.

Table 2.11 Congo red removal by adsorbents

Adsorbent	**Isotherm model**	**Kinetic model**	**Reaction nature**	**Tendency**	**Removal %**	**Adsorption capacity mgg^{-1}**	**Source**
Bottom ash	-	PSO	EXTR	SP	96.95	-	(Mittal, et al., 2009)
Deoiled soya	-	PSO	EXTR	SP	97.4	-	(Mittal, et al., 2009)
Zinc peroxide	FIM	PSO	-	-	-	208	(Chawla, et al., 2017)
Multi Wall Carbon Nano Tubes (MWCNT)	LIM	PSO	EDTR	-	92	-	(Zare, et al., 2015)
$Fe_xCo_{3-x}O_4$	LIM, FIM	PFO	-	-	-	-	(Liu, et al., 2019)
Nano CaO	-	-	-	-	-	357	(Xia, et al., 2013)
CaO	-	-	-	-	-	238	(Xia, et al., 2013)

2.11.2. Removal of congo red via biosorption

Some biosorbent materials tested to remove congo red are given in the Table 2.12.

Table 2.12 Congo red removal by biosorbents

Adsorbent	**Isotherm model**	**Kinetic model**	**Reaction nature**	**Tendency**	**% Removal**	**Adsorption capacity mgg^{-1}**	**Source**
Immobilized *Aspergillus Niger*	LIM	PSO	EDTR	NSP	98.8	-	(Hamad & Saied, 2021)
Tunics of corm of saffron	LIM	PSO	-	-	68	-	(Dbik, et al., 2020)
Tea waste	LIM	PSO	EDTR	SP	-	-	(Dahr, et al., 2014)
Cladodes of *Cereus* sp.	LIM	PSO	-	-	-	27	(Jeyavishnu & Alagesan, 2020)
Cuticle of *Cereus* sp.	LIM	PSO	-	-	-	52.6	(Jeyavishnu & Alagesan, 2020)
Bengal gram fruit shell	LIM	PSO	EDTR	SP	-	22.2	(Krishna, et al., 2014)
Activated pomelo peel	LIM	PSO	-	SP	-	144.9	(Zheng, et al., 2020)
Aspergillus carbonarius	LIM	PSO	EDTR	SP	-	99	(Bouras, et al., 2017)
Penicillium glabrum	LIM	PSO	EDTR	SP	-	101	(Bouras, et al., 2017)
Euro-American poplar	LIM	PSO	-	-	71.8	3.3	(Stjepanović, et al., 2021)
Phoenix dactylifera seeds	LIM	PSO	EDTR	SP	76.1	61.7	(Pathania, et al., 2016)
Eichhornia crassipes roots	FIM	PSO	-	-	96	-	(Wanyonyi, et al., 2014)
Activated *Tectona grandis* leaf	FIM	PSO	EDTR	SP	-	-	(Gedam, et al., 2019)
Modified chitosan	SIM	PSO	EDTR	-	-	-	(Zahir, et al., 2017).
Treated coconut residual fibre	LIM, FIM	PSO	-	-	-	129	(Rani, et al., 2017)
Dried cabbage waste powder	LIM, FIM	PSO	-	-	91	-	(Wekoye, et al., 2020)
Pineapple plant stems	LIM, TIM	PSO	EXTR	-	-	11.966	(Chan, et al., 2016)

2.11.3. Removal of congo red by other methods

Degradation and mineralization of aqueous CR using ozone, strong enough to decolourize CR by pseudo-first-order oxidation with COD drop up to 54 % and TOC drop up to 32 % (Khadhraoui, et al., 2009).

Natural coagulant alginate extracted from *Sargassum sp.* brown algae can coagulate 96 % of the aqueous CR with optimum alginate and calcium dose in pH 4.0 (Vijayaraghavan & Shanthakumar, 2015). Seed kernel extracted from *Leucaena leucocephala* as a natural coagulant can remove 99.9 % colour of aqueous CR with generating a half amount of sludge compared to chemical standard coagulants (Kristianto, et al., 2019).

Chitosan-based ternary selenide nanocomposites can 99 % of photocatalytic degradation at pH 6.0, 60 ppm of dye concentration, 0.2 g of catalyst amount and with good sunlight irradiation with second-order reaction and capable of up to five degradation cycles (Yang, et al., 2021).

Haematococcus sp. has 98 % decolouration at 10 ppm of aqueous CR among microalgae *Haematococcus sp*., *Chlorella sp*., *Chlorella vulgaris*, *Scenedesmus obliquuss, S. officinalis*, and *S. quadricauda* and blue-green algae *Arthospira maxima* (Mahalakshmi, et al., 2015).

Electrochemical pre-treatment using titanium electrode anode with coating RuO_2-IrO_2 with bio decolourization using bacteria consortium of *Pseudomonas stutzeri* MN1 and *Acinetobacter baumannii* MN3 has 98 % of aqueous CR decolouration (Sathishkumar, et al., 2019).

2.12. Reactive Black B Dye

Reactive Black 5 (RB5) has a Chemical formula of $C_{26}H_{21}N_5Na_4O_{19}S_6$ and a Molar mass of 991.82 with a Colour index number of 20505 (Won, et al., 2006). RB5 is manufactured by coupling of 2-(4-Aminophenylsulfonyl) ethyl hydrogen sulphate, and 4-Amino-5-hydroxynaphthalene-2,7-disulfonic acid (reactive-black-5, 2012). The generic name of RB5 is CI Reactive Black 5 (Eren & Acar, 2006) and the

synonym used is Remazol black B (Sarvestani & Doroudi, 2020) with the product name Reactive Black B (REACTIVE DYES, 2021). RB5 is a diazo acidic reactive dye (Munagapati, et al., 2019) and contains sulfonic acid groups which cause anionic nature in the molecule (Munagapati, et al., 2018). Molecular structure of RB B is given in the Figure 2.2.

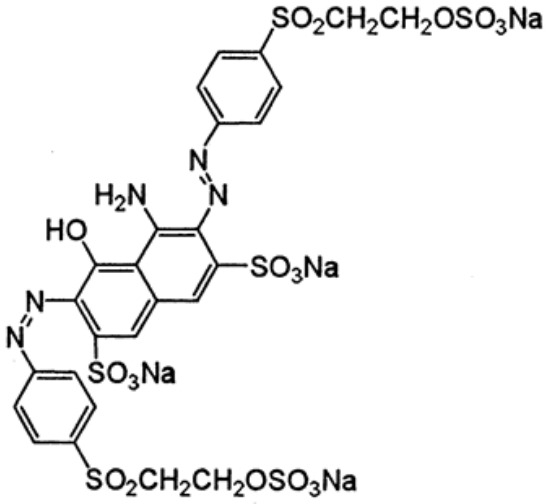

Figure 2.2 Molecular structure of Reactive Black B

Due to its toxicity to aquatic components, and the carcinogenic and mutagenic behaviour of breakdown compounds, it should be highly concern when it presents in the water (Bhaumik, et al., 2016). Due to the presence of reactive groups in the molecule covalent bonds form with fibre and have a higher solubility in water (Bouraie & Din, 2016). Due to poor bonding with fibre, it washes away into the wastewater stream (Qureshi, et al., 2017). Due to economically viable, highly stable, higher colour brightness, and less energy usage RB5 is very much popular in many different industries like production of textile, paper, plastic, leather mineral processing, electroplating and leather etc. and hence the environmental discharge is higher. The presence of RB5 in water in trace amounts can induce colour and hinder light penetration which causes environmental problems such as disturbing plant growth by reducing photosynthesis and then decreasing oxygen concentration and leading to eutrophication. RB5 can be caused health problems due to long exposure. Such as Skin rashes, Bladder cancer, Chromosomal aberration, Respiratory and kidney failure, Blindness, Shock, Cardiovascular collapse, and Asthma (Sarvestani & Doroudi, 2020).

2.12.1. Removal of reactive black b via adsorption

Remove Reactive Black B (RBB) in aqueous solutions different types of adsorbents can be applied. Natural adsorbents are environmentally friendly and low cost, but have low stability in harsh conditions and are less reusable. Nanomaterials are more efficient, stable, and reusable, but expensive to produce. Chitosan-based adsorbents are environmentally friendly with low cost but less efficient in adsorption (Sarvestani & Doroudi, 2020).

Some adsorbent materials tested to remove reactive black b are given in the Table 2.13

Table 2.13 Reactive black B removal by adsorbents

Adsorbent material	**Isotherm model**	**Kinetic model**	**Reaction nature**	**Tendency**	**Removal %**	**Adsorption capacity mgg^{-1}**	**Source**
Bentonite clay	-	PSO	EXTR	SP and NSP	-	-	(Amin, et al., 2015)
Powdered Activated Carbon (AC)	LIM, FIM	PSO	-	-	-	58.8	(Eren & Acar, 2006)
Afsin-Elbistan fly ash	LIM, FIM	PSO	-	-	-	7.9	(Eren & Acar, 2006)
Activated red mud	FIM	PSO	-	-	-	83.0	(Shirzad-Siboni, et al., 2014)
Bone char	RPIM	-	-	-	-	286	(Ip, et al., 2010)
Bamboo AC impregnation ratio (IMR) 2	LIM, FIM	-	-	-	-	473	(Ip, et al., 2010)
Bamboo AC IMR 6	LIM, FIM	-	-	-	-	160	(Ip, et al., 2010)
Granular AC filtrasorb	RPIM	-	-	-	-	198	(Ip, et al., 2010)

The higher adsorption capacity of bone char over the activated carbon may be due to differences in temperatures which adsorption experiments were conducted. With PAC as adsorbent, the experiment conducted at 20 ^{0}C and with Bone char 25 ^{0}C. The adsorption experiment done at 25 ^{0}C, for both activated carbon and bone char, shows activated carbon have higher adsorption capacity than Bone char (Ip, et al., 2010).

2.12.2. Removal of reactive black b via biosorption

Some biosorbent materials tested to remove reactive black b are given in the Table 2.14.

Table 2.14 Reactive black B removal by biosorbent

Adsorbent material	Isotherm model	Kinetic model	Reaction nature	Tendency	Removal %	Adsorption capacity mgg^{-1}	Source
Pumpkin seed hulls	LIM	PSO	EXTR	less SP	-	9.18	(Çelebi, 2019)
Eggshells	LIM	PSO	EXTR	less SP	-	18.46	(Çelebi, 2019)
Dried *Penicillium restrictum* biomass	-	PSO	-	-	-	142.04	(Iscen, et al., 2007)
Banana peel	LIM	PSO	-	-	-	49.2	(Munagapati, et al., 2018)
Sunflower seed shell	FIM	PSO	-	-	85	-	(Osma, et al., 2007)
Mandarin peels	FIM	PSO	-	-	71	-	(Osma, et al., 2007)
Corynebacterium glutamicum	LIM	PSO	EDTR	SP	-	185.2	(Won, et al., 2006)
Sisal fibers	BET	-	-	SP	85	310.2	(Vargas, et al., 2019)
Plyaniline nano fibers	LIM	PSO	EDTR	SP	-	312.5	(Bhaumik, et al., 2016)
Aqai stalk of *Euterpe oleracea*	SIM	AFO	-	-	-	52.3	(Cardoso, et al., 2011)
Acidified aqai stalk of *Euterpe oleracea*	SIM	AFO	-	-	-	72.3	(Cardoso, et al., 2011)
Chemically modified banana peel powder	LIM	PSO	EDTR	SP	-	211.8	(Munagapati, et al., 2019)
Nontoxic biodegradable Zein nanofiber	LIM	PSO	-	-	99.8	-	(Qureshi, et al., 2017)
Sawdust	LIM, FSIM	-	-	-	93	-	(Chakraborty, et al., 2006)

2.12.3. Removal of reactive black b by other methods

Colour of aqueous RBB can be remove up to 99.99% with the use of a 108.5 ppm dose of $KMnO_4$ (Ullah, et al., 2013). Fenton's oxidation using $FeSO_4$ and H_2O_2 remove 99 % of the colour in RBB aqueous solutions (Meriç, et al., 2004). Fe^{2+} and H_2O_2 pre-treatment before remediation of RBB using bacteria consortium are much more productive due to less chemical usage, less time for treatment and low sludge generation (Bahmani, et al., 2013). Fenton (H_2O_2/Fe^{2+}) and photo Fenton (H_2O_2/Fe^{2+}/UV) processes can decolourise RBB up to 97.5 % and 98.1 % (Lucas & Peres, 2005). Photolysis and photocatalysis of ferrioxalate with H_2O_2 remove 98 % of RBB and 71 % of COD at pH 5.0, 2-hour reaction time, molar ratio $C_2O_4^{2-}$: Fe^{3+} =1:3 (Huang, et al., 2007). A slurry membrane batch reactor with ZnO is better than with TiO_2 and the increment of ZnO can reduce the RBB removal. 100 % removal can obtain in pH 11.0 within 1-hour with combined reactions of ZnO photolysis and photoactivity (Laohaprapanon, et al., 2015). With co-metabolic functions of H_2O_2 and the presence of glucose *Debaryomyces polymorphus* and *Candida tropicalis* yeasts remove RBB colour (Qingxiang, et al., 2007). Photocatalytic oxidation with a UV/ TiO_2 reactor can remove RBB in textile effluent (Tang & Chen, 2004). TiO_2 photocatalytic treatment can remove RBB in artificial greywater up to 97 % with optimum conditions of 150 min. In real greywater 76 % removal in 330 min (Chong, et al., 2015). Anaerobic Sequential Batch Reactor, aerobic Membrane Bio Reactor (MBR) with immobilized suspended bio cells and an integrated MPR with UV/TiO_2 slurry can remove RBB. Integrated membrane photocatalytic reactor with UV/TiO_2 slurry reactor has a faster removal than the other types (You, et al., 2010). *Aeromonas hydrophila was* able to 76 % decolouration of RBB in optimal static conditions such as pH 7.0 and temperature 35 °C with modified mineral salt medium $(NH_4)_2SO_4$, KH_2PO_4, K_2HPO_4, $MgSO_4.7H_2O$ and NaCl (Bouraie & Din, 2016). Decolouration of RBB capable with bacteria strain Bacillus cereus strain HJ-1 isolated from river sediment contaminated with azo dye. After decolouration in the optimal conditions microbial sample can amend with original sediment and the microbial community can survive up to 12 days of incubation in natural river conditions (Liao, et al., 2013). Anaerobic hydrogen-based denitrification and

combined anaerobic/aerobic hydrogen-based denitrification can remove nitrate and RBB dye. *Xanthomonadaceae, Rhodocyclaceae*, and *Thauera spp* are the major bacteria that done a major role to remove nitrate and RBB in the hydrogen-based denitrification process. In both methods combined anaerobic/aerobic hydrogen-based denitrification process can recommend the removal of textile dye RBB in wastewater (Singhopon , et al., 2021). About 80 % aqueous RBB remove using consortia of thermophilic bacteria with aerobic conditions in less than 12 h with *Anoxybacillus* genus. The rate of decolouration can double in bench-scale bioreactors than in the flask cultures with the bacterial consortia (Deive, et al., 2010). Batch electrocoagulation using iron and aluminium electrodes can remove aqueous RBB with respective removal rates for both electrodes of 96 %, and 89.45 % in the same conditions (Baneshi, et al., 2016).

2.13. Methylene Blue Dye

The MB has a formula of $C_{16}H_{18}N_3SCl_3H_2O$ with a molar mass of 319.85 g mol^{-1} and the dye is cationic. MB is not acutely toxic, but it can cause breathing difficulties when inhaled and if swallowed through the mouth, it can cause nausea, vomiting, diarrhoea, and gastritis. When expose to large amounts cause abdominal and chest pain, severe headache, sweating, pain in micturition and methemoglobinemia (Bhattacharyya & Sharma, 2005). MB is used in different types of industries such as paper, textile processing etc. MB can create fever, hypertension, and mental problems when expose to high concentrations (Chaukura, et al., 2017). Chemical dose of 500.0 mg of MB can cause anaemia, dizziness, abdominal pain, etc (Ooi, et al., 2016). Molecular structure of MB is given in the Figure 2.3.

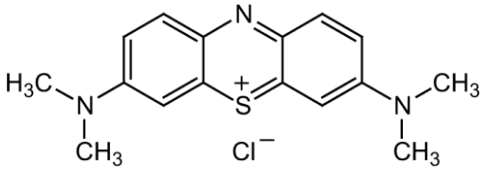

Figure 2.3 Molecular structure of Methylene Blue

2.13.1. Removal of methylene blue via adsorption

Some adsorbent materials tested to remove methylene blue are given in the Table 2.15.

Table 2.15 Methylene blue removal by adsorbents

Adsorbent material	**Isotherm model**	**Kinetic model**	**Reaction nature**	**Tendency**	**Removal %**	**Adsorption capacity mgg^{-1}**	**Source**
Sulphuric acid-treated and microwaved bentonite	LIM,	PSO	-	-	-	92.6	(Banat, et al., 2006)
Biochar derived from pulp and paper sludge	FIM	PSO	-	-	-	33	(Chaukura, et al., 2017)
Fe_2O_3–biochar nanocomposite derived from pulp and paper sludge	LIM	PFO	-	-	-	50	(Chaukura, et al., 2017)
AC	LIM	PSO	-	-	-	192.31	(Cheng, et al., 2018)
Iron/Cerium modified AC	LIM	PSO	-	-	-	264.55	(Cheng, et al., 2018)
Heap Fired Rice Husk Ash	LIM, FIM	PSO	EDTR	SP	-	17.36	(Salem, et al., 2018)
Ash of Treated Rice Husk	LIM, FIM	PSO	EDTR	SP	-	15.64	(Salem, et al., 2018)
Polyaniline zirconium (IV) silico phosphate nanocomposite	FIM	PSO	EDTR	SP	-	12	(Gupta, et al., 2014)
Acid treated zeolite	KCIM	PSO	-	-	98.8	-	(Hor, et al., 2016)
Metal-organic frameworks based on copper-benzene tricarboxylates	LIM	PSO	EXTR	SP	-	-	(Lin, et al., 2014)

2.13.2. Removal of methylene blue via biosorption

Some biosorbent materials tested to remove methylene blue are given in the Table 2.16.

Table 2.16 Methylene blue removal by biosorbents

Adsorbent material (biosorbent)	**Isotherm model**	**Kinetic model**	**Reaction nature**	**Tendency**	**Removal %**	**Adsorption capacity mgg^{-1}**	**Source**
Typha latifolia L. stem and leaf powder	LIM	PSO	-	-	98.69	126.6	(Orozco, et al., 2018)
Leaves of the Neem tree (*Azadirachta indica*)	FIM, LIM	PFO	EDTR	-	-	8.76	(Bhattacharyya & Sharma, 2005)
Shaddock peel	LIM	PSO	-	-	-	305.81	(Liang, et al., 2012)
Sugar extracted spent rice biomass	LIM	PSO	EDTR	SP	-	8.13	(UrRehman, et al., 2012)
Mangosteen peel derived ferric oxide magnetic biochar	LIM	-	-	-	95	46.296	(Ruthiraan, et al., 2017)
Immobilized *Agrobacterium fabrum* biomass with iron oxide nanoparticles	FIM	PSO	EXTR	SP	-	91	(Sharma, et al., 2018)
Tamarind Fruit Shell	LIM	PSO	EDTR	SP	-	1.72	(Saha, 2010)
Natural Carica papaya wood	LIM	PSO	EDTR	SP	-	32.25	(S, Lata, & P, 2018)
Papaya seeds	LIM	PSO	-	-	-	637.29	(Paz, et al., 2013)
Haloxylon recurvum plant stems	FIM	PFO	EXTR	SP	-	22.93	(Hassan, et al., 2017)
Brazil nutshells	LIM	PSO	EXTR	SP	-	7.81	(Brito, et al., 2010)

2.13.3. Removal of methylene blue by other methods

Degussa P25 TiO_2 was able to degrade 81.4 % of MB using a photocatalytic reaction. At optimised conditions, 95 % degradation was achieved. When copper doping it can be able to increase the degradation by up to 2 % (Tichapondwa, et al., 2020). The degradation of MB using nano TiO_2 powder was observed under photolysis and sonolysis systems. According to the results, lower initial concentration and higher UV radiation are effective for removal. The rates of sonophotocatalytic processes are higher than the photocatalytic process (Salehi, et al., 2012).

Phytoremediation of MB using Water hyacinth was done to evaluate the removal efficiency. It has been shown that 98.42 % of removal was achieved (Ooi, et al., 2016).

Oxidation of MB using in-situ generated H_2O_2 with the presence of Fe^{2+} catalyst was observed. In the conditions of 100 mg dm^{-3} MB solution with 1×10^{-3} mol dm^{-3} Fe^{2+}, 88.2 % removal was achieved (Lacasa, et al., 2019).

2.14. Reactive Red Dye

Reactive red (RR) dye has a molecular weight of 968.21 g mol^{-1}, and the molecular formula is $C_{27}H_{18}ClN_7Na_4O_{15}S_5$ (Dehghani, et al., 2019). Molecular structure of RR is given in the Figure 2.4.

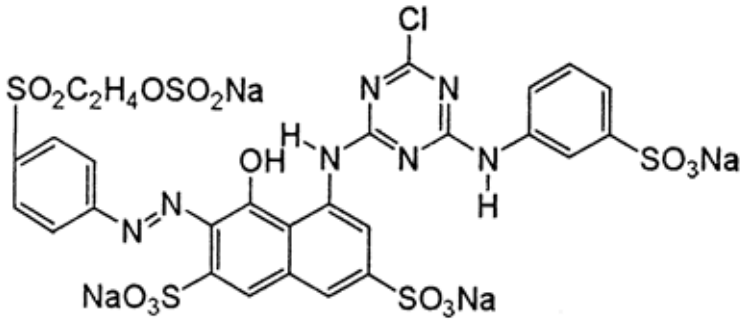

Figure 2.4 Molecular structure of Reactive Red

RR dye is an anionic azo dye (Gül, 2013) a deep red powder produced by coupling of 2-(4-Aminophenylsulfonyl) ethyl hydrogen sulphate diazo and 4-Amino-5-hydroxynaphthalene-2,7-disulfonic acid, then condensation with 2,4,6-Trichloro-1,3,5-triazine, finally condensation with 3-Aminobenzenesulfonic acid (Reactive red 198, n.d.). RR dye has toxic and carcinogenic properties in nature. It is used in many industries like textile dyeing, tannery, printing, etc (Surana, et al., 2011). This dye is also known as Remazol Red 198.

2.14.1. Removal of reactive red via adsorption

Some adsorbent materials tested to remove reactive red are given in the Table 2.17.

Table 2.17 Reactive red removal by adsorbents

Adsorbent material	**Isotherm model**	**Kinetic model**	**Reaction nature**	**Tendency**	**Removal %**	**Adsorption capacity mgg^{-1}**	**Source**
Shrimp chitosan	LIM	PSO	-	-	-	357.1	(Haffad, et al., 2019)
Cuttlefish bone powder	LIM, FIM	PSO	-	-	77	-	(Mahboobeh, et al., 2017)
MWCNT	FIM	-	EDTR	SP	-	169.73	(Baghapour, et al., 2013)
Alumina carbon nano tube hybrid	FIM	PSO	EXTR	-	91.54	-	(Malakootian, et al., 2015)
Cellulose	SIM, RPIM	ELM	EDTR	SP	-	-	(Silva, et al., 2015)
Magnetic Activated Carbon	LIM	PSO	-	-	78.9	-	(Abuzerr, et al., 2018)
Polyaniline/Fe3O4 magnetic nanoparticles	LIM	PSO	EDTR	SP	-	45.454	(Tayebi, et al., 2016)

2.14.2. Removal of reactive red via biosorption

Some biosorbent materials tested to remove reactive red are given in the Table 2.18.

Table 2.18 Reactive red removal by biosorbents

Adsorbent material (biosorbent)	Isotherm model	Kinetic model	Reaction nature	Tendency	Removal %	Adsorption capacity mgg^{-1}	Source
Sawdust	LIM, FSIM	-	-	-	89	-	(Chakraborty, et al., 2006)
Eggshell biocomposite beads	LIM, TIM	PSO	EXTR	SP	-	46.9	(Elkady, et al., 2011)
Pomegranate seed powder	FIM	PSO	-	-	87.64	10.95	(Ghaneian, et al., 2015)
Potamogeton crispus native	-	PSO	-	-	-	14.3	(Gulnaz, et al., 2011)
Potamogeton crispus acid-treated	-	PSO	-	-	-	26.8	(Gulnaz, et al., 2011)
Potamogeton crispus alkali-treated	-	PSO	-	-	-	44.2	(Gulnaz, et al., 2011)
Canola hull	TIM	PSO	-	-	-	-	(Mahmoodi, et al., 2011)

2.14.3. Removal of reactive red by other methods

A consortium of bacteria *Enterococcus faecalis* and *Klebsiella variicola* concentrated to 3.5 mL × 10^5 cells m L^{-1} can remove 10–25 mg L^{-1} RR dye in an aqueous solution up to 99.26 % with 72-hour incubation, pH 8.0 and 37 ℃ (Eslami, et al., 2019). Removal of aqueous RR dye utilising fungus *Rhizopus oryzae was* done in the experiment. Under the optimal conditions of pH, dye concentration, reaction time and fungal volume, the removal rate was obtained at 98 % (Esmaeili & Kalantari, 2015).

Photocatalytic degradation of RR dye in aqueous solutions was succeeded using TiO_2/UV-C photocatalytic process. With 0.4-1.0 g L^{-1} TiO_2 dose can obtain up to 97-100 % removal at pH 4.0 and 100 mg L^{-1} dye concentration. When increasing the pH and dye concentration shows a decrease in removal efficiency (Rahimi, et al., 2013).

Feasibility of the Photo Fenton process (UV/ H_2O_2/Fe (II)) for removal of RR dye from aqueous solutions was studied and 99 % removal was achieved in optimal conditions (Mansooreh, et al., 2015). When comparing the removal of aqueous RR dye by Fenton and Photo Fenton processes the Photo Fenton process is much more effective than the Fenton process (Dehghani, et al., 2019).

A comparison of the Ozonation process of RR dye aqueous solutions with and without the use of MgO nanocrystal catalysts shows the presence of MgO nanocrystals increases the treatment process (Moussavi & Mahmoudi, 2009).

2.15. Crystal Violet Dye

Crystal violet has a molecular weight of 407.99 g mol^{-1} and a molecular formula of $C_{25}H_{30}ClN_3$ (Fabryanty, et al., 2017). CV dye is produced by reacting dimethylaniline with phosgene and getting 4, 41-bis (dimethylamino) benzophenone intermediate it again reacts with dimethylaniline presence of phosphorus oxychloride and hydrochloric acid. CV is categorised as a biohazard substance (Mani & Bharagava, 2016). CV is generally used for bacterial staining applications in a bacterial classification other than the textile and dying applications. This dye can cause severe environmental damage when mixed into the aquatic environment due to it being readily absorbed into fish tissue and interfering with metabolic activities. Some studies report mutagenic and carcinogenic effects on rodents (Lim, et al., 2020). CV is a cationic dye under the triphenylmethane group. CV causes mitotic poisoning and Vitro clastogenic effects which are reasons for chromosomal damage. CV cause fish tumours and hepatocarcinoma, reticular cell sarcoma in organs like the vagina, uterus, ovary, and bladder. It can cause skin irritations, digestive tract irritations, and respiratory and renal failures in humans (Lellis, et al., 2019). Molecular structure of CV is given in the Figure 2.5

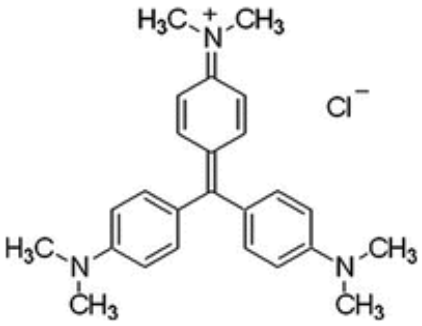

Figure 2.5 Molecular structure of Crystal Violet

2.15.1. Removal of crystal violet via adsorption

Some adsorbent materials tested to remove crystal violet are given in the Table 2.19.

Table 2.19 Crystal violet removal by adsorbents

Adsorbent material	**Isotherm model**	**Kinetic model**	**Reaction nature**	**Tendency**	**Removal %**	**Adsorption capacity mgg^{-1}**	**Source**
Gliricidia sepium tree Biochars at 700 ^{0}C	HIM	PSO	-	-	-	125.5	(Wathukarage A et al., 2019)
CaO modified fly ash	LIM	PSO	EXTR	SP	-	38.57	(Chakraborty, et al., 2021)
Bentonite-alginate composite	FIM, LIM	PSO	-	-	-	601.9	(Fabryanty, et al., 2017)
The hydrogel of biodegradable polymers Xanthan gum and N-vinyl imidazole	LIM	PFO	-	-	-	453	(Mohamed, et al., 2018)

2.15.2. Removal of crystal violet via biosorption

Some biosorbent materials tested to remove crystal violet are given in the Table 2.20.

Table 2.20 Crystal violet removal by biosorbents

Adsorbent material (biosorbent)	**Isotherm model**	**Kinetic model**	**Reaction nature**	**Tendency**	**Removal %**	**Adsorption capacity mgg^{-1}**	**Source**
Coffee husks	FIM, LIM	PSO	EXTR	SP	94	12.0360	(Cheruiyot, et al., 2019)
Tea dust	LIM, FIM	PSO	-	-	-	175.4	(Khan, et al., 2016)
Pineapple leaf (*Ananas comosus*) powder	LIM	PSO	-	-	-	158.73	(Neupane, et al., 2015)
Water hyacinth (*Eichhornia crassipes)* root powder	LIM	PSO	EDTR	SP	-	322.58	(Kulkarni, et al., 2017)
Cordia trichotoma sawdust	LIM	-	EDTR	SP	83.35	129.77	(Grassi, et al., 2020)
Diaporthe schini inactive biomass	SIM	ELM	EDTR	SP	87	642.3	(Grassi, et al., 2019)
Olive leaves powder	LIM, FIM	PSO	-	-	99.2	181.1	(Elsherif, et al., 2021)
Corn stalk	LIM	PSO	-	-	-	-	(Muhammad, et al., 2019)
Avocado seed powder	Liu	-	EXTR	-	92.9	95.98	(Bazzo, et al., 2015)
Rubber (*hevea brasillensis)* seed shell	LIM	PSO	-	-	-	23.81	(Tan & Hameed, 2012)
Arundo donax L	LIM	PSO	EXTR	SP	-	19.6	(Krika, et al., 2019)
Treated ginger waste	FIM	PSO	EDTR	SP	-	277.7	(Kumar & Ahmad, 2011)
Artocarpus altilis (breadfruit) skin	LIM, SIM	PSO	EDTR	SP	-	150.1	(Lim, et al., 2015)

2.15.3. Removal of crystal violet by other methods

There are negligible effects when using UV light or H_2O_2 alone for Decolouration of aqueous CV dye using Fenton regent and UV/H_2O_2. The decolourisation is independent of pH value. In both ways, reactions occur with first-order reaction kinetics. Hydrogen phosphate ion inhibits decolourisation (Alshamsi, et al., 2007).

Decolourisation of CV aqueous using *Bacillus sp*., possible and according to phytotoxicity and microbial toxicity studies CV is less toxic for the bacteria (Ayed, et al., 2009). The removal efficiency of CV using *Bacillus pumilus* and *Micrococcus lylae* respectively 89.47 % and 88.4 % (Selim, et al., 2015).

Electrochemical degradation of CV aqueous solution using synthetic boron-doped diamond thin-film electrodes able to oxidize CV completely with high efficiency without generating by-products (Palma-Goyes, et al., 2010).

Degradation of CV aqueous solution using AgC doped TiO_2 (more effective than the TiO_2 alone) stimulated by UV and solar light respectively 99 % and 88 % (Sahoo, et al., 2005).

2.16. Comparison of Different Removal Methods for Different Dyes

For removal of each five dyes there are number of different methods have been tested. Most of them are goes under biological or chemical process. Those methods have obtained different removal efficiency values and most of them are obtained removal higher than 90%. There are few reasons can be identified behind that observation. The experimental conditions they used in different experiments are different. Such as pH of dye solution, catalyst used, temperature used, and source of energy used to activate the catalyst are vary by experiment to experiment.

3. MATERIAL AND METHODS

3.1. Preparation of Biosorbent (Adsorbent)

Rampe leaves were obtained from the healthy and well-grown bush in the wetland area located in Kotavila, Matara district. Only the matured leaf part was selected, and dead contents were removed. The leaves were washed well three times using clean well water to remove dust, mud, and debris and kept in an open atmosphere under sunshine to sundry for two weeks. Dried leaves were trimmed up to 1.0 cm size pieces using a pair of scissors. Trimmed leaves were heated using an oven up to 150 ^{0}C for 3 minutes while mixing well. Heating of trimmed leaves using an oven is given in Figure 3.1.

Figure 3.1 Heating leaves in the oven

After the heating, the leaves were immediately grounded into powder using a grinder. Prepared powder was sieved using the sieve shaker with a range of 710-250 µm sieves. Fine and coarse particles were removed, and particles retained on a 250 µm sieve were used for the experiment. The separated leaf powder was washed using flowing clean water to remove colour with a filter using 100 µm stainless steel mesh. Then powder was again washed three times using 80 ^{0}C hot water and cold water to

remove tannin (brown colour) in the leaves powder solution. Sieving of PALP is in Figure 3.2.

Figure 3.2 Sieve Shaker

After the removal of colour, powdered leaves were kept in an open atmosphere for 3 hours to remove excess water. Then powdered leaves were dried using a laboratory drier operating at 110 ^{0}C for 24 hours. Drying of PALP using laboratory drier is given in Figure 3.3.

Figure 3.3 Drying PALP by laboratory drier

Finally, the dried powder was stored in a sealed container to prevent absorbing moisture (Amarasinghe & Amarasinghe, 2020).

The physical properties such as true density and bulk density were measured using the A&D Company Limited GF- 200 precision balance density measuring kit and gravimetric bottle method respectively. For true density measurement weight of empty kit (W1), weight of kit with full of water (W2), weight of known amount of PALP with kit (W3), Weight of same PALP with water and kit (W4) and were measured and memorize internally. Then true density was calculated by obtaining true volume of PALP (W2+W3-W1-W4). For bulk density measurement, known amount of PALP was taken (W5) and volume of same PALP measured (V1) using measuring cylinder. For the batch adsorption tests, a weighed amount of adsorbent was kept in a stirrer to achieve steady mixing.

3.2. Preparation of Dye Solutions (Adsorbate)

Five types of dyes were purchased from a local industrial chemical supplier named Kannan and company. A spatula was used to get enough amount of dye for weighing

and prepare dye solution. The required quantity of dye was carefully weighed using GIBERTINI CENT-2 4000 PT electronic precision balance. Weighted dye was dissolved in 1.0 L of distilled water in a volumetric flask to obtain the desired concentration. The dye solution was mixed thoroughly using a stirrer until all dye clusters disappear. The prepared dye solutions were diluted to obtain the dye concentration required for the experiments.

3.3. Analysing Using UV Visible Spectrophotometer

Sample analysis was done by SHIMADZU UV 1800 UV- Vis Spectrophotometer with a wavelength range of 190 – 1100 nm. Distilled water was kept as the reference. All the dyes are separately undergone for spectrum analysis using 0.03 g L^{-1} dye solutions. Then maximum absorbance was obtained for every dye from the maximum peak obtained. Wavelength vs. absorbance values in APPENDIX A: ABSORBANCE SPECTRUM VALUES FOR MB, CV, CR, RR, AND RBB DYE SOLUTIONS. Analysing dye sample with UV Visible spectrophotometer is given in Figure 3.4.

Figure 3.4 UV Visible Spectrophotometer

3.4. Calibration Curves

Calibration curves were obtained for all five dyes for the range which can detect using the UV-Vis spectrophotometer using a known concentration of dye solutions. Calibration curves were prepared using dye concentrations as given in APPENDIX B: CALIBRATION CURVE DATA

The spectrometer was able to interpret absorbance linearly without creating error up to 3.0 of absorbance. Therefore, higher concentrations of dye solutions could be prepared for the experiments. The higher concentrations (which can give accurate absorbance values) was selected to reduce the error occur at weighing of the dye. Therefore, solutions with absorbance above 0.9 were used as initial dye concentrations.

Calibration curves obtained for all five dyes related to absorbance vs concentration are given in the Figure 3.5.

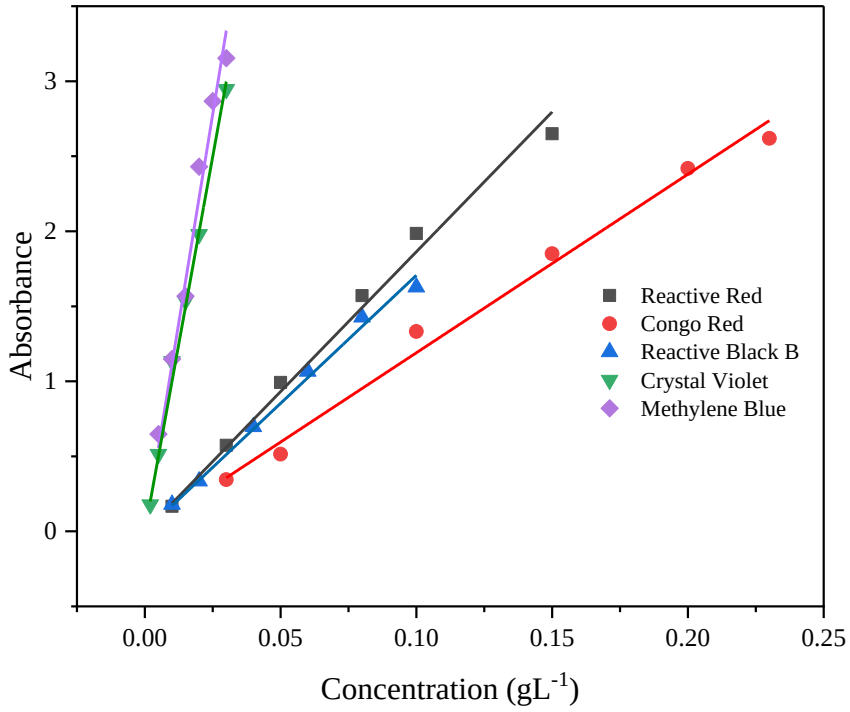

Figure 3.5 Concentration vs. absorbance linear fit of selected dyes

3.5. Batch Adsorption Experiment

Variable speed IKA® RW 20 digital mechanical stirrer was used for agitation of the solution. Batch adsorption studies were performed using a 1.0 L beaker filled with 1.0 L of the dye solution and then PALP was added when starting the timer. Batch adsorption test with agitation using the mechanical stirrer is given in the Figure 3.5.

Figure 3.6 Variable speed mechanical stirrer

Dye type, initial dye concentration, agitator speed rounds per minute (RPM), dye solution pH, dye solution temperature and PALP weight used for the experiments are given in Table 3.1.

Table 3.1 Experimental setup details

Test No	**Dye**	**Initial dye concentration gL^{-1}**	**Agitator speed RPM**	**pH**	**Temperature ^0C**	**Adsorbent weight g**
T01	MB	0.030	315	7.08	27.9	5.0
T02	MB	0.025	315	7.09	27.5	5.0
T03	MB	0.020	315	7.08	27.9	5.0
T04	MB	0.010	315	6.91	27.2	5.0
T05	CV	0.030	315	6.91	27.2	5.0

T06	CV	0.025	315	6.97	27.5	5.0
T07	CV	0.020	315	6.97	27.5	5.0
T08	CV	0.010	315	7.09	27.5	5.0
T09	RBB	0.025	315	6.87	27.3	5.0
T10	CR	0.050	315	6.85	26.8	5.0
T11	CR	0.040	315	6.85	26.8	5.0
T12	CR	0.030	315	6.96	27.6	5.0
T13	CR	0.010	315	6.96	27.6	5.0
T14	RR	0.030	315	6.87	27.3	5.0
T15	CR	0.100	315	6.93	27.5	5.0

3.6. Collecting Samples

Samples were collected to 10.00 ml glass bottles with caps. Before the samples taken, the bottles and cap were cleaned well with boiling water, distilled water respectively. Cleaned bottles were allowed to dry until remove all the remaining water. After samples were drawn into the dry glass bottles immediately closed using a plastic cap.

Samples were drawn from the initial solution and thereafter 1 minute, 2 minutes, 5 minutes, 15 minutes, 30 minutes, and 300 minutes of contact time intervals after starting each test. When the sample collecting from the batch adsorption experiment, 100 μm stainless steel mesh was used to separate the solution from the adsorbent media. All sample bottles were labelled with the sample identification to prevent possible errors. Samples were named properly for identification as in Table 3.2.

Table 3.2 Nomenclature for samples

Test No	**Sample No 01**	**Sample No 02**	**Sample No 03**	**Sample No 04**	**Sample No 05**	**Sample No 06**
	1 min	***2 min***	***5 min***	***15 min***	***30 min***	***300 min***
T1	T1-S1	T1-S2	T1-S3	T1-S4	T1-S5	T1-S6
T2	T2-S1	T2-S2	T2-S3	T2-S4	T2-S5	T2-S6
T3	T3-S1	T3-S2	T3-S3	T3-S4	T3-S5	T3-S6
T4	T4-S1	T4-S2	T4-S3	T4-S4	T4-S5	T4-S6
T5	T5-S1	T5-S2	T5-S3	T5-S4	T5-S5	T5-S6
T6	T6-S1	T6-S2	T6-S3	T6-S4	T6-S5	T6-S6
T7	T7-S1	T7-S2	T7-S3	T7-S4	T7-S5	T7-S6
T8	T8-S1	T8-S2	T8-S3	T8-S4	T8-S5	T8-S6
T9	T9-S1	T9-S2	T9-S3	T9-S4	T9-S5	T9-S6
T10	T10-S1	T10-S2	T10-S3	T10-S4	T10-S5	T10-S6
T11	T11-S1	T11-S2	T11-S3	T11-S4	T11-S5	T11-S6

T12	T12-S1	T12-S2	T12-S3	T12-S4	T12-S5	T12-S6
T13	T13-S1	T13-S2	T13-S3	T13-S4	T13-S5	T13-S6
T14	T14-S1	T14-S2	T14-S3	T14-S4	T14-S5	T14-S6
T15	T15-S1	T15-S2	T15-S3	T15-S4	T15-S5	T15-S6

The samples were analysed for the dye concentration and the absorbance values observed are given in APPENDIX C: ABSORBANCE VALUES READINGS GIVEN BY UV-VIS SPECTROPHOTOMETER FOR ALL FIVE DYES. Relevant concentration values for samples in all tests were obtained using relevant calibration curve data given in APPENDIX D: CONCENTRATION VALUES OBTAINED BY CONVERSION OF ABSORBANCE VALUE READINGS USING CALIBRATION CURVES

3.7. FTIR Spectroscopy and SEM Imaging

Fourier Transform Infrared (FTIR) spectroscopy of raw PALP and dye adsorbed dry PALP were obtained using BRUKER ALPHA FTIR scanner to observe bonds formations of PALP after adsorption of dyes. Attenuated total reflection (ATR) method was used with wave number range of 650 - 4000 cm^{-1} to generate FTIR spectroscopy. Dried PALP Samples before and after adsorption of dye were taken for the analyse. Only MB, CV, and CR dyes selected due to further experiments carried out only for them.

Scanning Electron Microscope (SEM) images of raw PALP and dye adsorbed dry PALP samples were taken to observe the surface topography using ZEISS EVO | 18 Research SEM. In SEM imaging, magnification applied was 2500 and beam voltage was 10 kV. As same as in the FTIR, dried PALP Samples before and after adsorption of dye were taken for the analyse. Only MB, CV, and CR dyes selected due to further experiments carried out only for them.

4. RESULTS AND DISCUSSION

4.1. Adsorbent Characterization

The true density and bulk density of PALP were obtained as 1176 kg m^{-3} and 128.67 kg m^{-3}. Measuring of true density and bulk density of PALP is important. Because PALP have to mix with aqueous dye solutions in experiment. If the true density of PALP is less than the density of water, PALP tent to float on water surface. Then it may not mix homogeneously with dye solution and may produce errors. However, obtained true density value is higher than the density of water. Therefore, PALP can use for the experiment. Particle size distribution of PALP was selected between 710-250 µm.

4.2. Absorbance Spectrum Analysis

Absorbance spectrums obtained from UV visible spectrophotometer for all five dyes are given in Figure 4.1.

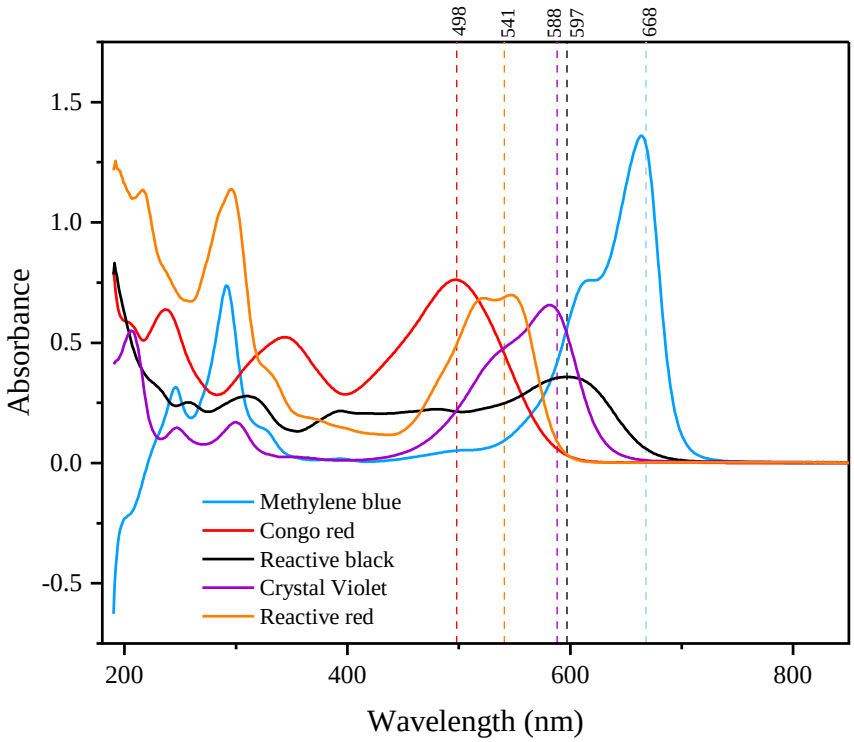

Figure 4.1 Absorbance spectra of selected dyes

The range of wavelength 190 nm to 1100 nm was analysed for all five dyes. UV radiation region is normally 200 nm to 400 nm and the visible region is between 400 nm to 800 nm. Absorbance is a value calculated as Equation 7.

$$A = \log \frac{I}{I_0} \tag{7}$$

A is absorbance and the I is the intensity of the reference beam and I_0 is the intensity of the sample beam. The wavelength that belongs to the strongest absorbance peak of the absorbance spectrum is denoted as maximum absorbance or λ_{max}. It is a characteristic value for a substance. Obtained maximum absorbance values are given in Table 4.1.

Table 4.1 Maximum absorbance values of selected dyes

Name of the Dye	**The wavelength of maximum absorbance λ_{max} (nm)**
Methylene blue	668
Cristal violet	588
Congo red	498
Reactive red	541
Reactive black	597

Obtained Maximum absorbance value for each dye used to analyse all samples.

4.3. Calibration Curves

Calibration curves were obtained from the data in APPENDICES B: CALIBRATION DATA and plotted into a linear fit in Figure 3.5. The equation details of straight lines obtained are in Table 4.2. Where R^2 is the coefficient of determination. Values of slope, intercept, and coefficient of determination for calibration curves obtained in Figure 3.5 are tabulated in the Table 4.2.

Table 4.2 Calibration curves data of selected dyes

Coefficient	**Reactive Red**	**Congo Red**	**Reactive Black B**	**Crystal Violet**	**Methylene Blue**
slope	18.635	11.901	17.066	99.925	111.248
intercept	0	0	0	0	0
R^2	0.9968	0.9974	0.9981	0.9986	0.9963

4.4. Selecting of Best Adsorbing Dye for Further Studies

Percentage removed at equilibrium was calculated for all five dyes. The highest removal percentage at equilibrium obtained for MB, CV, and CR were 94.9 %, 89.56 %, and 80.95 % respectively. RR and RBB dyes were shown minimum removal at equilibrium. The removal for RR and RBB were 10.57 % and 3.43 % respectively. The percentage removal of dyes at equilibrium is given in Table 4.3 and the bar chart for percentage removed in each dye at equilibrium given in Figure 4.2.

Table 4.3 Percentage removed of dyes at the equilibrium

	MB T1	**CV T5**	**CR T12**	**RR T14**	**RB B T9**
Percentage removal %	94.99	89.56	80.95	10.57	3.43

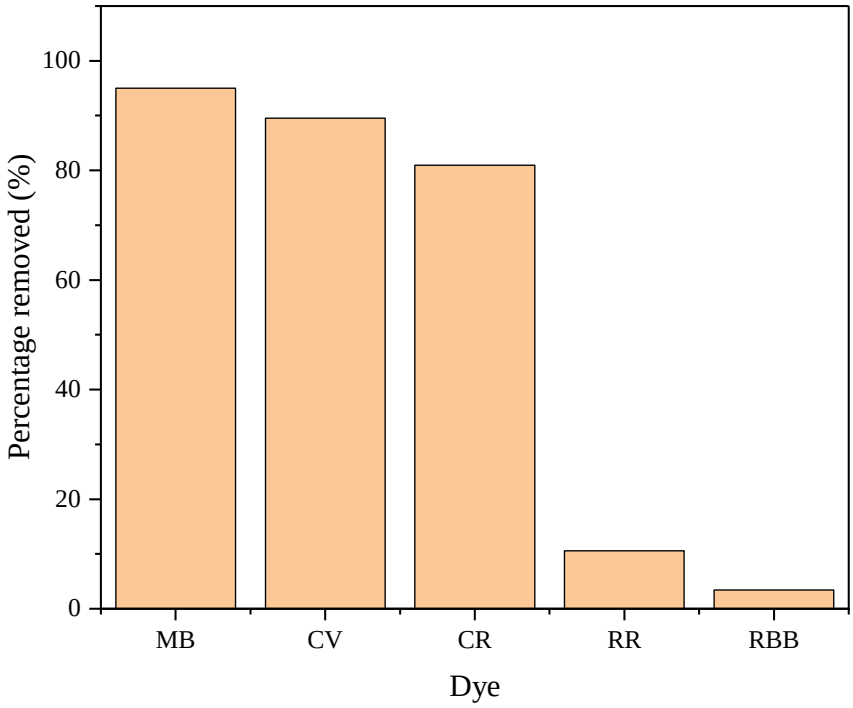

Figure 4.2 Percentage removed of dyes at the equilibrium after 300 min with 5.0 g of PALP for an initial dye concentration of MB, CV, CR and RR 0.03 g L^{-1} and RBB 0.025 g L^{-1}

According to Figure 4.2, the RR and RB B have the least percentage removal. The pH value range for this experiment is conducted around 7.00. In industrial scenario, reactive dyes are applied to the fibre with using alkaline solution. Which means the pH value is more than 7.00 required for effective dying process. Therefore, pH

around 7.00 may not be favourable for adsorption of reactive dyes onto PALP. That can also reason for less removal of both reactive dyes According to data in Table 4.4, with an increase in molecular weight, molecular lengths also increase significantly. The presence of large molecular dimensions in adsorbate molecules can block access to the active pore sites present in the adsorbent material (Al-Degs, et al., 2008). The adsorption of CR onto PALP shows anionic nature with slow adsorption. So molecular anionic nature also can be a reason for cause low adsorption in both reactive dyes. Data related to molecular weight, molecular dimension, and nature of the molecule for all five dyes are given in the Table 4.4.

Table 4.4 Comparison of dye molecule size, weight, and nature

Dye	**Molecular weight ($gmol^{-1}$)**	**Molecular length (nm)**	**Molecular width (nm)**	**Nature**
MB	319.85	1.447 (ref a)	0.95 (ref a)	Cationic
CV	407.99	1.4 (ref b)	1.4 (ref b)	Cationic
CR	696.66	2.29 (ref c)	0.8 (ref c)	Anionic
RR	968.21	No data found		Anionic
RBB	991.82			Anionic

ref a: (Jia, et al., 2018)
ref b: (Wathukarage A. , et al., 2017)
ref c: (Liang, et al., 2016)

Molecular structures of dyes Reactive red and Reactive black b are given in the Figure 4.3.

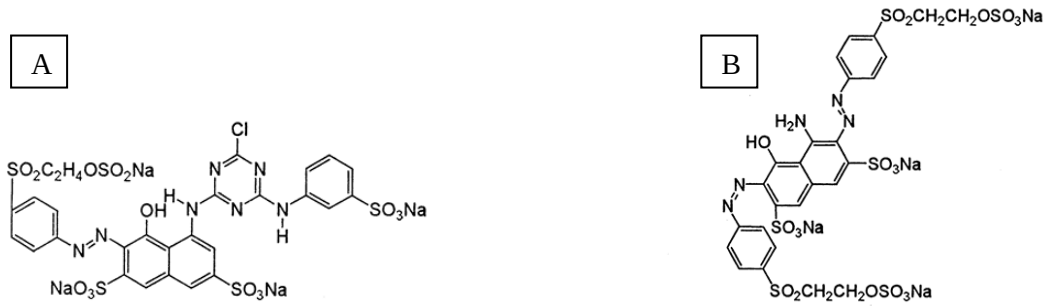

Figure 4.3 (A) - Reactive Red, (B) - Reactive black B

Presence of hydrogen bonds or benzene rings in dye molecules, there is a possibility to create dye aggregates in the solution. Dye aggregation can depend on the dye concentration and the pH of the solution. Molecular aggregates have a larger particle size than the molecular alone and it can affect to reduce the adsorption mass transport (Liang, et al., 2016). In Figure 4.3 (A) RR and (B) RBB there are many

hydrogens bond sites and benzene rings are available. Therefore, dye aggregation is possible.

C_t/C_0 vs contact time curve plotted for the comparison between each dye's fraction of remaining with the time consumed. Figure 4.4 shows the C_t/C_0 vs. time (min) plot for all five types of dyes for Test no T1, T5, T9, T12, and T14.

Table 4.5 shows C_t/C_0 values for Test no T1, T5, T9, T12 and T14.

Table 4.5 Fraction of remaining dye in the solution as a function of time

Contact Time (min)	**C_t/C_0**				
	MB T1	***CV T5***	***RB B T9***	***CR T12***	***RR T14***
0	1.000	1.000	1.000	1.000	1.000
1	0.671	0.682	0.994	0.997	0.985
2	0.515	0.568	0.991	0.958	0.965
5	0.298	0.374	0.966	0.832	0.945
15	0.151	0.165	0.973	0.588	0.951
300	0.083	0.133	0.963	0.403	0.972

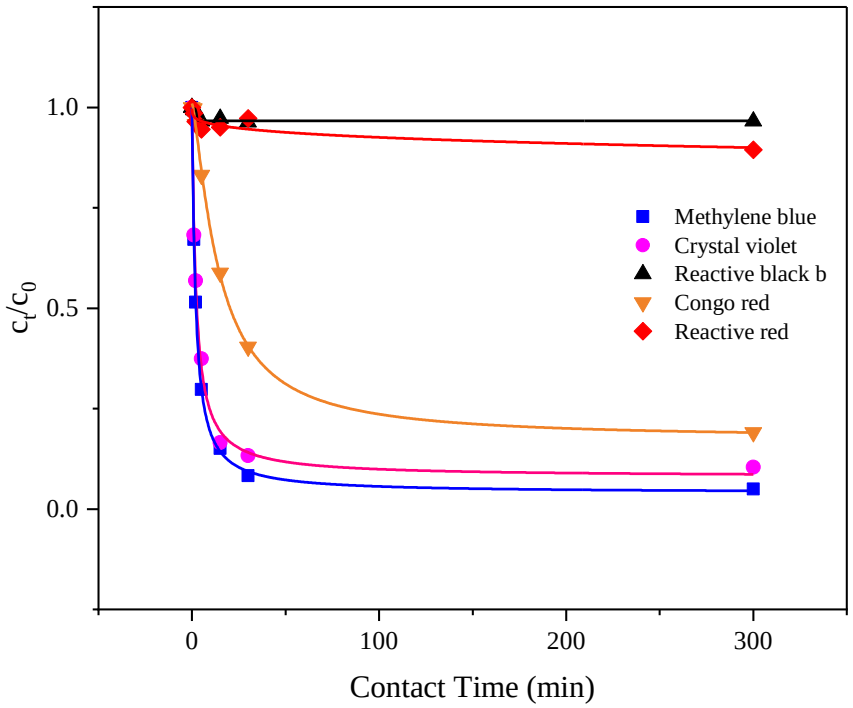

Figure 4.4 Fraction of remaining dye in the solution as a function of time at 5.0 g PALP dose, 315 RPM agitator speed, 7.0 pH, 27 ^{0}C with initial concentrations for MB, CV, CR, RR, and RBB 0.03, 0.03, 0.03, 0.03, and 0.025 g L^{-1}respectively

According to Figure 4.4, RBB and RR show high fraction of remaining at the end of the 300 minutes. Due to the negligible adsorption of RBB, and RR; MB, CV, and CR

dyes were selected to carry out further experiments. In Figure 4.4 CR shows a slow removal than the MB and CV in the initial 30 minutes. That may be due to the presence of larger molecular dimensions in CR compared to MB and CV as given in Table 4.4.

4.5. Effect of Dye Concentration for Adsorption onto PALP

Percentage removal (%) vs contact time (min) obtained for MB, CV, and CR dyes are given in the Figure 4.5, Figure 4.6, and Figure 4.7 respectively. Figure 4.5, Figure 4.6, and Figure 4.7 clearly show at the beginning of the adsorption there is a rapid removal and within a few minutes,' the removal rate gets reduced till obtaining the equilibrium. That is due to the presence of a high number of active sites at the beginning for adsorption. Within a few minutes, dye molecules start to attach to those sites and attached molecules act as a layer of repulsive forces by forming a barrier to adsorbing of remaining dye molecules in the solution (Ahmad, et al., 2009).

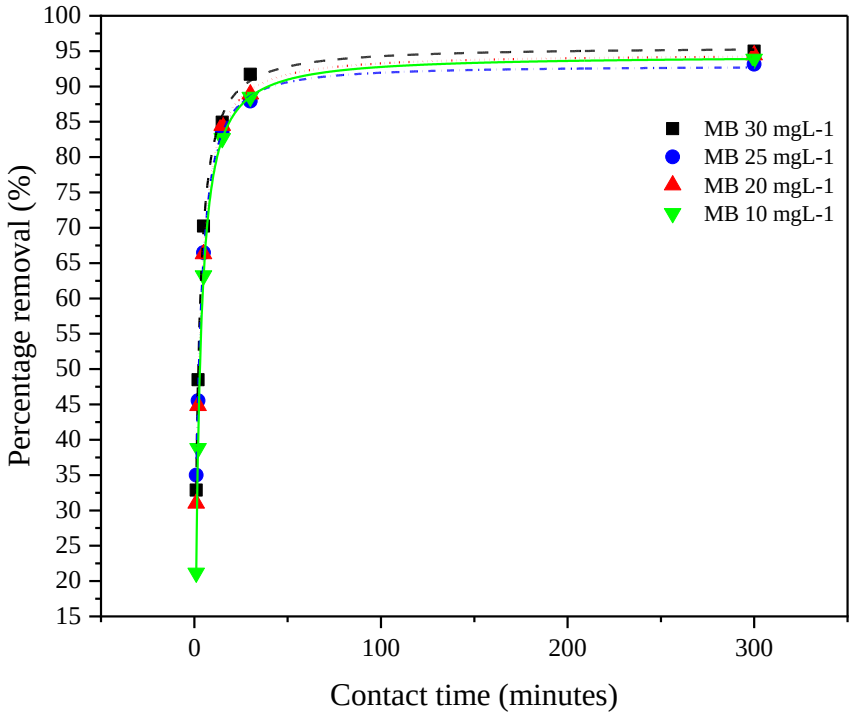

Figure 4.5 Percentage removal of MB for different initial concentrations at 5.0 g PALP dose, 315 RPM agitator speed, 7.0 pH and 27 ^{0}C

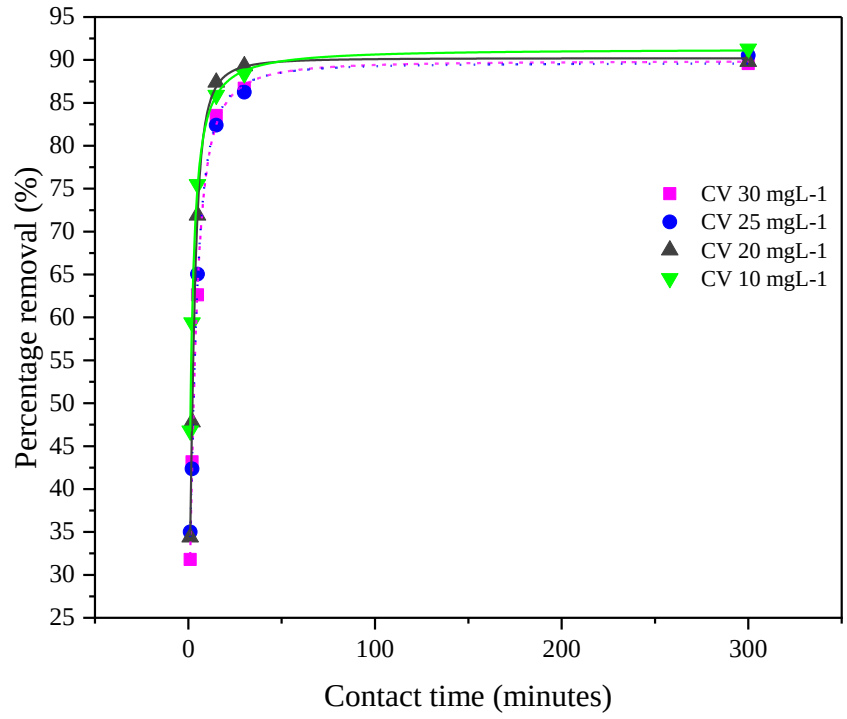

Figure 4.6 Percentage removal of CV for different initial concentrations at 5.0 g PALP dose, 315 RPM agitator speed, 7.0 pH and 27 ^{0}C

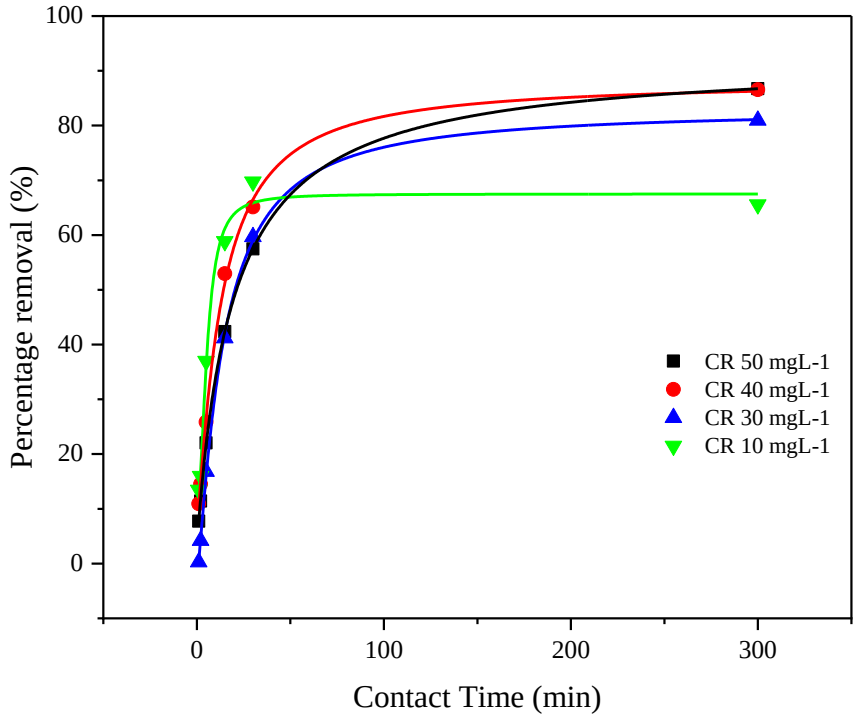

Figure 4.7 Percentage removal of CR for different initial concentrations at 5.0 g PALP dose, 315 RPM agitator speed, 7.0 pH and 27 ^{0}C

According to Figure 4.7, 10 mg L^{-1} data series have lower percentage removal than others.

4.6. Dye Adsorption Per Unit Weight of Adsorbent

Dye adsorbed per gram of PALP vs contact time (min) for MB, CV, and CR dyes are given in Figure 4.8, Figure 4.9, and Figure 4.10. These figures are generated by q_t vs t values obtained from Equation 1. All values are related to 27 ^{0}C, 7.0 pH, 315 RPM agitation speed and 5.0 g of adsorbent dose. The objective was to observe each dye mass removal with the change of initial concentration.

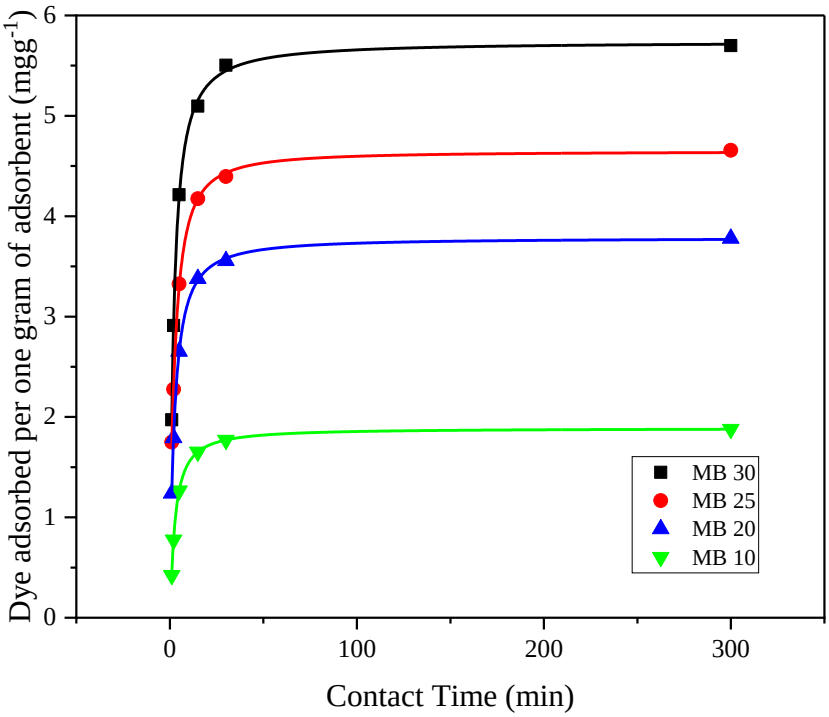

Figure 4.8 Different initial concentrations of MB adsorbed per 1.0 g of PALP, 315 RPM agitator speed, 7.0 pH and 27 ^{0}C

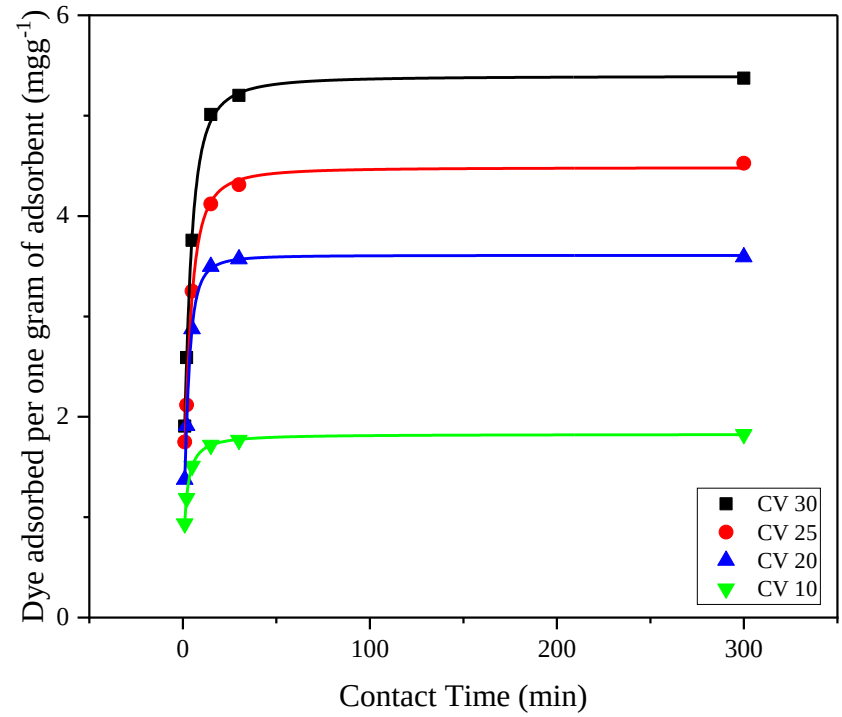

Figure 4.9 Different initial concentrations of CV adsorbed per 1.0 g of PALP, 315 RPM agitator speed, 7.0 pH and 27 ^{0}C

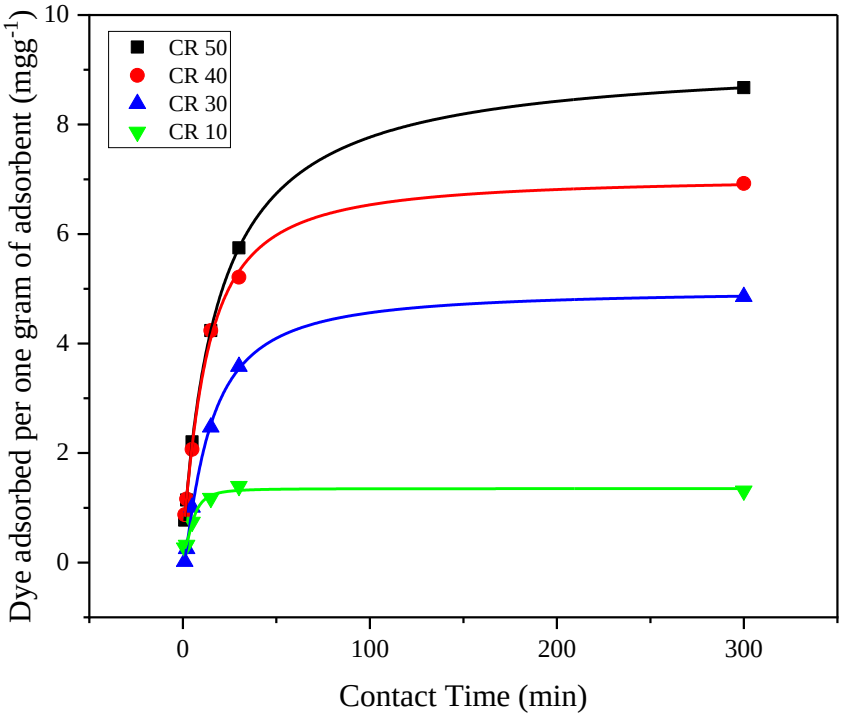

Figure 4.10 Different initial concentrations of CR adsorbed per 1.0 g of PALP, 315 RPM agitator speed, 7.0 pH and 27 ^{0}C

According to Figure 4.8, Figure 4.9, and Figure 4.10 it can be observed that the amount of dye adsorbed for one gram of adsorbent increases when the initial dye

concentration increases. That is because the number of dye molecules around the active sites of the adsorbent gets higher when the initial concentration increase. Therefore, the mass transfer rate to the adsorbent gets high for higher initial concentrations due to forming a considerable driving force for mass transfer between aqueous and solid phases (Ahmad, et al., 2009).

4.7. Adsorption Isotherm Model Studies

Obtained q_e and c_e values for MB, CV, and CR dyes each test with different initial concentration, are tabulated in Table 4.6.

Table 4.6 q_e and c_e of MB, CV, and CR for different initial dye concentrations

Dye	**Initial Concentration (mg L^{-1})**	**q_e (mg g^{-1})**	**c_e (mg L^{-1})**
MB	30	5.700	1.500
	25	4.660	1.700
	20	3.778	1.110
	10	1.878	0.611
CV	30	5.374	3.130
	25	4.526	2.370
	20	3.592	2.040
	10	1.826	0.870
CR	50	8.672	6.638
	40	6.924	5.377
	100	16.521	17.393

4.7.1. Langmuir adsorption isotherm model fit

Langmuir adsorption isotherm model fit obtained for MB, CV, and CR with plotting 1/ q_e (mg g^{-1}) vs 1/ c_e (mg L^{-1}) is given in the Figure 4.11.

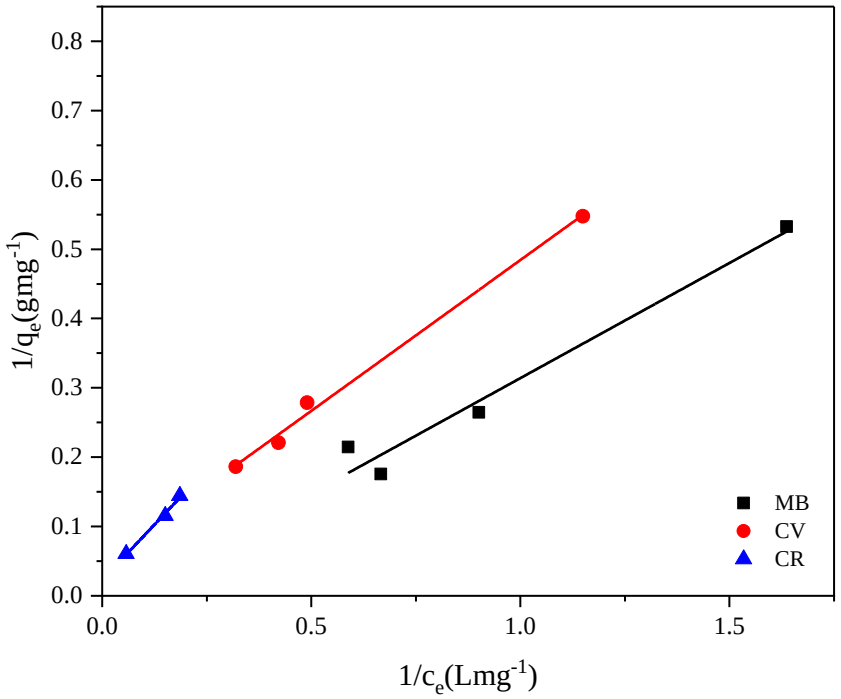

Figure 4.11 Langmuir isotherm model fit

4.7.2. Freundlich adsorption isotherm model fit

Freundlich adsorption isotherm model fit is given in the Figure 4.12.

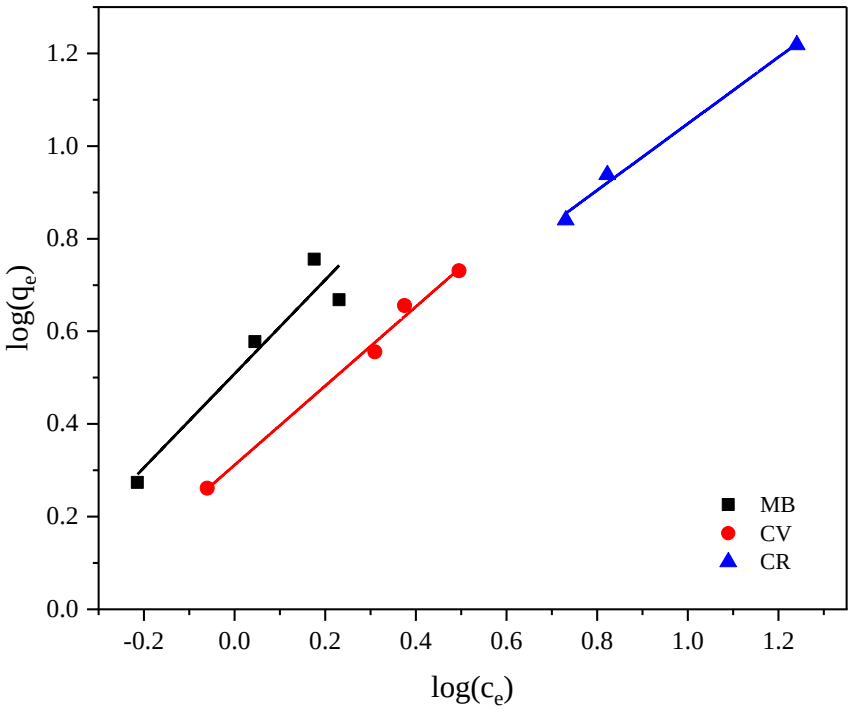

Figure 4.12 Freundlich isotherm model fit

4.7.3. Temkin adsorption isotherm model fit

Temkin adsorption isotherm model fit obtained for MB, CV, and CR with plotting ln (c_e) vs q_e is given in the Figure 4.13.

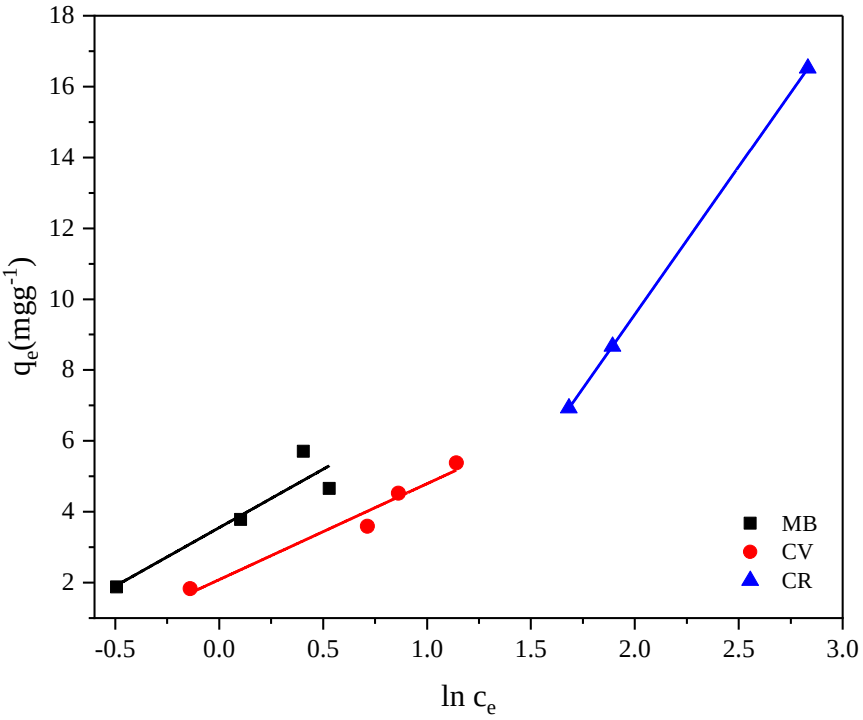

Figure 4.13 Temkin isotherm model fit

4.7.4. Isotherm model fit data comparison

Obtained parameters by analysing Langmuir isotherm model, Freundlich isotherm model and Temkin isotherm model fits generated for MB, CV, and CR dyes are tabulated in the Table 4.7.

Table 4.7 Comparison for Langmuir, Freundlich, and Temkin isotherms fitting

Dye	Langmuir isotherm			Freundlich isotherm			Temkin isotherm		
	q_m (mg g^{-1})	K_a (L mg^{-1})	R^2	K_f	1/n	R^2	A_T	B_T	R^2
MB	38.46	0.08	0.9681	3.22	1.013	0.9165	2.936	3.297	0.8621
CV	20.33	0.11	0.9950	2.046	0.854	0.9918	2.158	2.708	0.9648
CR	44.05	0.035	0.9937	2.133	0.718	0.9931	0.426	8.340	1.0000

According to the results shown in Table 4.7 MB, and CV, dyes were adsorbed onto PALP according to the Langmuir isotherm. The maximum monolayer adsorption capacity of PALP for adsorption of MB and CV were respectively 38.46 and 20.33 mg g^{-1}. CR was adsorbed according to Temkin isotherm.

4.8. Adsorption Kinetics Studies

Adsorption kinetic data were analysed by fitting results to Pseudo-first order, Pseudo-second order and intra-particle diffusion kinetic models and their results are explained in the preceding sections.

4.8.1. Pseudo-first order kinetic model fit

Pseudo-first order kinetic model fit for MB, CV, and CR dyes are given in Figure 4.14, Figure 4.15, and Figure 4.16 respectively.

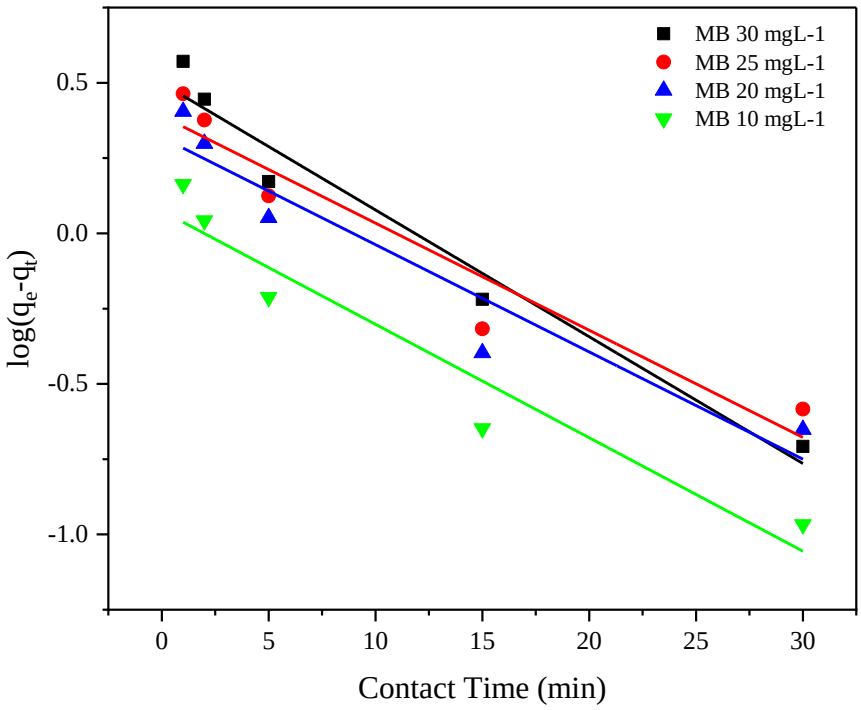

Figure 4.14 Pseudo-first order model fit for MB

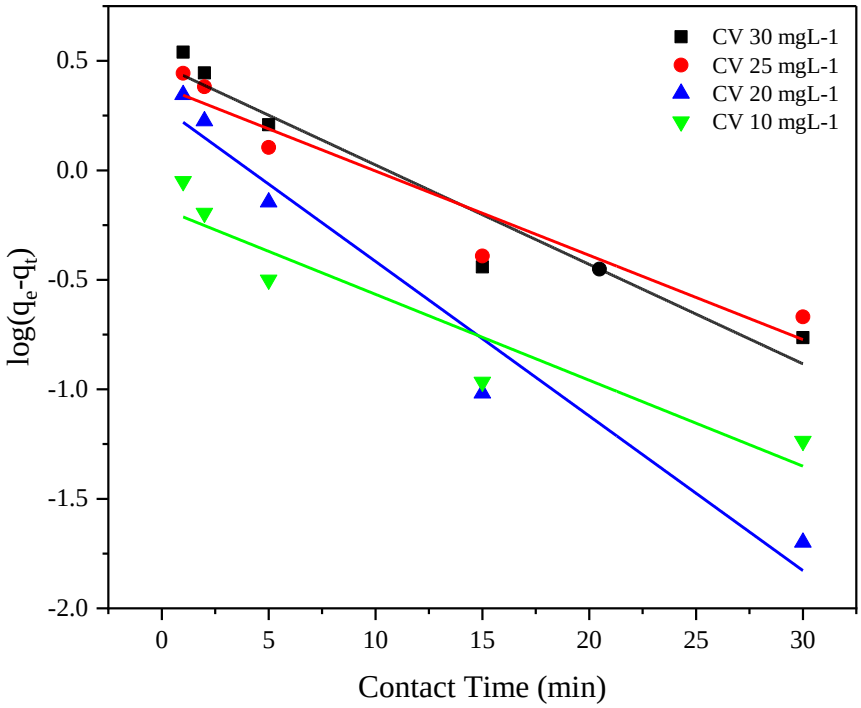

Figure 4.15 Pseudo-first order model fit for CV

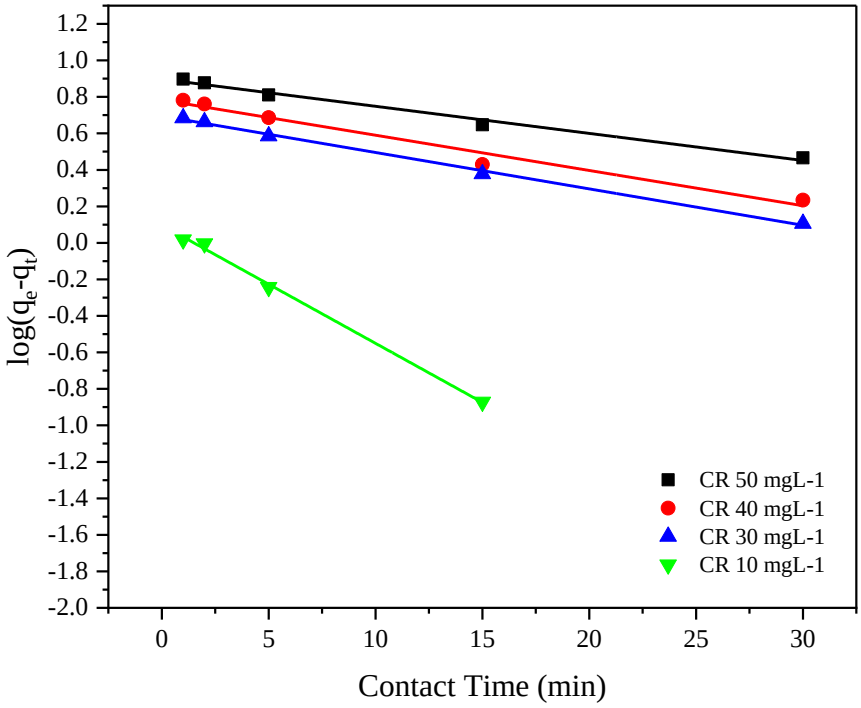

Figure 4.16 Pseudo-first order model fit for CR

4.8.2. Pseudo-second order kinetic model fit

Pseudo-second order kinetic model fit for MB, CV, and CR dyes are given in Figure 4.17, Figure 4.18, and Figure 4.19 respectively.

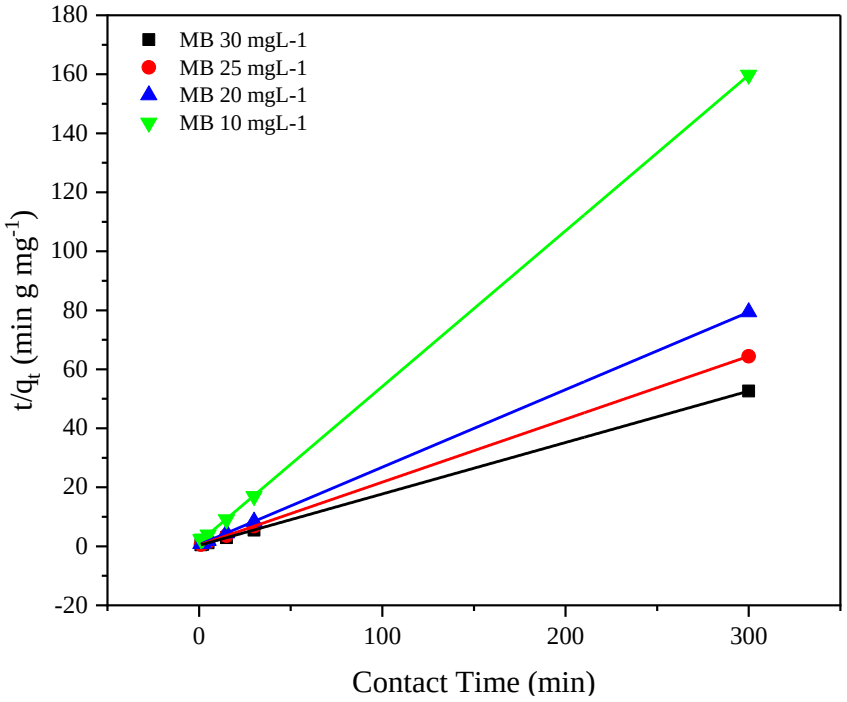

Figure 4.17 Pseudo-second order model fit for MB

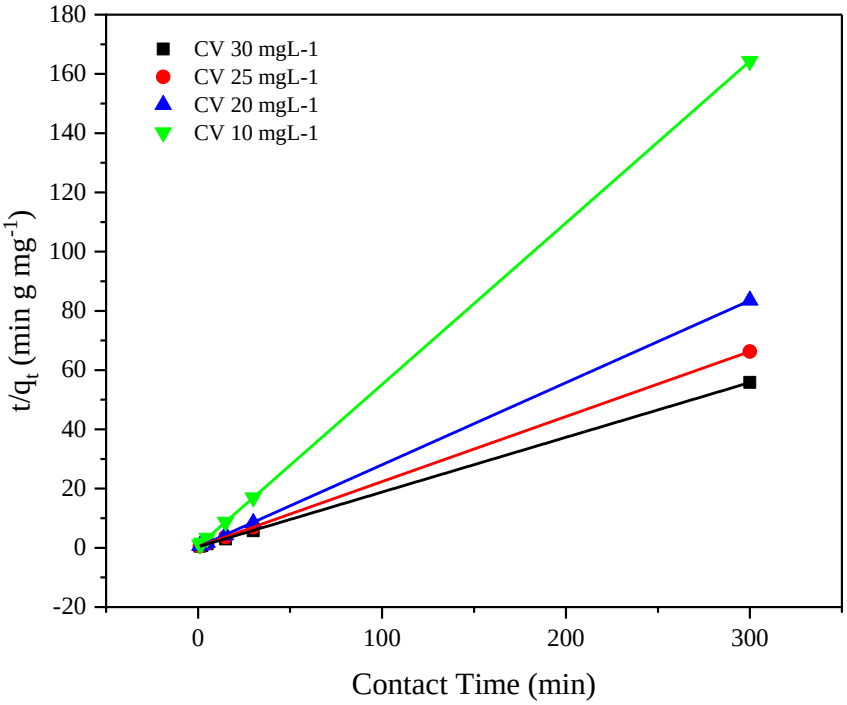

Figure 4.18 Pseudo-second order model fit for CV

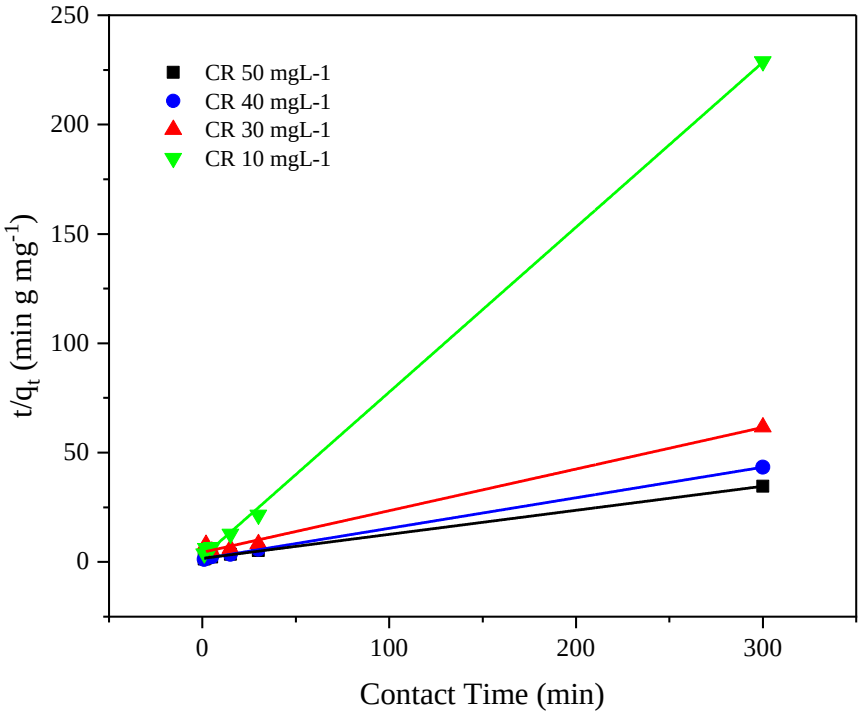

Figure 4.19 Pseudo-second order model fit for CR

4.8.3. Kinetic parameter comparison

Obtained parameters by analysing pseudo-first order and pseudo-second order kinetic model plots generated for MB, CV, and CR dyes are tabulated in the Table 4.8.

Table 4.8 Kinetic parameters for PSO and PFO obtained by adsorption of MB, CV, and CR

Dye	**Initial Concentration (mgL^{-1})**	**PFO**			**PSO**		
		q_e (mgg^{-1})	$K1$ (min^{-1})	R^2	q_e (mgg^{-1})	$K2$ $(gmg^{-1}min^{-1})$	R^2
MB	30	3.148	-0.097	0.9649	5.734	0.099	1.0000
	25	2.449	-0.081	0.9240	4.711	0.109	1.0000
	20	2.080	-0.081	0.9175	3.805	0.125	1.0000
	10	1.186	-0.085	0.9333	1.895	0.199	0.9999
CV	30	3.006	-0.104	0.9331	5.406	0.107	0.9999
	25	2.399	-0.088	0.9242	4.554	0.120	1.0000
	20	1.950	-0.161	0.9651	3.606	0.251	0.9999
	10	0.671	-0.090	0.9000	1.835	0.524	1.0000
CR	50	7.889	-0.034	0.9892	9.174	0.007	0.9995
	40	6.070	-0.044	0.9754	7.194	0.013	0.9997
	30	4.952	-0.046	0.9971	5.263	0.008	0.9940
	10	1.251	-0.149	0.9974	1.326	0.250	0.9995

According to the comparison in Table 4.8, it can conclude by observing R^2 values for MB, CV and CR dyes adsorb onto PALP as a pseudo-second order model. Therefore, q_e can calculate by pseudo-second order model fit equation. Values for q_e experimental and calculated to MB, CV, and CR dyes are tabulated in Table 4.9.

Table 4.9 q_e experimental vs calculated

Dye	**Initial Concentration (mg L^{-1})**	**q_e experimental (mg g^{-1})**	**q_e calculated (mg g^{-1})**
MB	30	5.70	5.73
	25	4.66	4.71
	20	3.78	3.81
	10	1.88	1.90
CV	30	5.37	5.41
	25	4.53	4.55
	20	3.59	3.61
	10	1.83	1.83
CR	50	8.67	9.17
	40	6.92	7.19
	30	4.86	6.85
	10	1.31	1.33

The results in Table 4.9, show the accuracy of the data set due to experimental and calculated values for q_e lie in closer. Further, it confirms the conclusion of the pseudo-second order model as the adsorption kinetic model is correct. Therefore, adsorption achieved an equilibrium state within the considered time duration.

4.8.4. Intra-particle diffusion study

Intra-particle diffusion study for MB, CV and CR dyes adsorption onto PALP was done using Morris and Weber diagram. The Morris and Weber model fit for MB, CV, and CR dyes are given in Figure 4.20, Figure 4.21, and Figure 4.22 respectively.

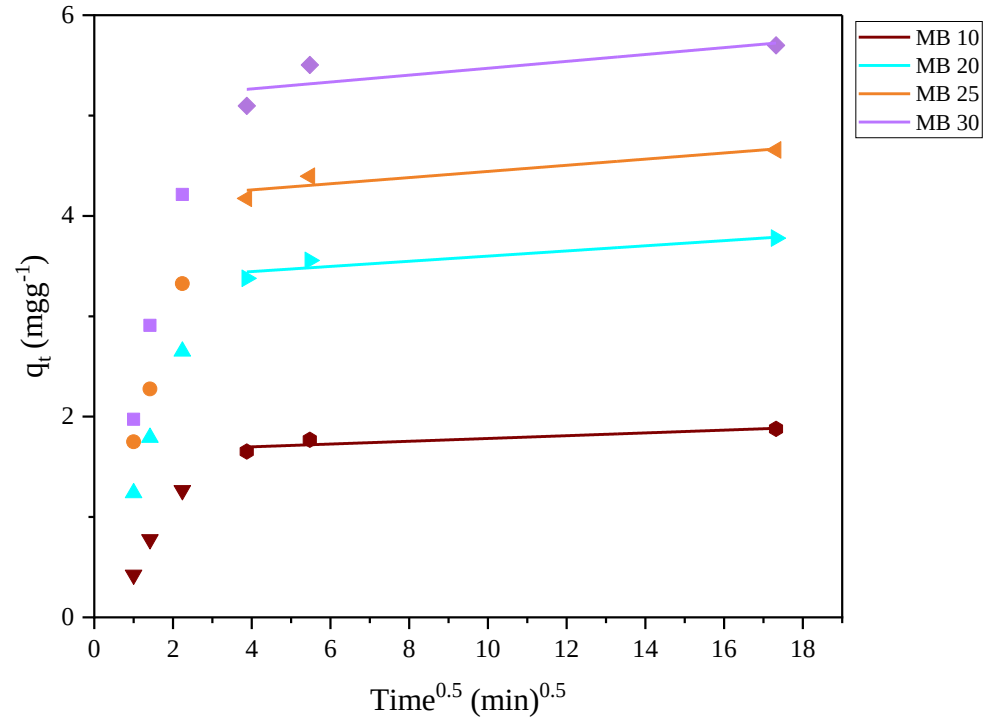

Figure 4.20 Morris and weber diagram for intra-particle diffusion of MB

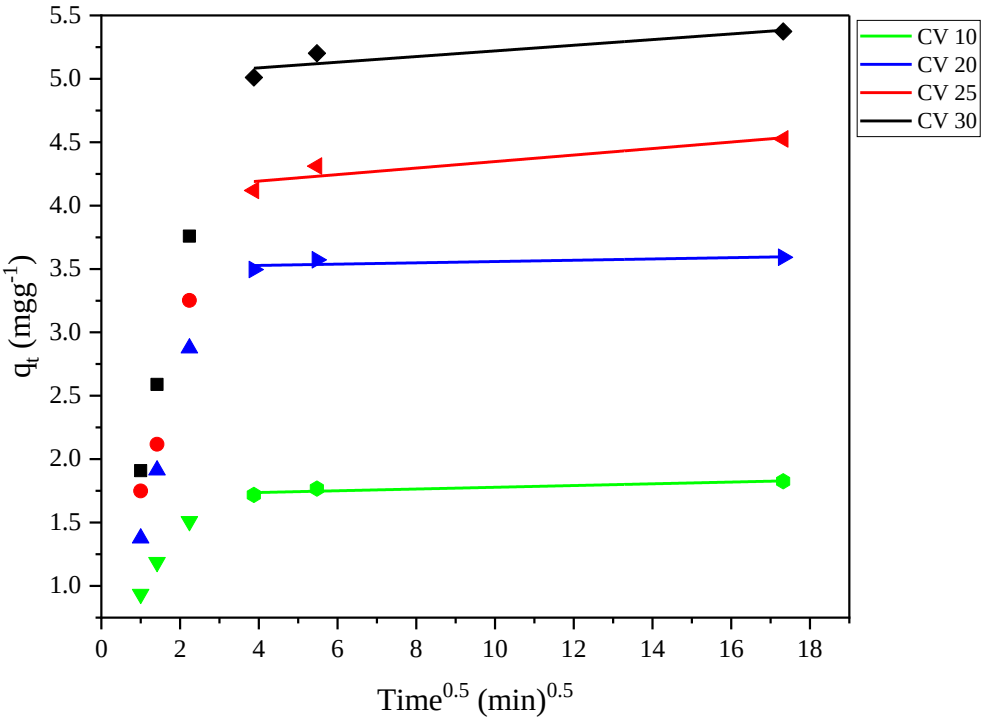

Figure 4.21 Morris and weber diagram for intra-particle diffusion of CV

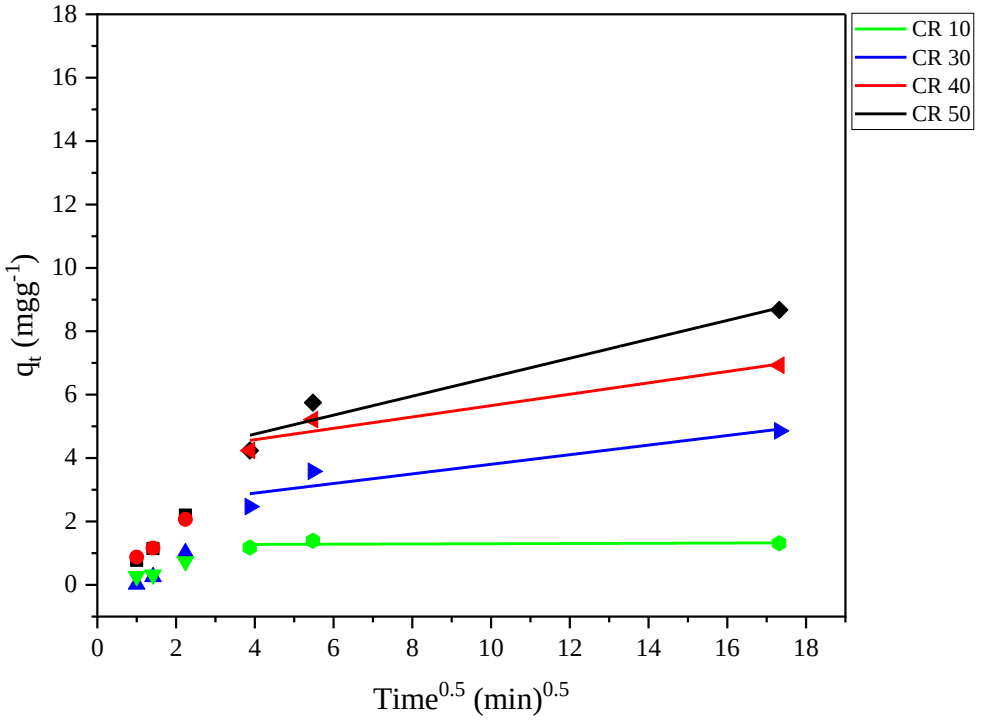

Figure 4.22 Morris and weber diagram for intra-particle diffusion of CR

Figures 4.20, 4.21 and 4.22 contain more than one straight line in each data set and indicate the adsorption is not limited to intra-particle diffusion. If the straight lines go through the origin, it can conclude that only the intra-particle diffusion is present as a rate-limiting step (Dahr, et al., 2014). Due to the first part of the diagram being related to external mass transfer by surface adsorption and the second part related to intra-particle diffusion (Belhachemi, et al., 2009). Only the second part was fitted. According to Figure 4.20, Figure 4.21, and Figure 4.22 intra-particle diffusion have initiated after 16 minutes of adsorption start. Obtained parameters by analysing Morris and Webber model plots generated for MB, CV, and CR dyes are tabulated in the Table 4.10.

Table 4.10 Morris and weber model fit parameters of Intra-particle diffusion

Dye	**Initial concentration mgL^{-1}**	**δ (mgg^{-1})**	**k_d (mgg^{-1}min$^{-0.5}$)**	***R*^{2}**
MB	30	1.643	0.013	0.6678
	25	3.342	0.025	0.8713
	20	4.136	0.030	0.8827
	10	5.128	0.034	0.8206
CV	30	1.709	0.006	0.8163
	25	3.507	0.005	0.8604
	20	4.090	0.025	0.5463
	10	4.997	0.022	0.8682
CR	50	3.562	0.298	0.9469

	40	3.863	0.179	0.9355
	30	2.290	0.151	0.8668
	10	1.262	0.003	0.0573

The mass transfer has two resistance components. One component is resistance to mass transfer by solute to solid interface and the other component is resistance to mass transfer by the solid interface to pore sites. According to the results in Table 4.10 boundary layer effect decrease when the initial dye concentration increases. Intra-particle diffusion rate constant decreases when the initial dye concentration increases. This reveals when the initial dye concentration increase, solute solid interface mass transfer increases due to resistance decrease (Dahr, et al., 2014). Here value of R^2 highly deviated from 1.0000 in some experiments. That may be due to coordinates related to 16 minutes create error. If that point shifted to right further through x- axis that error will disappear. Which means need to take a sample about 25 min of adsorption to obtain more accurate straight line for intra-particle diffusion studies.

4.9. FTIR Spectroscopy of PALP

FTIR spectroscopy can be obtained by two methods. Those methods are the KBr method and ATR method. The KBr method, can obtain good resolution than the ATR method but is time-consuming (Bunaciu, et al., 2013). In FTIR infra-red (IR) radiation beam emit toward the sample specimen and then the reflected IR beam is detected which contains the information of functional groups and bonds in the sample. That information is related to bond vibrations caused by the absorption of IR radiation (Aguilar, 2013). There are four regions according to the wavenumber range. Fingerprint region with a range of 450-1500 cm^{-1}, double bonds with a range of 1500-2000 cm^{-1}, triple bonds with a range of 2000-2500 cm^{-1} and single bonds with a range from 2500-4000 cm^{-1} (Nandiyanto, et al., 2019). In the Figure 4.23, Figure 4.24, and Figure 4.25 can see the FTIR spectrum received for MB adsorbed PALP, CV adsorbed PALP, and CR adsorbed PALP which were plotted with FTIR spectrum received for raw PALP to observe the changes occurred after dye adsorption.

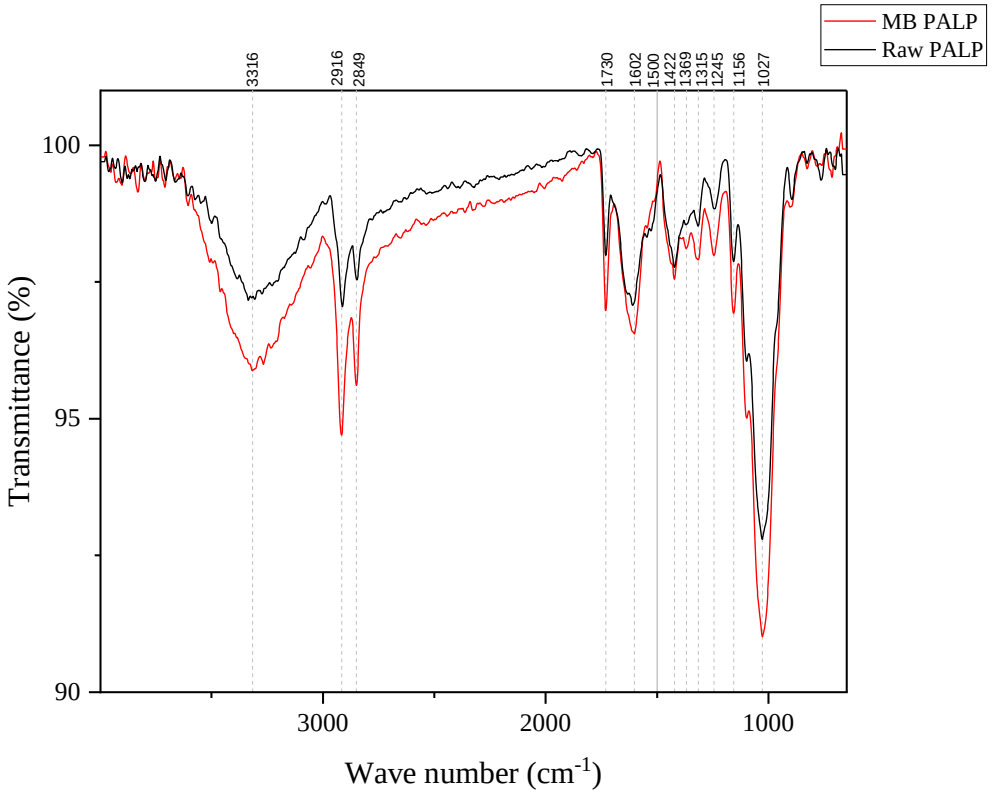

Figure 4.23 FTIR spectrum of PALP before and after adsorption of MB

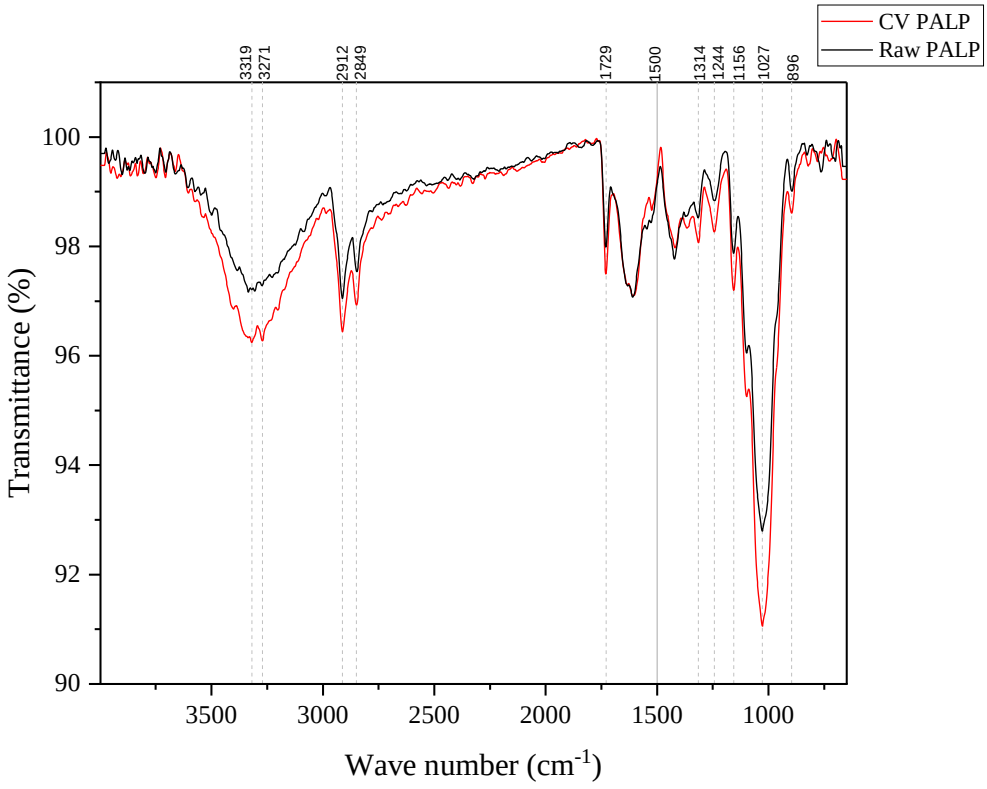

Figure 4.24 FTIR spectrum of PALP before and after adsorption of CV

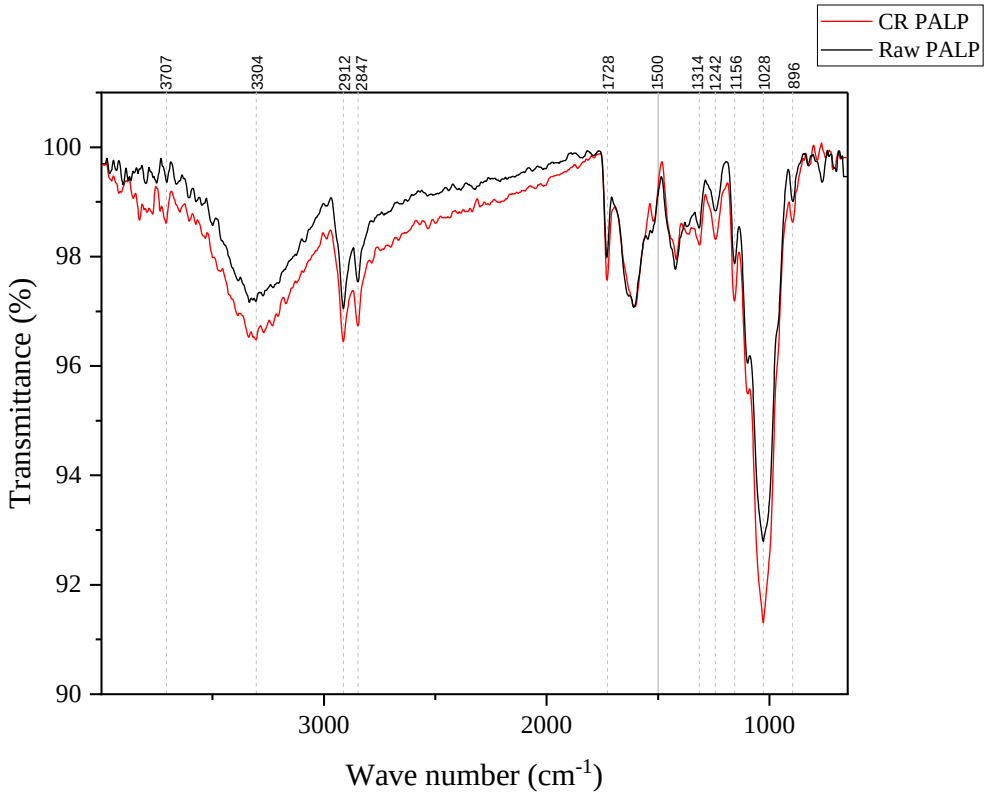

Figure 4.25 FTIR spectrum of PALP before and after adsorption of CR

According to FTIR spectrum obtained for raw PALP, it is much analogous to FTIR received to cellulose (Abderrahim, et al., 2015). Which is due to 40% of portion of plant leave contain cellulose fibers. According to obtained FTIR spectrum for PALP adsorbed by MB, CR, and CV it can see the intensity increased for all remarked peaks. This indicates an increase in the number of functional groups linked to the corresponding bond. The detail of corresponding bonds and groups related to changed peeks of FTIR spectrums by adsorption of MB, CV, and CR dyes on to PALP are tabulated in the Table 4.11.

Table 4.11 Functional groups related to increasing intensity after adsorbing of MB, CV and CR obtained by FTIR spectroscopy

MB		**CV**		**CR**	
Wavenumber cm^{-1}	***Group***	***Wavenumber cm^{-1}***	***Group***	***Wavenumber cm^{-1}***	***Group***
3316	O-H stretching	3319	O-H stretching	3707	O-H stretching
2916	C-H stretching	3271	O-H stretching	3304	N-H stretching
2849	C-H stretching	2912	C-H stretching	2912	C-H stretching

1730	C=O stretching	2849	C-H stretching	2847	C-H stretching
1602	C=C stretching	1729	C=O stretching	1728	C=O stretching
1422	O-H bending	1314	C-N stretching	1314	C-N stretching
1369	O-H bending	1244	C-O stretching	1242	C-O stretching
1315	C-N stretching	1156	C-N stretching	1156	C-N stretching
1245	C-O stretching	1027	S=O stretching	1028	S=O stretching
1156	C-N stretching	896	C=C bending	896	C=C bending
1027	S=O stretching				

(IR Spectrum Table & Chart, 2022)

According to the Table 4.11, increase of intensity of tabulated groups and bonds can be due to dispersion of relevant groups by adsorbing dye molecules after adsorption to PALP surface.

According to the Figure 4.23, Figure 4.24, and Figure 4.25 it can see newly formed peaks after adsorption of MB, CV, and CR onto PALP at 3271, and 1369 cm^{-1}. Those peaks related to O-H stretching and O-H bending respectively. Therefore, it is a sufficient evidence to prove that the adsorption was happened by hydrogen bond formation within dye and PALP surface. This information further confirms surface adsorption happened as chemisorption.

4.10. SEM Analysis

4.10.1. Images of raw PALP

Topological observation of raw PALP leave surface using SEM images are given in Figure 4.26. Figure 4.26 is a view of epidermal cells of PALP. Circle B indicated there is a papillose cell and circle A shows stomata. According to the Figure 4.26, papillose cells show significant amount of extrusion from the plane of surface of PALP.

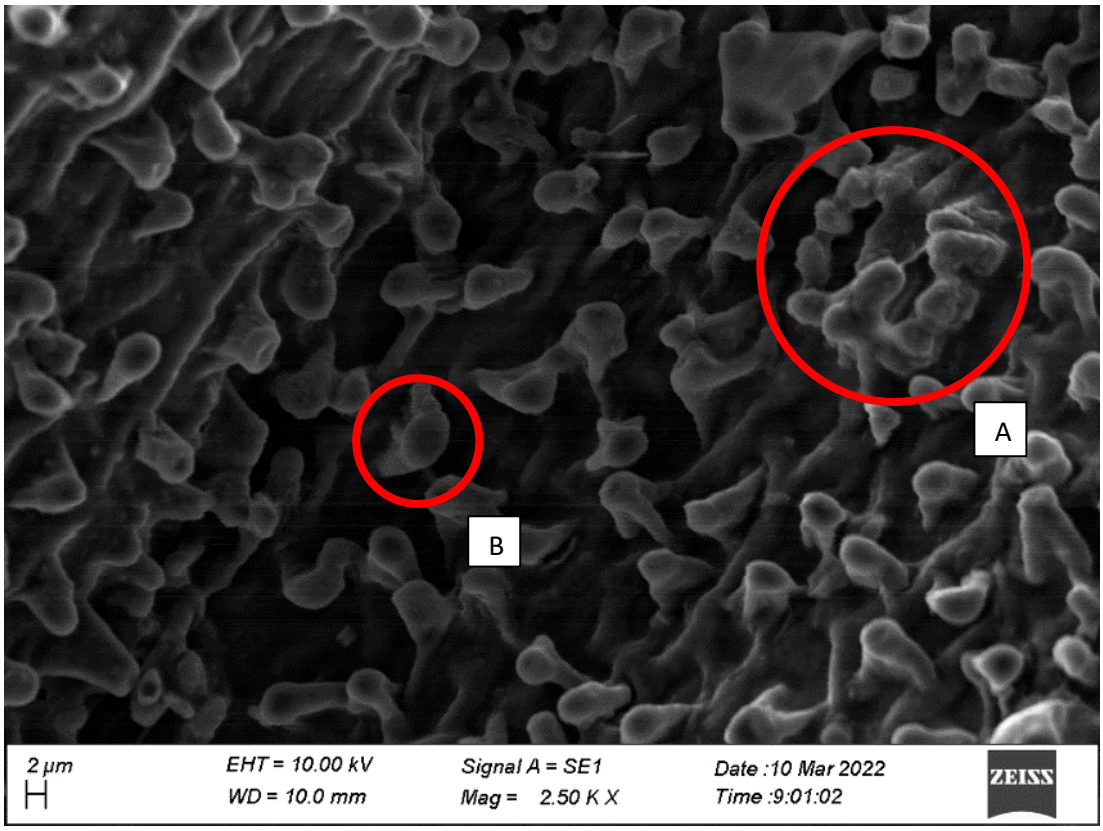

Figure 4.26 SEM image of raw PALP with 2500 magnification

Surface cell structure and internal cell structure of PALP are given in Figure 4.28.

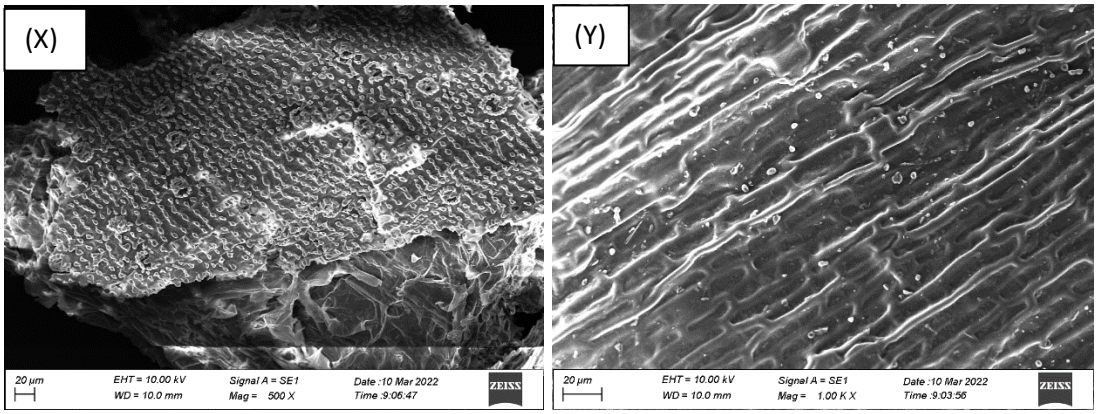

Figure 4.27 X: SEM image of raw PALP with 500 magnification, Y: SEM image of raw PALP with 1000 magnification

Figure 4.27 Image X can see the epidermal cell layer with papillose cells, stomata, and a sectional view with internal cell walls. In Figure 4.27 image Y can see the internal cell structure of long cells (Almeida, et al., 2013).

4.10.2. Images of PALP after adsorption of dye

Comparison with raw PALP and MB, CV, CR dyes adsorbed PALP leave surface changes using SEM images are given in the Figure 4.28.

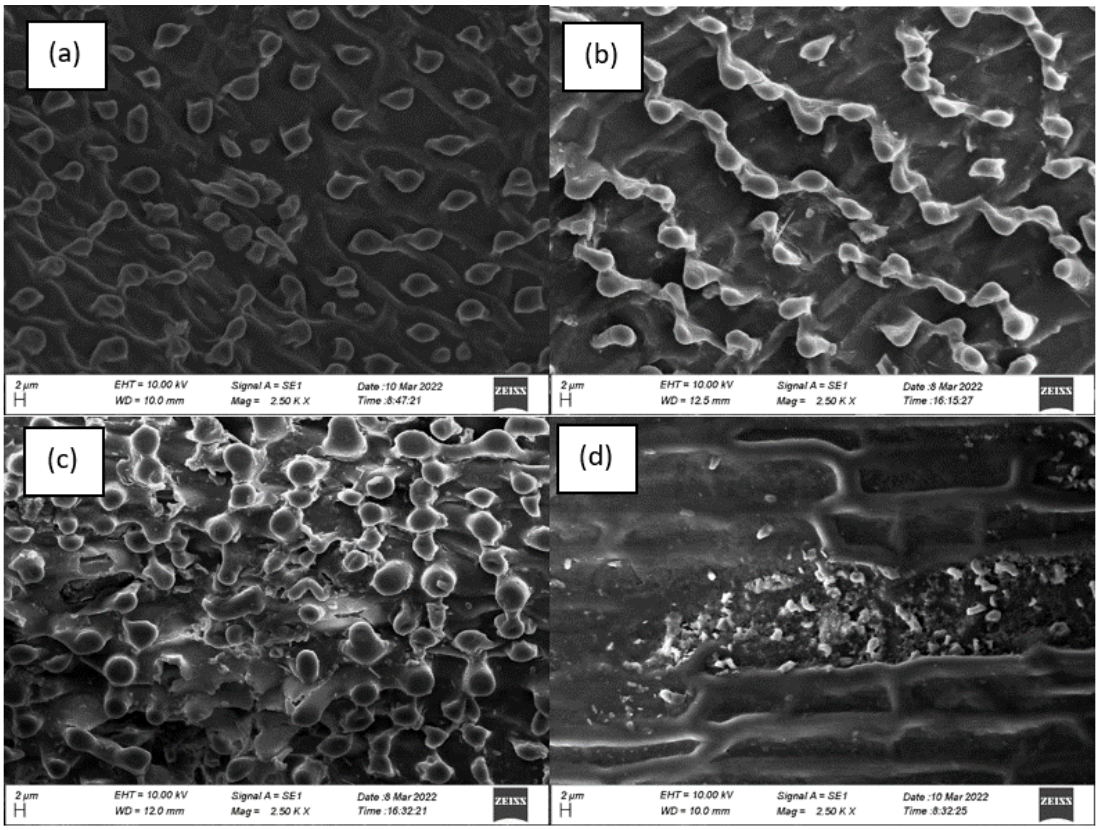

Figure 4.28 a: SEM image of raw PALP with 2500 magnification, b: SEM image of MB adsorbed PALP with 2500 magnification, c: SEM image of CV adsorbed PALP with 2500 magnification, d: SEM image of CR adsorbed PALP with 2500 magnification

In Figure 4.28 pictures b, c, and d it can see the volume of the papillose cell get increases. It is indicated that adsorption of dye molecules on papillose cells. Papillose cells are extruded from the leave surface. Therefore, those cells contact with water more than the surface of the PALP. The water film over the papillose cells creates surface area for mass transfer which is higher than other areas of leave surface. So, the micropores located on papillose cells can continue the adsorption process. In image d can see the cross-sectional view of PALP which adsorbed CR.

According to image d the adsorption vs happened onto cell walls other than the cellulose fibre structure.

5. CONCLUSIONS AND RECOMMENDATIONS

In this research, experiment analysis was carried out to check the adsorption of reactive, anionic, and cationic dyes to PALP in natural atmospheric conditions and neutral pH levels. The experimental study shows that the reactive red and reactive black B dyes in aqueous solutions with a temperature around 27 ^{0}C and pH around 07.00 cannot remove using PALP as an adsorbent. PALP adsorbent able to remove MB, CV, and CR dyes in aqueous solutions at the temperature around 27 ^{0}C and pH around 07.00. The removal percentages are respectively 95%, 90% and 81%. According to the experiment, at the beginning of adsorption all three dyes MB, CV, and CR show rapid adsorption and with time increases adsorption reduced until achieves the equilibrium state. Adsorption kinetics was followed by MB, CV and CR dyes with PALP are pseudo-second order kinetic model. Rate limiting factors for adsorption of MB, CV, and CR dyes with PALP consist of both intra-particle diffusion and surface adsorption. MB, and CV are adsorbed onto PALP according to the Langmuir isotherm model and have a maximum monolayer adsorption capacity of 38.46 mg g^{-1}, and 20.33 mg g^{-1} respectively. CR adsorbed onto PALP according to Temkin isotherm model.

Although there are many low-cost biosorbents available for the removal of MB and CV, PALP is also recommended as a low-cost biosorbent candidate and can be used as new alternative material. Therefore, mass-scale cultivation can be encouraged for economic purposes.

It can recommend checking the performance of column adsorption trials using PALP as an adsorbent to remove aqueous MB and CV due to the very fast removal shown in the batch experiments within 30 minutes.

It can recommend checking the ability to use PALP as an adsorbent for the removal of other available polar compounds with 1.5 nm molecular length and molecular mass around 400 g mol^{-1}.

REFERENCES

Abderrahim, B., Abderrahman, E., Mohamed, A., Fatima, T., Abdesselam, T., & Krim, O. (2015). Kinetic Thermal Degradation of Cellulose, Polybutylene Succinate and a Green Composite: Comparative Study. *World Journal of Environmental Engineering*, 95-110. doi:10.12691/wjee-3-4-1

Abuzerr, S., Darwish, M., & Mahvi, A. H. (2018, April). Simultaneous removal of cationic methylene blue and anionic reactive red 198 dyes using magnetic activated carbon nanoparticles: equilibrium, and kinetics analysis. (W. Rauch, Ed.) *Water Science Techonology, 2017*(2), 534–545. doi:10.2166/wst.2018.145

Aguilar, Z. P. (2013). Nanomaterials for Medical Applications. In *Types of Nanomaterials and Corresponding Methods of Synthesis* (pp. 33-82). doi:10.1016/B978-0-12-385089-8.00002-9

Ahmad, A., Rafatullah, M., Sulaiman, O., Ibrahim, M. H., & Hashim, R. (2009, October). Scavenging behaviour of meranti sawdust in the removal of methylene blue from aqueous solution. (Z. (. He, Ed.) *Journal of Hazardous Materials, 170*(1), 357-365. doi:10.1016/j.jhazmat.2009.04.087

Al-Degs, Y., El-Barghouthi, M., El-Sheikh, A., & Walker, G. (2008). Effect of solution pH, ionic strength, and temperature on adsorption behavior of reactive dyes on activated carbon. *Dyes and Pigments*, 16-23. doi:10.1016/j.dyepig.2007.03.001

Almeida, S. L., Schmidt, É. C., Pereira, D. T., Kreusch, M., Felix, M. R., Osorio, L. K., Bouzon, Z. L. (2013, May). Effect of ultraviolet-B radiation in laboratory on morphological and ultrastructural characteristics and physiological parameters of selected cultivar of Oryza sativa L. doi:10.1007/s00709-013-0512-0

Alshamsi, F. A., Albadwawi, A. S., Alnuaimi, M. M., Rauf, M. A., & Ashraf, S. S. (2007). Comparative efficiencies of the degradation of Crystal Violet using

UV/hydrogen peroxide and Fenton's reagent. (B. M. Heron, & M. Wainwright, Eds.) *Dyes and Pigments, 74*(2), 283-287. doi:10.1016/j.dyepig.2006.02.016

Amarasinghe, B., & Amarasinghe, A. (2020, October). Study on Mass Transfer, Kinetic Parameters and Rate Determining Step with Statistical Analysis in Adsorption of Pb ions onto Coir Pith. *International Journal of Scientific Research and Innovative Technology, 7*(9). Retrieved from https://ijsrit.com/uploaded_all_files/2494925667_f4.pdf

Amarasinghe, P., & Amarasinghe, K. (2020). Determination of Mass Transfer Coefficients for Adsorption of Pb and Cd Onto Coir Pith and Statistical Analysis. *Fortune journals, 2*(3), 139. doi:DOI: 10.26502/jatri.017

Amin, M. T., Alazba, A. A., & Shafiq, M. (2015, November). Adsorptive Removal of Reactive Black 5 from Wastewater Using Bentonite Clay: Isotherms, Kinetics and Thermodynamics. (M. A. Rosen, Ed.) *Sustainability, 7*(11), 15302-15318. doi:10.3390/su71115302

Ayed, L., Cheriaa, J., Laadhari, N., Cheref, A., & Bakhrouf, A. (2009). Biodegradation of crystal violet by an isolatedBacillus sp. (F. Cappitelli, Ed.) *Annals of Microbiology, 59*(2), 267-272. doi:10.1007/BF03178327

Baghapour, A. M., Mahvi, A. H., & Pourfadakari, S. (2013). Thermodynamic analysis of reactive red 198 removal from synthetic wastewater by using multiwall carbon nanotubes. (R. Mirzaei, Ed.) *Health Scope, 2*(3), 149-155. Retrieved from https://www.sid.ir/en/Journal/ViewPaper.aspx?ID=437199

Bahmani, P., Kalantary, R. R., Esrafili, A., Gholami, M., & Jafari, A. J. (2013, June). Evaluation of Fenton oxidation process coupled with biological treatment for the removal of reactive black 5 from aqueous solution. (S. Nasseri, Ed.) *Journal of Environmental Health Science and Engineering, 11*(1). doi:10.1186/2052-336X-11-13

Banat, F., Al-Asheh, S., Al-Anbar, S., & Al-Refaie , S. (2006, June). Microwave- and acid-treated bentonite as adsorbents of methylene blue from a simulated

dye wastewater. (L. Wong, & A. Basu, Eds.) *Bulletin of Engineering Geology and the Environment, 66*(1), 53-58. doi:10.1007/s10064-006-0054-1

Baneshi, M., Naraghi, B., Rahdar, S., Biglari, H., Saeidi, M., Ahamadabadi, M., Alipour, V. (2016). Removal of remazol black B dye from aqueous solution by electrocoagulation equipped with iron and aluminium electrodes. (V. Azevedo, Ed.) *The IIOAB Journal, 7*, 529-535. Retrieved from https://www.iioab.org/articles/IIOABJ_7.S2_529-535.pdf

Bazzo, A., Adebayo, M. A., Dias, S. L., Lima, E. C., Vaghetti, J. C., & de Oliveira, E. R. (2015, January). Avocado seed powder: characterization and its application for crystal violet dye removal from aqueous solutions. *Desalination and Water Treatment, 57*(34), 15873-15888. doi:10.1080/19443994.2015.1074621

Belhachemi, M., Belala, Z., Lahcene, D., & Addoun, F. (2009). Adsorption of phenol and dye from aqueous solution using chemically modified date pits activated carbons. *Desalination and Water Treatment*, 182-190. doi:10.5004/dwt.2009.729

Berradi, M., Hsissou, R., Khudhair, M., Assouag, M., Cherkaoui, O., Bachiri, A. E., & Harfi, A. E. (2019, November 05). Textile finishing dyes and their impact on aquatic environs. *Heliyon, 05*(11). doi:10.1016/j.heliyon.2019.e02711

Bhattacharyya, K. G., & Sharma, A. (2005, April). Kinetics and thermodynamics of Methylene Blue adsorption on Neem (Azadirachta indica) leaf powder. (B. M. Heron, & M. Wainwright, Eds.) *Dyes and Pigments, 65*(1), 51-59. doi:10.1016/j.dyepig.2004.06.016

Bhaumik, M., McCrindle, R. I., Maity, A., Agarwal, S., & Gupta, V. K. (2016, March). Polyaniline nanofibers as highly effective re-usable adsorbent for removal of reactive black 5 from aqueous solutions. (M. Malmsten, Ed.) *Journal of Colloid and Interface Science, 466*, 442-451. doi:10.1016/j.jcis.2015.12.056

Bouraie, M. E., & Din, W. S. (2016, September). Biodegradation of Reactive Black 5 by Aeromonas hydrophila strain isolated from dye-contaminated textile wastewater. *Sustainable Environment Research, 26*(5), 209-216. doi:10.1016/j.serj.2016.04.014

Bouras, H. D., Yeddou, A. R., Bouras, N., Hellel, D., Holtz, M. D., Sabaou, N., Nadjemi, B. (2017, November). Biosorption of Congo red dye by Aspergillus carbonarius M333 and Penicillium glabrum Pg1: Kinetics, equilibrium and thermodynamic studies. (H.-K. Tsao, Ed.) *Journal of the Taiwan Institute of Chemical Engineers, 80*, 915-923. doi:10.1016/j.jtice.2017.08.002

Brito, S. M., Andrade, H. M., Soares, L. F., & Azevedo, R. P. (2010, February). Brazil nut shells as a new biosorbent to remove methylene blue and indigo carmine from aqueous solutions. (D. Aga, A. J. Daugulis, & Z. (. He, Eds.) *Journal of Hazardous Materials, 174*(1-3), 84-92. doi:10.1016/j.jhazmat.2009.09.020

Bunaciu, A. A., Fleschin, Ş., & Aboul-Enein, H. Y. (2013). Evaluation of the Protein Secondary Structures Using Fourier Transform Infrared Spectroscopy. *Gazi University Journal of Science, 27*(1), 637-644. Retrieved from https://www.researchgate.net/publication/286655543_Evaluation_of_the_protein_secondary_structures_using_fourier_transform_infrared_spectroscopy

Cardoso, N. F., Lima, E. C., Calvete, T., Pinto, I. S., Amavisca, C. V., Fernandes, T. H., Alencar, W. S. (2011, March). Application of Aqai Stalks As Biosorbents for the Removal of the Dyes Reactive Black 5 and Reactive Orange 16 from Aqueous Solution. (J. Siepmann, Ed.) *Journal of Chemical & Engineering Data, 56*(5), 1857–1868. doi:10.1021/je100866c

Carneiro, P. A., Umbuzeiro, G. A., Oliveira, D. P., & Zanoni, M. V. (2010, February). Assessment of water contamination caused by a mutagenic textile. (D. Aga, A. J. Daugulis, G. Lyberatos, & Z. He, Eds.) *Journal of Hazardous Materials, 174*(1-3), 694-699. doi:10.1016/j.jhazmat.2009.09.106

Çelebi, H. (2019, January). The applicability of evaluable wastes for the adsorption of Reactive Black 5. (M. Abbaspour, Ed.) *International Journal of Environmental Science and Technology, 16*(1), 135-146. doi:10.1007/s13762-018-1969-3

Chakraborty, S., Basu, J. K., De, S., & DasGupta, S. (2006, May). Adsorption of Reactive Dyes from a Textile Effluent Using Sawdust as the Adsorbent. (P. E. Savage, Ed.) *Industrial & Engineering Chemistry Research, 45*(13), 4732–4741. doi:10.1021/ie050302f

Chakraborty, S., Mukherjee, A., Das, S., Maddela, N. R., Iram, S., & Das, P. (2021, February). Study on isotherm, kinetics, and thermodynamics of adsorption of crystal violet dye by calcium oxide modified fly ash. (C. Kwang-Ho, Ed.) *Environmental Engineering Research, 26*(1). doi:10.4491/eer.2019.372

Chan, S.-L., Tan, Y., Abdullah, A., & Ong, S.-T. (2016, April). Equilibrium, kinetic and thermodynamic studies of a new potential biosorbent for the removal of Basic Blue 3 and Congo Red dyes: Pineapple (Ananas comosus) plant stem. (H.-K. Tsao, Ed.) *Journal of the Taiwan Institute of Chemical Engineers, 61*, 306-3015. doi:10.1016/j.jtice.2016.01.010

Chaukura, N., Murimba, E. C., & Gwenzi, W. (2017, November). Sorptive removal of methylene blue from simulated wastewater using biochars derived from pulp and paper sludge. (R. Naidu, D. L. Nghiem, & M. Rood, Eds.) *Environmental Technology & Innovation, 8*, 132-140. doi:10.1016/j.eti.2017.06.004

Chawla, S., Uppal, H., Yadav, M., Bahadur, N., & Singh, N. (2017, January). Zinc peroxide nanomaterial as an adsorbent for removal of Congo red dye from waste water. (R. Handy, & B. Yan, Eds.) *Ecotoxicology and Environmental Safety, 135*, 68-74. doi:10.1016/j.ecoenv.2016.09.017

Cheng, S., Zhang, L., Ma, A., Xia, H., Peng, J., Li, C., & Shu, J. (2018, March). Comparison of activated carbon and iron/cerium modified activated carbon to

remove methylene blue from wastewater. (J. Hao, & X. C. Le, Eds.) *Journal of Environmental Sciences, 65*, 92-102. doi:10.1016/j.jes.2016.12.027

Cheruiyot, G. K., Wanyonyi, W. C., Kiplimo, J. J., & Maina, E. N. (2019, September). Adsorption of toxic crystal violet dye using coffee husks: Equilibrium, kinetics and thermodynamics study. (B. Gyampoh, Ed.) *Scientific African, 5*. doi:10.1016/j.sciaf.2019.e00116

Chong, M., Cho, Y., Poh, P., & Jin, B. (2015, February). Evaluation of Titanium dioxide photocatalytic technology for the treatment of reactive Black 5 dye in synthetic and real greywater effluents. (J. J. Klemeš, C. M. de Almeida, & Y. Wang, Eds.) *Journal of Cleaner Production, 89*, 196-202. doi:10.1016/j.jclepro.2014.11.014

Croce, R., Cina, F., Lombardo, A., Crispeyn, G., Cappelli, C. I., Vian, M., Baderna, D. (2017, October). Aquatic toxicity of several textile dye formulations: Acute and chronic assays with Daphnia magna and Raphidocelis subcapitata. (R. Handy, & B. Yan, Eds.) *Ecotoxicology and Environmental Safety, 144*, 79-87. doi:10.1016/j.ecoenv.2017.05.046

Dahr, M. F., Abolghasemi, H., Esmaili, M., Shojamoradi, A., & Fatoorehchi, H. (2014, September). Adsorption Characteristics of Congo Red from Aqueous Solution onto Tea Waste. (A. Gill, Ed.) *Chemical Engineering Communications, 202*(2), 181-193. doi:10.1080/00986445.2013.836633

Dbik, A., Bentahar, S., Khomri, M. E., Messaoudi, N. E., & Lacherai, A. (2020). Adsorption of Congo red dye from aqueous solutions using tunics of the corm of the saffron. *Materials Today : Proceedings, 22*, 134-139. doi:10.1016/j.matpr.2019.08.148

Dehghani, M., Shahsavani, S., Jamshidi, F., & Shamsedini, N. (2019). Comparison of the Efficiency of Fenton and Photo–Fenton Processes for the Removal of Reactive Red 198 Dye from the Aqueous Solution. *Iranian Journal of Health, Safety & Environment, 6*(4), 1336-1342. Retrieved from https://www.ijhse.ir/index.php/IJHSE/article/view/419

Deive, F. J., Domínguez, A., Barrio, T., Moscoso, F., Morán, P., Longo, M. A., & Sanromán, M. A. (2010, October). Decolorization of dye Reactive Black 5 by newly isolated thermophilic microorganisms from geothermal sites in Galicia (Spain). (D. Aga, A. J. Daugulis, & Z. He, Eds.) *Journal of Hazardous Materials, 182*(1-3), 735-742. doi:10.1016/j.jhazmat.2010.06.096

Elkady, M. F., Ibrahim, A. M., & AbdEl-Latif, M. M. (2011, September). Assessment of the adsorption kinetics, equilibrium and thermodynamic for the potential removal of reactive red dye using eggshell biocomposite beads. (N. Hilal, Ed.) *Desalination, 278*(1-3), 412-423. doi:10.1016/j.desal.2011.05.063

Elsherif, K. M., El-Dali, A., Alkarewi, A. A., Ewlad-Ahmed, A. M., & Treban, A. (2021). Adsorption of Crystal Violet Dye Onto Olive Leaves Powder: Equilibrium and Kinetic Studies. *Chemistry International , 7*(2), 79-89. doi:10.5281/zenodo.4441851

Eren, Z., & Acar, F. N. (2006, June). Adsorption of Reactive Black 5 from an aqueous solution: equilibrium and kinetic studies. (N. Hilal, Ed.) *Desalination, 194*(1-3), 1-10. doi:10.1016/j.desal.2005.10.022

Eslami, H., Shariatifar, A., Rafiee, E., Shiranian, M., Salehi, F., Hosseini, S. S., Ebrahimi, A. A. (2019, February). Decolorization and biodegradation of reactive Red 198 Azo dye by a new Enterococcus faecalis–Klebsiella variicola bacterial consortium isolated from textile wastewater sludge. (P. J. Large, Ed.) *World Journal of Microbiology and Biotechnology, 35*. doi:10.1007/s11274-019-2608-y

Esmaeili, A., & Kalantari, M. (2015, February). Bioremoval of an azo textile dye, Reactive Red 198, by Rhizopus oryzae. *Desalination and Water Treatment, 57*(14), 6401-6410. doi:10.1080/19443994.2015.1010237

Fabryanty, R., Valencia, C., Soetaredjo, F. E., Putro, J. N., Santoso, S. P., Kurniawan, A., Ismadji, S. (2017, December). Removal of crystal violet dye by adsorption using bentonite – alginate composite. (G. L. Dotto, D. Fatta-

Kassinos, & Y. Lee, Eds.) *Journal of Environmental Chemical Engineering, 5*(6), 5677-5687. doi:10.1016/j.jece.2017.10.057

Gedam, V. V., Raut, P., Chahande, A., & Pathak , P. (2019, March). Kinetic, thermodynamics and equilibrium studies on the removal of Congo red dye using activated teak leaf powder. (E. Drioli, & S. A. Aljlil, Eds.) *Applied Water Science, 9*(3). doi:10.1007/s13201-019-0933-9

Ghaneian, M. T., Jamshidi, B., Dehvari, M., & Amrollahi, M. (2015, May). Pomegranate seed powder as a new biosorbent of reactive red 198 dye from aqueous solutions: adsorption equilibrium and kinetic studies. (M. Anpo, Ed.) *Research on Chemical Intermediates, 41*(5), 3223–3234. doi:10.1007/s11164-013-1427-2

Gita, S., Hussan, A., & Choudhury, T. G. (2017, December). Impact of Textile Dyes Waste on Aquatic Environments and its Treatment. (S. K. Konar, Ed.) *Environment & Ecology, 35*(3C), 2349-2353. Retrieved from https://www.researchgate.net/publication/321443064_Impact_of_Textile_Dyes_Waste_on_Aquatic_Environments_and_its_Treatment

Grassi, P., Drumm, F. C., Georgin, J., Franco, D. S., Dotto, G. L., Foletto, E. L., & Jahn, S. L. (2020, October). Application of Cordia trichotoma sawdust as an effective biosorbent for removal of crystal violet from aqueous solution in batch system and fixed-bed column. (P. Garrigues, Ed.) *Environmental Science and Pollution Research*, 6771–6783. doi:https://doi.org/10.1007/s11356-020-11005-6

Grassi, P., Reis, C., Drumm, F. C., Georgin, J., Tonato, D., Escudero, L. B., Dotto, G. L. (2019, February). Biosorption of crystal violet dye using inactive biomass of the fungus Diaporthe schini. (W. Rauch, Ed.) *Water Science & Technology, 79*(4), 709-717. doi:10.2166/wst.2019.091

Gül, Ü. D. (2013, October). Treatment of dyeing wastewater including reactive dyes. *WaterSA, 39*(5). doi:10.4314/wsa.v39i5.2

Gulnaz, O., Sahmurova, A., & Kama, S. (2011, Nov). Removal of Reactive Red 198 from aqueous solution by Potamogeton crispus. (S. Allen, T. Aminabhavi, & D. Dionysiou, Eds.) *Chemical Engineering Journal, 174*(2-3), 579-585. doi:10.1016/j.cej.2011.09.061

Gupta, V. K., Pathania, D., Kothiyal, N. C., & Sharma, G. (2014, February). Polyaniline zirconium (IV) silicophosphate nanocomposite for remediation of methylene blue dye from waste water. (W. Schröer, T. Yamaguchi, & A. J. Valente, Eds.) *Journal of Molecular Liquids, 190*, 139-145. doi:10.1016/j.molliq.2013.10.027

Haffad, H., Zbair, M., Anfar, Z., Ahsaine, H. A., Bouhlal, H., & Khallok, H. (2019, March). Removal of reactive red-198 dye using chitosan as an adsorbent: optimization by Central composite design coupled with response surface methodology. (R. M. Kini, Ed.) *Toxin Reviews, 40*(2), 225-237. doi:10.1080/15569543.2019.1584822

Hamad, M. T., & Saied, M. S. (2021, January). Kinetic studies of Congo red dye adsorption by immobilized Aspergillus niger on alginate. (E. Drioli, Ed.) *Applied Water Science, 11*(2). doi:10.1007/s13201-021-01362-z

Han, R., Ding, D., Xu, Y., Zou, W., Wang, Y., Li, Y., & Zou, L. (2008, May). Use of rice husk for the adsorption of congo red from aqueous solution in column mode. (A. Pandey, Ed.) *Bioresource Technology, 99*(8), 2938-2946. doi:https://doi.org/10.1016/j.biortech.2007.06.027

Hassaan, M. A., & Nemr, A. E. (2017, August). Health and Environmental Impacts of Dyes: Mini Review. (M. Minaei, Ed.) *American Journal of Environmental Science and Engineering, 1*(3), 64-67. doi:10.11648/j.ajese.20170103.11

Hassan, W., Farooq, U., Ahmad, M., Athar, M., & Khan, M. A. (2017, May). Potential biosorbent, Haloxylon recurvum plant stems, for the removal of methylene blue dye. (A. A. Alwarthan, Ed.) *Arabian Journal of Chemistry, 10*(2), S1512-S1522. doi:10.1016/j.arabjc.2013.05.002

Hor, K. Y., Chee, J. M., Chong, M. N., Jin, B., Saint, C., Poh, P. E., & Aryal, R. (2016, April). Evaluation of physicochemical methods in enhancing the adsorption performance of natural zeolite as low-cost adsorbent of methylene blue dye from wastewater. (J. J. Klemeš, C. M. Bôas de Almeida, & Y. Wang, Eds.) *Journal of Cleaner Production, 118*, 197-209. doi:10.1016/j.jclepro.2016.01.056

Huang, Y.-H., Tsai, S.-T., Huang, Y.-F., & Chen, C.-Y. (2007, February). Degradation of commercial azo dye reactive Black B in photo/ferrioxalate system. (D. Aga, A. J. Daugulis, Z. He, & G. Lyberatos, Eds.) *Journal of Hazardous Materials, 140*(1-2), 382-388. doi:10.1016/j.jhazmat.2006.10.083

Hulme, A. N., Ferreira, E. S., McNab, H., & Quye, A. (2004, February). The natural constituents of historical textile dyes. (J. Love, Ed.) *Chemical Society Reviews*(6), 329-336. doi:10.1039/B305697J

Ip, A. W., Barford, J. P., & McKay, G. (2010, March). A comparative study on the kinetics and mechanisms of removal of Reactive Black 5 by adsorption onto activated carbons and bone char. (S. Allen, T. (. Aminabhavi, & D. Dionysiou, Eds.) *Chemical Engineering Journal, 157*(2-3), 434-442. doi:10.1016/j.cej.2009.12.003

IR Spectrum Table & Chart. (2022, January 18). Retrieved April 18, 2022, from www.sigmaaldrich.com: https://www.sigmaaldrich.com/LK/en/technical-documents/technical-article/analytical-chemistry/photometry-and-reflectometry/ir-spectrum-table

Iscen, C. F., Kiran, I., & Ilhan, S. (2007, May). Biosorption of Reactive Black 5 dye by Penicillium restrictum: The kinetic study. (D. Aga, A. J. Daugulis, & Z. He, Eds.) *Journal of Hazardous Materials, 143*(1-2), 335-340. doi:10.1016/j.jhazmat.2006.09.028

Jeyavishnu, K., & Alagesan, V. (2020, April). Cereus sp. as potential biosorbent for removal of Congo red from aqueous solution: isotherm and kinetic

investigations. (G. B. Wiersma, Ed.) *Environmental Monitoring and Assessment, 192*(4). doi:10.1007/s10661-020-8197-2

Jia, P., Tan, H., Liu, K., & Gao, W. (2018, August). Removal of Methylene Blue from Aqueous Solution. *Applied science,* 1-11. doi:10.3390/app8101903

Katheresan, V., Kansedo, J., & Lau, S. Y. (2018, June). Efficiency of Various Recent Wastewater Dye Removal Methods: A Review. *Journal of Environmental Chemical Engineering, 6*(4), 4676-4697. doi:10.1016/j.jece.2018.06.060

Khadhraoui, M., Trabelsi, H., Ksibi, M., Bouguerra, S., & Elleuch, B. (2009, January). Discoloration and detoxicification of a Congo red dye solution by means of ozone treatment for a possible water reuse. (D. Aga, A. J. Daugulis, Z. He, & G. Lyberatos, Eds.) *Journal of Hazardous Materials, 161*(2-3), 974-981. doi:10.1016/j.jhazmat.2008.04.060

Khan, M. R., Rahman, W., Ong, H. R., Ismail, A. B., & Cheng, C. K. (2016). Tea dust as a potential low-cost adsorbent for the removal of crystal violet from aqueous solution. *Desalination and Water Treatment, 57*(31), 14728-14738. doi:10.1080/19443994.2015.1066272

Khan, S., Mohammad, A., & Abdul, M. (2019). Mutagenicity and genotoxicity evaluation of textile industry wastewater using bacterial and plant bioassays. (A. M. Tsatsakis, & A. Anadón, Eds.) *Toxicology Reports, 6*, 193-201. doi:10.1016/j.toxrep.2019.02.002

Khattab, T. A., Abdelrahman, M. S., & Rehan, M. (2020). Textile dyeing industry: environmental impacts and remediation. (P. Garrigues, Ed.) *Environmental Science and Pollution Research, 27*, 3803–3818. doi:10.1007/s11356-019-07137-z

Krika, F., Krika, A., & Azizi, A. (2019). Arundo donax L. as a low-cost and promising biosorbent for the removal of crystal violet from aqueous media: kinetic, isotherm and thermodynamic investigations. (E. Vessally, Ed.) *Chemical Review and Letters, 2*, 59-68. doi:10.22034/CRL.2019.187434.1015

Krishna, L. S., Reddy, A. S., Muralikrishna, A., Zuhairi, W. Y., Osman, H., & Reddy, A. V. (2014, September). Utilization of the agricultural waste (Cicer arientinum Linn fruit shell biomass) as biosorbent for decolorization of Congo red. *Desalination and Water Treatment, 56*(8), 2181-2192. doi:10.1080/19443994.2014.958540

Kristianto, H., Rahman, H., Prasetyo, S., & Sugih, A. K. (2019, May). Removal of Congo red aqueous solution using Leucaena leucocephala seed's extract as natural coagulant. (E. Drioli, & S. A. Aljlil, Eds.) *Applied Water Science, 9*(4). doi:10.1007/s13201-019-0972-2

Kulkarni, M. R., Revanth, T., Acharya, A., & Bhat, P. (2017, March). Removal of Crystal Violet dye from aqueous solution using water hyacinth: Equilibrium, kinetics and thermodynamics study. *Resource-Efficient Technologies, 3*(1), 71-77. doi:10.1016/j.reffit.2017.01.009

Kumar, R., & Ahmad, R. (2011). Biosorption of hazardous crystal violet dye from aqueous solution onto treated ginger waste (TGW). (N. Hilal, Ed.) *Desalination, 265*(1-3), 112-118. doi:10.1016/j.desal.2010.07.040

Lacasa, E., Cañizares, P., Walsh, F. C., Rodrigo, M. A., & Ponce-de-León, C. (2019, June). Removal of methylene blue from aqueous solutions using an Fe2+ catalyst and in-situ H2O2 generated at gas diffusion cathodes. (A. R. Hillman, Ed.) *Electrochimica Acta, 308*, 45-53. doi:10.1016/j.electacta.2019.03.218

Laohaprapanon, S., Matahum, J., Tayo, L., & You, S.-J. (2015, April). Photodegradation of Reactive Black 5 in a ZnO/UV slurry membrane reactor. (H.-K. Tsao, Ed.) *Journal of the Taiwan Institute of Chemical Engineers, 49*, 136-141. doi:10.1016/j.jtice.2014.11.017

Lellis, B., Polonio, C. Z., Pamphile, J. A., & Polonio, J. C. (2019, December). Effects of textile dyes on health and the environment and bioremediation potential of living organisms. *Biotechnology Research and Innovation, 3*(2), 275-290. doi:10.1016/j.biori.2019.09.001

Liang, H.-q., Li, M., Liu, B.-t., Xu, Z.-k., & Wu, Q.-y. (2016). Hierarchically Porous Carbon Membranes Derived from PAN and Their Selective Adsorption of Organic Dyes. *Chinese Journal of Polymer Science, 34*(1), 23-33. doi:10.1007/s10118-016-1723-6

Liang, J., Wu, J., Li, P., Wang, X., & Yang, B. (2012, Feb). Shaddock peel as a novel low-cost adsorbent for removal of methylene blue from dye wastewater. *Desalination and Water Treatment, 39*(1-3), 70-75. doi:10.1080/19443994.2012.669160

Liao, C.-S., Hung, C.-H., & Chao, S.-L. (2013, February). Decolorization of azo dye reactive black B by Bacillus cereus strain HJ-1. (J. d. Boer, T. Galloway, & Y. Yoon, Eds.) *Chemosphere, 90*(7), 2109-2114. doi:10.1016/j.chemosphere.2012.10.077

Lim, L. B., Priyantha, N., & Mansor, N. H. (2015). Artocarpus altilis (breadfruit) skin as a potential low-cost biosorbent for the removal of crystal violet dye: equilibrium, thermodynamics and kinetics studies. (J. W. LAMOREAUX, Ed.) *Environmental Earth Sciences, 73*(7), 3239–3247. doi:10.1007/s12665-014-3616-8

Lim, L. B., Usman, A., Hassan, M. H., & Mohamad Zaidi, N. A. (2020). Tropical wild fern (Diplazium esculentum) as a new and effective low-cost adsorbent for removal of toxic crystal violet dye. (S. Y. Alraqa, Ed.) *Journal of Taibah University for Science, 14*(1), 621-627. doi:10.1080/16583655.2020.1761122

Lin, S., Song, Z., Che, G., Ren, A., Li, P., Liu, C., & Zhang, J. (2014, July). Adsorption behavior of metal–organic frameworks for methylene blue from aqueous solution. (W. Schmidt, P. Dietzel, & F. Kleitz, Eds.) *Microporous and Mesoporous Materials, 139*, 27-34. doi:10.1016/j.micromeso.2014.03.004

Liu, J., Wang, N., Zhang, H., & Baeyens, J. (2019, May). Adsorption of Congo red dye on FexCo3-xO4 nanoparticles. (R. Dewil, J. Evans, & L. X. Zhang, Eds.)

Journal of Environmental Management, 238, 473-483. doi:10.1016/j.jenvman.2019.03.009

Lucas, M. S., & Peres, J. A. (2005, September). Decolorization of the azo dye Reactive Black 5 by Fenton and photo-Fenton oxidation. (B. M. Heron, & M. Wainwright, Eds.) *Dyes and Pigments, 71*(3), 236-244. doi:10.1016/j.dyepig.2005.07.007

Mahalakshmi, S., Lakshmi, D., & Menaga, U. (2015, Spring). Biodegradation of Different Concentration of dye (Congo red dye) by using Green and Blue Green Algae. (M. Ardestani, & M. H. Niksokhan, Eds.) *International Journal of Environmental Research, 9*(2), 735-744. doi:10.22059/IJER.2015.947

Mahboobeh, D., Hassan, M. E., & Taghi, M. G. (2017). Adsorption Kinetics and Equilibrium Studies of Reactive Red 198 Dye by Cuttlefish Bone Powder. (J. T. Darian, Ed.) *Iranian Journal of Chemistry and Chemical Engineering, 36*(2), 143-151. doi:10.30492/IJCCE.2017.26703

Mahmoodi, N. M., Arami, M., Bahrami, H., & Khorramfar, S. (2011, June). The effect of pH on the removal of anionic dyes from colored textile wastewater using a biosorbent. (S. Spiegel, Ed.) *Applied Polymer Science, 120*(5), 2996–3003. doi:10.1002/app.33406

Malakootian, M., Mansoorian, H. J., Hosseini, A., & Khanjani, N. (2015, July). Evaluating the efficacy of alumina/carbon nanotube hybrid adsorbents in removing Azo Reactive Red 198 and Blue 19 dyes from aqueous solutions. (G. Chen, F. Khan, & M. Hailwood, Eds.) *Process Safety and Environmental Protection, 96*, 125–137. doi:10.1016/j.psep.2015.05.002

Mani, S., & Bharagava, R. N. (2016). Exposure to Crystal Violet, Its Toxic,Genotoxic and Carcinogenic Effects on Environment and Its Degradationand Detoxification for Environmental Safety. *Reviews of Environmental Contamination and Toxicology*, 71-104. doi:10.1007/978-3-319-23573-8_4

Mansooreh, D., Medhi, T. M., Talat, G., Mashid, G., Laila, K., Elhameyan, Z., Ghanbarian, M. (2015, April). Optimization of the parameters influencing the photo-fenton process for the decolorization of reactive red 198 (rr198). (M. Ahamadizadeh, Ed.) *Jundishapur journal of health sciences, 7*(2), 38-43. doi:10.5812/jjhs.7(2)2015.28243

Meriç, S., Kaptan, D., & Ölmez, T. (2004, January). Color and COD removal from wastewater containing Reactive Black 5 using Fenton's oxidation process. (J. d. Boer, Ed.) *Chemosphere, 54*(3), 435-441. doi:10.1016/j.chemosphere.2003.08.010

Merlot, C., & Bruschweiler, B. J. (2017, August). Azo dyes in clothing textiles can be cleaved into a series of mutagenic aromatic amines which are not regulated yet. (L. Aylward, & M. v. Berg, Eds.) *Regulatory Toxicology and Pharmacology, 88,* 214-226. doi:10.1016/j.yrtph.2017.06.012

Mittal, A., Mittal, J., Malviya, A., & Gupta, V. K. (2009, December). Adsorptive removal of hazardous anionic dye ''Congo red" from wastewater. (M. Malmsten, Ed.) *Journal of Colloid and Interface Science, 340*(1), 16-26. doi:10.1016/j.jcis.2009.08.019

Mohamed, R. R., Abu Elell, M. H., Sabaa, M. W., & Saad, G. R. (2018). Synthesis of an efficient adsorbent hydrogel based on biodegradable polymers for removing crystal violet dye from aqueous solution. (A. D. French, Ed.) *Cellulose, 25*(11), 6513–6529. doi:10.1007/s10570-018-2014-x

Moussavi, G., & Mahmoudi, M. (2009, October). Degradation and biodegradability improvement of the reactive red 198 azo dye using catalytic ozonation with MgO nanocrystals. (S. Allen, T. (. Aminabhavi, & D. Dionysiou, Eds.) *Chemical Engineering Journal, 152*(1), 1-7. doi:10.1016/j.cej.2009.03.014

Muhammad, U. L., Zango, Z. U., Kadir, H. A., & Usman, A. U. (2019). Crystal Violet removal from aqueous solution using corn stalk biosorbent. (S. G. Abdu, Ed.) *Science World Journal, 14*(1), 133-138. Retrieved from https://www.ajol.info/index.php/swj/article/view/208516

Munagapati, S. V., & Kim, D. S. (2016, August). Adsorption of anionic azo dye Congo Red from aqueous solution. (W. Schröer, & T. Yamaguchi, Eds.) *Journal of Molecular Liquids, 220*, 540-548. doi:10.1016/j.molliq.2016.04.119

Munagapati, V. S., Wen, J.-C., Pan, C.-L., Gutha, Y., Wen, J.-H., & Reddy, G. M. (2019, August). Adsorptive removal of anionic dye (Reactive Black 5) from aqueous solution using chemically modified banana peel powder: kinetic, isotherm, thermodynamic, and reusability studies. (L. A. Newman, Ed.) *International Journal of Phytoremediation, 22*(3), 267-278. doi:10.1080/15226514.2019.1658709

Munagapati, V. S., Yarramuthi, V., Kim, Y., Lee, K. M., & Kim, D.-S. (2018, February). Removal of anionic dyes (Reactive Black 5 and Congo Red) from aqueous solutions using Banana Peel Powder as an adsorbent. (R. Handy, & B. Yan, Eds.) *Ecotoxicology and Environmental Safety, 148*, 601-607. doi:10.1016/j.ecoenv.2017.10.075

Nandiyanto, A. B., Oktiani, R., & Ragadhita, R. (2019). How to Read and Interpret FTIR Spectroscope of Organic Material. *Indonesian Journal of Science & Technology*, 97-118. doi:10.17509/ijost.v4i1.15806

Neupane, S., Ramesh, S. T., Gandhimathi, R., & Nidheesh, P. V. (2015). Pineapple leaf (Ananas comosus) powder as a biosorbent for the removal of crystal violet from aqueous solution. *Desalination and Water Treatment, 54*(7), 2041-2054. doi:10.1080/19443994.2014.903867

Nikfar, S., & Jaberidoost, M. (2014). Dyes and Colorants. In P. Wexler (Ed.), *Encyclopedia of Toxicology* (3 ed., Vol. 2, pp. 252-261). Academic Press. doi:10.1016/B978-0-12-386454-3.00602-3

Ooi, J. Q., Morad, N., & Tan, A. K. (2016, October). Phytoremediation of Methylene Blue and Methyl Orange Using Eichhornia crassipes. (R. Haynes, Ed.) *International Journal of Environmental Science and Development, 7*(10), 724-728. doi:10.18178/ijesd.2016.7.10.869

Orozco, R. S., Martínez-Juan, M., García-Sánchez, J. J., & Ureña-Núñez, F. (2018, January). Removal of Methylene Blue from Aqueous Solution Using Typha Stems and Leaves. (L. Lucia, & M. Hubbe, Eds.) *BioResources, 13*(1), 1696-1710. doi:10.15376/biores.13.1.1696-1710

Osma, J. F., Saravia, V., Toca-Herrera, J. L., & Couto, S. R. (2007, August). Sunflower seed shells: A novel and effective low-cost adsorbent for the removal of the diazo dye Reactive Black 5 from aqueous solutions. (D. Aga, A. J. Daugulis, & Z. He, Eds.) *Journal of Hazardous Materials, 147*(3), 900-905. doi:10.1016/j.jhazmat.2007.01.112

Pal, P. (2017). Industry-Specific Water Treatment: Case Studies. In P. Pal, *Industrial Water Treatment Process Technology* (1 ed., pp. 243-511). Butterworth-Heinemann. doi:10.1016/B978-0-12-810391-3.00006-0

Palma-Goyes, R. E., Guzmán-Duque, F. L., Peñuela, G., González, I., Nava, J. L., & Torres-Palma, R. A. (2010, September). Electrochemical degradation of crystal violet with BDD electrodes: Effect of electrochemical parameters and identification of organic by-products. (J. de Boer, T. Galloway, & Y. Yoon, Eds.) *Chemosphere, 81*(1), 26-32. doi:10.1016/j.chemosphere.2010.07.020

Patel, H., & Vashi, R. T. (2012, April). Removal of Congo Red dye from its aqueous solution. (A. A. Mayouf, Ed.) *Journal of Saudi Chemical Society, 16*(2), 131-136. doi:10.1016/j.jscs.2010.12.003

Pathania, D., Sharma, A., & Siddiqi, Z.-M. (2016, July). Removal of congo red dye from aqueous system using Phoenix dactylifera seeds. (W. Schröer, T. Yamaguchi, & A. J. Valente, Eds.) *Journal of Molecular Liquids, 219*, 359-367. doi:10.1016/j.molliq.2016.03.020

Paz, D. S., Baiotto, A., Schwaab, M., Mazutti, M. A., Bassaco, M. M., Bertuol, D. A., Meili, L. (2013, July). Use of papaya seeds as a biosorbent of methylene blue from aqueous solution. (W. Rauch, Ed.) *Water Science & Technology, 68*(2), 441–447. doi:10.2166/wst.2013.185

Pimentel, P., Oliveira, R., Melo, D., Melo, M., Assunção, A., & Gonzales, G. (2011). dsorption of chromium ions on oil shale waste. *Brazilian journal of petroleum and gas, 5*(2), 065-073. doi:doi:10.5419/bjpg2011-0008

Qingxiang, Y., Lingxia, T., Min, Y., & Hao, Z. (2007, June). Effects of glucose on the decolorization of Reactive Black 5 by yeast isolates. (J. Hao, X. Le, & W. Mitch, Eds.) *Journal of Environmental Sciences, 20*(1), 105-108. doi:10.1016/S1001-0742(08)60016-9

Qureshi, U. A., Khatri, Z., Ahmed, F., Khatri, M., & Kim, I.-S. (2017, April). Electrospun Zein Nanofiber as a Green and Recyclable Adsorbent for the Removal of Reactive Black 5 from the Aqueous Phase. (D. T. Allen, Ed.) *ACS Sustainable Chemistry & Engineering, 5*(5), 4340–4351. doi:10.1021/acssuschemeng.7b00402

Rahimi, s., Ehrampoush, m. h., Ghaneian, m. t., Reshadat, s., fatehizadeh, a., Ahmadian, m., Rahimi, s. (2013, October). Application of TiO2/UV-C Photocatalytic Process in Removal of Reactive Red 198 Dye from Synthetic Textile Wastewater. *Asian Journal of Chemistry, 25*(13), 7427-7432. doi:10.14233/ajchem.2013.14764

Rani, K. C., Naik, A., Chaurasiya, R. S., & Raghavarao, K. (2017, May). Removal of toxic Congo red dye from water employing low-cost coconut residual fiber. (W. Rauch, Ed.) *Water Science & Technology, 75*(9). doi:10.2166/wst.2017.109

Raymundo, A. S., Zanarotto, R., Belisário, M., Pereira, M. d., Ribeiro, J. N., & Ribeiro, A. V. (2010, August). Evaluation of Sugar-Cane Bagasse as Bioadsorbent in the Textile Wastewater Treatment Contaminated with Carcinogenic Congo Red Dye. *Brazilian Archives of Biology and Technology, 53*(4), 931-938. doi:10.1590/S1516-89132010000400023

REACTIVE DYES. (2021, August 20). (Global Colors, Inc) Retrieved July 10, 2021, from Global Colors Inc: https://globalcolorsinc.com/reactive-dyes/

Reactive red 198. (n.d.). Retrieved 9 2021, from ChemicalBook.com: https://www.chemicalbook.com/ChemicalProductProperty_EN_CB9260610.htm

reactive-black-5. (2012, May 18). Retrieved from worlddyevariety: http://www.worlddyevariety.com/reactive-dyes/reactive-black-5.html

Ruthiraan, M., Abdullah, E. C., Mubarak, N. M., & Noraini, M. N. (2017, April). A promising route of magnetic based materials for removal of cadmium and methylene blue from waste water. (G. L. Dotto, & D. Fatta-Kassinos, Eds.) *Journal of Environmental Chemical Engineering, 5*(2), 1447-1455. doi:10.1016/j.jece.2017.02.038

S, R., Lata, S., & P, B. (2018, March). Biosorption characteristics of methylene blue and malachite green from simulated wastewater onto Carica papaya wood biosorbent. (M. Chipara, H. Deng, & J. Gao, Eds.) *Surfaces and Interfaces, 10*, 197-215. doi:10.1016/j.surfin.2017.09.011

Saha, P. (2010). Assessment on the Removal of Methylene Blue Dye using Tamarind Fruit Shell as Biosorbent. (J. T. Trevors, Ed.) *Water, Air, & Soil Pollution, 213*(1-4), 287–299. doi:10.1007/s11270-010-0384-2

Sahoo, C., Gupta, A. K., & Pal, A. (2005, September). Photocatalytic degradation of Crystal Violet (C.I. Basic Violet 3) on silver ion doped TiO2. (B. M. Heron, & M. Wainwright, Eds.) *Dyes and Pigments, 66*(3), 189-196. doi:10.1016/j.dyepig.2004.09.003

Saini, R. D. (2017). Textile Organic Dyes: Polluting effects and Elimination Methods from Textile Waste Water. (R. Gupta, Ed.) *International Journal of Chemical Engineering Research, 9*, 121-136. Retrieved from http://www.ripublication.com/ijcher17/ijcherv9n1_10.pdf

Salehi, M., Hashemipour, H., & Mirzaee, M. (2012). Experimental Study of Influencing Factors and Kinetics in Catalytic Removal of Methylene Blue with TiO2 Nanopowder. (S. Bonacci, Ed.) *American Journal of Environmental Engineering, 2*(1), 1-7. doi:10.5923/j.ajee.20120201.01

Salem, E. A., Fayed, T. A., El-Nahass, M. N., & Dawood, M. (2018, January). A Comparative Study for Adsorption of Methylene Blue Dye from Wastewater on to Three Different Types of Rice Ash. (A. El-Saghier, Ed.) *Journal of Pharmaceutical and Applied Chemistry, 4*(2), 99-107. doi:10.18576/jpac/040204

Sarvestani, M. R., & Doroudi, Z. (2020). Removal of Reactive Black 5 from Waste Waters by Adsorption: A Comprehensive Review. (S. A. Bidgoli, & M. Jahanshahi, Eds.) *Journal of Water and Environmental Nanotechnology, 5*(2), 180-190. doi:10.22090/JWENT.2020.02.008

Sathishkumar, K., AlSalhi, M. S., Sanganyado, E., Devanesan, S., Arulprakash, A., & Rajasekar, A. (2019, November). Sequential electrochemical oxidation and bio-treatment of the azo dye congo red and textile effluent. (A. L. Pinheiro, D. Ramaiah, & M. d. Baptista, Eds.) *Journal of Photochemistry and Photobiology B: Biology, 200*. doi:10.1016/j.jphotobiol.2019.111655

Sekar, N. (2011). Acid dyes. In M. Clark (Ed.), *Handbook of Textile and Industrial Dyeing: Principles, Processes and Types of Dyes* (1 ed., Vol. 1, pp. 486-514). Woodhead Publishing. doi:10.1533/9780857093974.2.486

Selim, K. A., Abdel-Khalek, N. A., El-Sayed, S. M., & Abdallah, S. S. (2015, Nvember). Bioremoval of Crystal Violet Dye from Egyptian Textile Effluent. *International Research Journal of Engineering and Technology (IRJET), 2*(8), 1038-1043. Retrieved from https://www.irjet.net/archives/V2/i8/IRJET-V2I8155.pdf

Sharma, S., Hasan, A., Kumar, N., & Pandey, L. M. (2018, May). Removal of methylene blue dye from aqueous solution using immobilized Agrobacterium fabrum biomass along with iron oxide nanoparticles as biosorbent. (P. Garrigues, Ed.) *Environmental Science and Pollution Research, 25*(22), 21605–21615. doi:10.1007/s11356-018-2280-z

Shirzad-Siboni, M., Jafari, S. J., Giahi, O., Kim, I., Lee, S.-M., & Yang, J.-K. (2014, July). Removal of acid blue 113 and reactive black 5 dye from aqueous

solutions by activated red mud. (B. R. Yoo, Ed.) *Journal of Industrial and Engineering Chemistry, 20*(4), 1432-1437. doi:10.1016/j.jiec.2013.07.028

Silva, L. S., Lima, L. C., Ferreira, F. J., Silva, M. S., Osajima, J. A., Bezerra, R. D., & Filho, S. E. (2015, April). Sorption of the anionic reactive red RB dye in cellulose: Assessment of kinetic, thermodynamic, and equilibrium data. (J. Plumet, Ed.) *Open Chemistry, 13*(1), 801-812. doi:10.1515/chem-2015-0079

Singhopon , T., Shinoda , K., Rujakom, S., & Kazama, F. (2021, March). Factors Affecting the Simultaneous Removal of Nitrate and Reactive Black 5 Dye via Hydrogen-Based Denitrification. (J.-L. PROBST, Ed.) *Water, 13*(7). doi:10.3390/w13070922

Stjepanović, M., Velić, N., Galić , A., Kosović , I., Jakovljević , T., & Stanić, M. H. (2021, February). From Waste to Biosorbent: Removal of Congo Red from Water by Waste Wood Biomass. (M. M. Manca, Ed.) *Water, 13*(3). doi:10.3390/w13030279

Surana, M., Mehta, P., Pamecha, K., & Kabra, B. V. (2011). Treatment of water contaminated with Reactive Red 198 (RR198) by Photo-Fenton Reagent. *Pelagia Research Library, 2*(2), 177-186. Retrieved from https://www.imedpub.com/articles/treatment-of-water-contaminated-with-reactive-red-198-rr198by-photofenton-reagent.pdf

Tan , I. A., & Hameed, B. H. (2012). Removal of crystal violet dye from aqueous solutions using rubber (hevea brasillensis) seed shell-based biosorbent. *Desalination and Water Treatment, 48*(1-3), 174-181. doi:10.1080/19443994.2012.698810

Tang, C., & Chen, V. (2004, June). The photocatalytic degradation of reactive black 5 using TiO2/UV in an annular photoreactor. (E. Morgenroth, G.-H. Chen, & A. Deletic, Eds.) *Water Research, 38*(11), 2775-2781. doi:10.1016/j.watres.2004.03.020

Tayebi, H.-A., Dalirandeh, Z., Rad, A. S., Mirabi, A., & Binaeian, E. (2016, January). Synthesis of polyaniline/Fe3O4 magnetic nanoparticles for removal

of reactive red 198 from textile waste water: kinetic, isotherm, and thermodynamic studies. *Desalination and Water Treatment, 57*(47), 22551-22563. doi:10.1080/19443994.2015.1133323

Technical report 123 Freundlich isotherms. (n.d.). Retrieved from ecetoc: https://www.ecetoc.org/report/measured-partitioning-property-data/adsorption-desorption-distribution-kd-and-organic-carbon-water-partition-koc-coefficients/freundlich-isotherms/

Tichapondwa, S., Newman, J., & Kubheka, O. (2020, October). Effect of TiO2 phase on the photocatalytic degradation of methylene blue dye. (J. Gottsmann, J. Liu, & M. Mul, Eds.) *Physics and Chemistry of the Earth, Parts A/B/C, 118-119*. doi:10.1016/j.pce.2020.102900

Ullah, I., Ali, S., & Akram, M. (2013). Degradation of Reactive Black B dye in wastewater using oxidation process. (M. A. Hanif, Ed.) *International Journal of Chemical and Biochemical Sciences, 4*, 96-100. doi:10.1.1.707.5470

UrRehman, M. S., Kim, I., & Han, J.-I. (2012, October). Adsorption of methylene blue dye from aqueous solution by sugar extracted spent rice biomass. (M. Coimbra, K. Edgar, & T. Budtova, Eds.) *Carbohydrate Polymers, 90*(3), 1314-1322. doi:10.1016/j.carbpol.2012.06.078

Vargas, V. H., Paveglio, R. R., Pauletto, P., Gonçalves Salau, N., & Dotto, L. (2019, April). Sisal fiber as an alternative and cost-effective adsorbent for the removal of methylene blue and reactive black 5 dyes from aqueous solutions. (A. Gill, Ed.) *Chemical Engineering Communications, 207*(4), 523-536. doi:10.1080/00986445.2019.1605362

Vijayaraghavan, G., & Shanthakumar, S. (2015, February). Performance study on algal alginate as natural coagulant for the removal of Congo red dye. *Desalination and Water Treatment, 57*(14), 6384-6392. doi:10.1080/19443994.2015.1008578

Wanyonyi, W. C., Onyari, J. M., & Shiundu, P. M. (2014, July). Adsorption of Congo Red Dye from Aqueous Solutions Using Roots of Eichhornia

Crassipes: Kinetic and Equilibrium Studies. *Energy Procedia, 50*, 862-869. doi:10.1016/j.egypro.2014.06.105

Wathukarage, A., Herath, I., Iqbal, M. C., & Vithanage, M. (2019). Mechanistic understanding of crystal violet dye sorption by woody biochar: implications for wastewater treatment. (M. H. Wong, Ed.) *Environmental Geochemistry and Health*, 1647–1661. doi:10.1007/s10653-017-0013-8

Wathukarage, A., Herath, I., Iqbal, M., & Vithanage, M. (2017, August). Mechanistic understanding of crystal violet dye sorption by woody biochar: implications for wastewater treatment. *Environ Geochem Health*. doi:10.1007/s10653-017-0013-8

Wekoye, J. N., Wanyonyi, W. C., Wangila, P. T., & Tonui, M. K. (2020). Kinetic and equilibrium studies of Congo red dye adsorption on cabbage waste powder. (K. Kannan, Ed.) *Environmental Chemistry and Ecotoxicology*, *2*, 24-31. doi:10.1016/j.enceco.2020.01.004

Won, S. W., Kim, H.-J., Choi, S.-H., Chung, B.-W., Kim, K.-J., & Yun, Y.-S. (2006, August). Performance, kinetics and equilibrium in biosorption of anionic dye Reactive Black 5 by the waste biomass of Corynebacterium glutamicum as a low-cost biosorbent. (S. Allen, T. Aminabhavi, & D. Dionysiou, Eds.) *Chemical Engineering Journal*, *101*(1), 37-43. doi:10.1016/j.cej.2006.04.005

Xia, H., Chen, L., & Fang, Y. (2013, August). Highly Efficient Removal of Congo red from Wastewater by Nano-Cao. (R. Wickramasinghe, Ed.) *Separation Science and Technology*, *48*(17), 2681-2687. doi:10.1080/01496395.2013.805340

Yang, Y., Ali, N., Khan, A., Khan, S., Khan, S., Khan, H., Bilal, M. (2021, January). Chitosan-capped ternary metal selenide nanocatalysts for efficient degradation of Congo red dye in sunlight irradiation. (A. Dong, & J. F. Kennedy, Eds.) *International Journal of Biological Macromolecules, 167*, 169-181. doi:10.1016/j.ijbiomac.2020.11.167

You, S.-J., Damodar, R. A., & Hou, S.-C. (2010, May). Degradation of Reactive Black 5 dye using anaerobic/aerobic membrane bioreactor (MBR) and photochemical membrane reactor. (D. Aga, A. J. Daugulis, & Z. He, Eds.) *Journal of Hazardous Materials, 173*(1-3), 1112-1118. doi:10.1016/j.jhazmat.2010.01.036

Zahir, A., Aslam, Z., Kamal, M. S., Ahmad, W., Abbas, A., & Shawabkeh, R. A. (2017, October). Development of novel cross-linked chitosan for the removal of anionic Congo red dye. (W. Schroer, T. Yamaguchi, & A. J. Valente, Eds.) *Journal of Molecular Liquids, 244*, 211-218. doi:10.1016/j.molliq.2017.09.006

Zamora, M. H., Jeronimo, F. M., Urbina, E. C., & Villanueva, R. O. (2016, September). Congo red dye affects survival and reproduction in the cladoceran Ceriodaphnia dubia. Effects of direct and dietary exposure. (L. R. Shugart, Ed.) *Ecotoxicology, 25*(10), 1832-1840. doi:10.1007/s10646-016-1731-x

Zare, K., Sadegh, H., ghoshekandi, R. S., Maazinejad, B., Ali, V., Tyagi, I., Gupta, V. K. (2015, December). Enhanced removal of toxic Congo red dye using multi walled carbon nanotubes: Kinetic, equilibrium studies and its comparison with other adsorbents. (W. Schröer, T. Yamaguchi, A. J. Valente, & L. F. Vega, Eds.) *Journal of Molecular Liquids, 212*, 266-271. doi:10.1016/j.molliq.2015.09.027

Zheng, H., Sun, Q., Li, Y., & Du, Q. (2020, April). Biosorbents prepared from pomelo peel by hydrothermal technique and its adsorption properties for congo red. (A. Balazs, & S. Banerjee, Eds.) *Materials Research Express, 7*. doi:10.1088/2053-1591/ab8a83

APPENDIX A: ABSORBANCE SPECTRUM VALUES FOR MB, CV, CR, RR, AND RBB DYE SOLUTIONS

Wavelength vs. absorbance for selected dyes

Wavelength (nm)	Methylene blue Abs.	Congo red Abs.	Reactive black B Abs.	Crystal Violet Abs.	Reactive red Abs.
190	-0.627	0.794	0.784	0.419	1.217
191	-0.513	0.761	0.832	0.415	1.238
192	-0.441	0.713	0.801	0.423	1.256
193	-0.379	0.672	0.776	0.427	1.224
194	-0.332	0.644	0.748	0.428	1.222
195	-0.301	0.626	0.723	0.435	1.216
196	-0.279	0.613	0.703	0.444	1.215
197	-0.261	0.604	0.679	0.456	1.194
198	-0.249	0.597	0.658	0.467	1.186
199	-0.238	0.593	0.639	0.482	1.166
200	-0.231	0.591	0.622	0.496	1.162
201	-0.227	0.59	0.598	0.509	1.149
202	-0.223	0.586	0.579	0.521	1.136
203	-0.219	0.586	0.56	0.532	1.129
204	-0.215	0.584	0.54	0.541	1.121
205	-0.212	0.581	0.522	0.546	1.109
206	-0.208	0.577	0.505	0.55	1.102
207	-0.201	0.572	0.487	0.549	1.098
208	-0.193	0.567	0.473	0.544	1.1
209	-0.183	0.561	0.458	0.534	1.102
210	-0.172	0.554	0.445	0.52	1.103
211	-0.159	0.544	0.433	0.501	1.108
212	-0.145	0.536	0.422	0.479	1.116
213	-0.13	0.527	0.412	0.452	1.119
214	-0.114	0.52	0.402	0.422	1.127
215	-0.098	0.514	0.394	0.389	1.131
216	-0.08	0.511	0.385	0.356	1.136
217	-0.064	0.509	0.378	0.323	1.134
218	-0.047	0.511	0.37	0.29	1.126
219	-0.031	0.515	0.364	0.258	1.118
220	-0.015	0.521	0.358	0.23	1.101
221	0	0.529	0.353	0.205	1.078
222	0.015	0.537	0.347	0.183	1.053
223	0.029	0.546	0.343	0.166	1.028
224	0.044	0.555	0.339	0.151	1
225	0.057	0.565	0.335	0.138	0.973
226	0.07	0.574	0.332	0.128	0.946
227	0.082	0.584	0.328	0.12	0.922
228	0.093	0.593	0.324	0.113	0.898
229	0.104	0.601	0.32	0.108	0.878
230	0.114	0.61	0.316	0.104	0.862
231	0.125	0.617	0.311	0.101	0.848
232	0.135	0.623	0.306	0.1	0.837
233	0.146	0.628	0.301	0.1	0.828
234	0.159	0.632	0.295	0.101	0.82
235	0.173	0.635	0.288	0.103	0.812
236	0.187	0.638	0.281	0.105	0.804
237	0.202	0.638	0.274	0.109	0.797
238	0.218	0.637	0.267	0.113	0.789
239	0.234	0.636	0.261	0.118	0.78
240	0.251	0.632	0.254	0.123	0.771
241	0.267	0.627	0.249	0.128	0.762
242	0.282	0.62	0.245	0.133	0.753
243	0.296	0.611	0.242	0.138	0.743
244	0.307	0.602	0.24	0.141	0.734
245	0.314	0.591	0.238	0.144	0.725
246	0.316	0.579	0.238	0.146	0.717
247	0.312	0.567	0.238	0.147	0.708
248	0.303	0.553	0.239	0.146	0.701
249	0.289	0.539	0.24	0.143	0.693
250	0.274	0.525	0.242	0.14	0.688
251	0.258	0.511	0.244	0.136	0.684
252	0.242	0.496	0.246	0.131	0.68
253	0.228	0.482	0.247	0.126	0.678
254	0.216	0.469	0.249	0.121	0.676
255	0.206	0.456	0.251	0.116	0.676
256	0.199	0.444	0.252	0.111	0.675

257	0.193	0.432	0.252	0.106	0.674
258	0.19	0.421	0.252	0.101	0.672
259	0.188	0.411	0.252	0.098	0.672
260	0.187	0.401	0.25	0.094	0.672
261	0.189	0.392	0.248	0.091	0.673
262	0.192	0.383	0.246	0.088	0.676
263	0.197	0.375	0.243	0.086	0.682
264	0.205	0.367	0.239	0.084	0.689
265	0.214	0.359	0.236	0.082	0.698
266	0.225	0.353	0.232	0.08	0.711
267	0.238	0.346	0.229	0.079	0.725
268	0.25	0.339	0.226	0.078	0.741
269	0.264	0.332	0.222	0.078	0.758
270	0.277	0.326	0.219	0.077	0.776
271	0.29	0.32	0.217	0.077	0.793
272	0.304	0.314	0.215	0.077	0.81
273	0.319	0.309	0.214	0.077	0.826
274	0.335	0.305	0.213	0.079	0.842
275	0.352	0.301	0.213	0.08	0.857
276	0.371	0.296	0.213	0.081	0.875
277	0.392	0.293	0.214	0.083	0.892
278	0.415	0.29	0.215	0.085	0.912
279	0.44	0.288	0.217	0.088	0.931
280	0.466	0.286	0.218	0.091	0.952
281	0.492	0.285	0.221	0.094	0.974
282	0.519	0.283	0.223	0.097	0.994
283	0.546	0.283	0.226	0.101	1.012
284	0.574	0.284	0.228	0.105	1.028
285	0.602	0.284	0.231	0.11	1.041
286	0.629	0.285	0.234	0.114	1.052
287	0.658	0.287	0.236	0.119	1.063
288	0.686	0.29	0.239	0.124	1.073
289	0.707	0.292	0.242	0.129	1.081
290	0.725	0.295	0.244	0.134	1.093
291	0.737	0.3	0.247	0.139	1.104
292	0.737	0.304	0.249	0.144	1.115
293	0.73	0.309	0.252	0.15	1.124
294	0.714	0.314	0.255	0.155	1.133
295	0.691	0.319	0.257	0.159	1.137
296	0.661	0.325	0.26	0.163	1.139
297	0.627	0.33	0.262	0.166	1.135
298	0.59	0.336	0.264	0.168	1.128
299	0.55	0.342	0.266	0.169	1.114
300	0.51	0.348	0.268	0.169	1.094
301	0.471	0.354	0.27	0.168	1.07
302	0.432	0.36	0.271	0.166	1.045
303	0.396	0.366	0.273	0.164	1.013
304	0.361	0.372	0.274	0.16	0.977
305	0.33	0.378	0.275	0.155	0.939
306	0.301	0.384	0.276	0.15	0.898
307	0.273	0.39	0.277	0.143	0.852
308	0.251	0.396	0.277	0.136	0.807
309	0.232	0.4	0.278	0.128	0.761
310	0.216	0.407	0.278	0.12	0.717
311	0.202	0.412	0.278	0.111	0.673
312	0.192	0.417	0.277	0.104	0.633
313	0.184	0.422	0.276	0.096	0.595
314	0.177	0.427	0.275	0.089	0.561
315	0.171	0.432	0.274	0.082	0.53
316	0.167	0.437	0.273	0.076	0.502
317	0.162	0.442	0.271	0.07	0.478
318	0.159	0.446	0.269	0.065	0.459
319	0.156	0.45	0.266	0.06	0.442
320	0.153	0.453	0.263	0.056	0.429
321	0.15	0.458	0.259	0.052	0.419
322	0.148	0.462	0.255	0.049	0.413
323	0.147	0.465	0.251	0.046	0.408
324	0.145	0.469	0.246	0.044	0.404
325	0.143	0.474	0.241	0.042	0.4
326	0.14	0.478	0.235	0.04	0.396
327	0.138	0.482	0.229	0.038	0.393
328	0.134	0.485	0.223	0.037	0.388
329	0.13	0.489	0.216	0.036	0.383
330	0.125	0.493	0.209	0.035	0.378
331	0.119	0.497	0.203	0.034	0.373
332	0.112	0.5	0.196	0.033	0.368

333	0.105	0.503	0.19	0.032	0.362
334	0.097	0.505	0.184	0.03	0.355
335	0.09	0.509	0.178	0.029	0.349
336	0.083	0.512	0.173	0.028	0.341
337	0.076	0.515	0.167	0.027	0.333
338	0.069	0.517	0.163	0.026	0.323
339	0.063	0.518	0.158	0.026	0.314
340	0.058	0.521	0.155	0.026	0.304
341	0.053	0.522	0.151	0.026	0.293
342	0.048	0.522	0.148	0.025	0.281
343	0.044	0.523	0.145	0.025	0.271
344	0.041	0.522	0.143	0.025	0.262
345	0.038	0.523	0.141	0.025	0.253
346	0.035	0.522	0.14	0.025	0.244
347	0.033	0.521	0.139	0.025	0.237
348	0.031	0.52	0.137	0.025	0.23
349	0.029	0.517	0.136	0.025	0.223
350	0.028	0.514	0.135	0.025	0.217
351	0.026	0.512	0.134	0.025	0.213
352	0.025	0.508	0.133	0.025	0.209
353	0.023	0.504	0.133	0.025	0.206
354	0.022	0.5	0.132	0.025	0.203
355	0.021	0.495	0.132	0.025	0.2
356	0.02	0.49	0.132	0.025	0.199
357	0.019	0.484	0.133	0.024	0.197
358	0.018	0.479	0.133	0.024	0.196
359	0.017	0.474	0.135	0.024	0.194
360	0.016	0.468	0.136	0.023	0.193
361	0.015	0.462	0.138	0.023	0.192
362	0.015	0.455	0.14	0.022	0.191
363	0.014	0.448	0.142	0.022	0.19
364	0.014	0.442	0.145	0.022	0.19
365	0.014	0.436	0.148	0.022	0.189
366	0.013	0.428	0.15	0.021	0.188
367	0.012	0.421	0.153	0.02	0.187
368	0.013	0.414	0.156	0.02	0.186
369	0.013	0.409	0.159	0.02	0.185
370	0.013	0.402	0.162	0.019	0.184
371	0.013	0.396	0.165	0.019	0.183
372	0.013	0.39	0.168	0.018	0.182
373	0.013	0.384	0.171	0.017	0.181
374	0.013	0.377	0.174	0.017	0.179
375	0.013	0.372	0.176	0.017	0.178
376	0.014	0.366	0.18	0.016	0.176
377	0.014	0.36	0.182	0.015	0.174
378	0.014	0.355	0.185	0.015	0.173
379	0.014	0.35	0.188	0.014	0.171
380	0.014	0.344	0.191	0.013	0.169
381	0.015	0.338	0.193	0.013	0.167
382	0.015	0.333	0.196	0.013	0.165
383	0.015	0.328	0.199	0.012	0.163
384	0.016	0.323	0.201	0.012	0.161
385	0.016	0.318	0.204	0.012	0.16
386	0.016	0.313	0.206	0.012	0.158
387	0.017	0.309	0.209	0.011	0.157
388	0.017	0.305	0.211	0.011	0.155
389	0.017	0.301	0.212	0.011	0.154
390	0.017	0.298	0.214	0.011	0.153
391	0.018	0.295	0.215	0.011	0.152
392	0.018	0.292	0.217	0.011	0.151
393	0.018	0.29	0.217	0.011	0.15
394	0.018	0.288	0.217	0.011	0.149
395	0.018	0.287	0.216	0.011	0.148
396	0.017	0.286	0.216	0.011	0.147
397	0.017	0.285	0.215	0.011	0.146
398	0.017	0.285	0.214	0.011	0.145
399	0.016	0.286	0.213	0.011	0.144
400	0.015	0.286	0.212	0.011	0.143
401	0.015	0.287	0.211	0.011	0.141
402	0.014	0.289	0.21	0.011	0.14
403	0.013	0.29	0.209	0.011	0.139
404	0.012	0.292	0.209	0.011	0.137
405	0.012	0.294	0.208	0.011	0.136
406	0.011	0.297	0.208	0.011	0.134
407	0.01	0.299	0.207	0.012	0.133
408	0.009	0.302	0.207	0.012	0.132

409	0.008	0.305	0.207	0.012	0.131
410	0.008	0.309	0.206	0.012	0.129
411	0.007	0.312	0.206	0.013	0.128
412	0.007	0.316	0.206	0.013	0.127
413	0.006	0.32	0.207	0.013	0.127
414	0.006	0.324	0.206	0.013	0.126
415	0.006	0.328	0.206	0.014	0.125
416	0.006	0.332	0.207	0.014	0.125
417	0.006	0.337	0.207	0.014	0.124
418	0.006	0.341	0.206	0.015	0.123
419	0.006	0.345	0.206	0.015	0.123
420	0.006	0.35	0.206	0.015	0.122
421	0.006	0.354	0.206	0.016	0.122
422	0.006	0.359	0.206	0.016	0.121
423	0.006	0.364	0.206	0.017	0.121
424	0.006	0.369	0.205	0.017	0.121
425	0.007	0.374	0.205	0.018	0.12
426	0.007	0.378	0.205	0.018	0.12
427	0.007	0.383	0.205	0.019	0.12
428	0.007	0.388	0.205	0.019	0.119
429	0.008	0.393	0.205	0.02	0.119
430	0.008	0.398	0.205	0.021	0.118
431	0.008	0.403	0.205	0.021	0.118
432	0.009	0.408	0.205	0.022	0.118
433	0.009	0.413	0.205	0.023	0.117
434	0.01	0.418	0.205	0.024	0.117
435	0.01	0.423	0.205	0.024	0.117
436	0.01	0.428	0.206	0.025	0.117
437	0.011	0.434	0.206	0.026	0.117
438	0.011	0.439	0.206	0.027	0.117
439	0.012	0.444	0.206	0.028	0.117
440	0.012	0.449	0.207	0.029	0.117
441	0.013	0.455	0.207	0.03	0.118
442	0.013	0.46	0.207	0.031	0.118
443	0.014	0.465	0.208	0.032	0.119
444	0.014	0.471	0.208	0.034	0.121
445	0.015	0.477	0.208	0.035	0.122
446	0.016	0.482	0.209	0.036	0.124
447	0.016	0.488	0.209	0.038	0.126
448	0.017	0.494	0.21	0.039	0.129
449	0.017	0.499	0.21	0.04	0.131
450	0.018	0.505	0.211	0.042	0.134
451	0.019	0.511	0.211	0.044	0.137
452	0.02	0.517	0.212	0.045	0.14
453	0.02	0.523	0.212	0.047	0.144
454	0.021	0.529	0.212	0.049	0.148
455	0.021	0.535	0.213	0.05	0.152
456	0.022	0.541	0.213	0.052	0.156
457	0.023	0.547	0.213	0.054	0.161
458	0.024	0.554	0.214	0.056	0.165
459	0.024	0.56	0.214	0.058	0.171
460	0.025	0.567	0.215	0.061	0.176
461	0.026	0.573	0.215	0.063	0.182
462	0.026	0.58	0.215	0.065	0.188
463	0.027	0.587	0.216	0.068	0.194
464	0.028	0.593	0.216	0.07	0.201
465	0.029	0.6	0.217	0.073	0.208
466	0.029	0.607	0.217	0.076	0.215
467	0.03	0.614	0.218	0.079	0.223
468	0.031	0.621	0.219	0.082	0.23
469	0.031	0.629	0.219	0.085	0.239
470	0.032	0.636	0.22	0.088	0.247
471	0.033	0.643	0.221	0.092	0.255
472	0.034	0.65	0.221	0.095	0.264
473	0.035	0.656	0.222	0.098	0.272
474	0.035	0.663	0.222	0.102	0.281
475	0.036	0.67	0.223	0.105	0.289
476	0.037	0.676	0.223	0.109	0.298
477	0.038	0.683	0.224	0.113	0.306
478	0.038	0.689	0.224	0.117	0.315
479	0.039	0.696	0.224	0.121	0.323
480	0.04	0.702	0.224	0.125	0.332
481	0.041	0.708	0.224	0.13	0.341
482	0.042	0.714	0.224	0.134	0.349
483	0.042	0.719	0.224	0.139	0.358
484	0.043	0.725	0.223	0.143	0.366

485	0.044	0.73	0.223	0.148	0.374
486	0.045	0.734	0.222	0.152	0.382
487	0.046	0.739	0.222	0.157	0.39
488	0.046	0.743	0.221	0.162	0.399
489	0.047	0.747	0.22	0.167	0.407
490	0.048	0.75	0.219	0.173	0.415
491	0.048	0.753	0.219	0.178	0.424
492	0.049	0.756	0.218	0.184	0.433
493	0.05	0.758	0.217	0.189	0.442
494	0.05	0.759	0.216	0.195	0.451
495	0.051	0.761	0.215	0.201	0.461
496	0.051	0.761	0.215	0.207	0.472
497	0.051	0.762	0.214	0.213	0.482
498	0.052	0.762	0.213	0.219	0.492
499	0.052	0.761	0.213	0.226	0.503
500	0.052	0.76	0.213	0.233	0.515
501	0.053	0.758	0.212	0.239	0.526
502	0.053	0.756	0.212	0.246	0.537
503	0.053	0.754	0.212	0.253	0.548
504	0.053	0.751	0.212	0.259	0.56
505	0.053	0.748	0.212	0.266	0.571
506	0.053	0.744	0.213	0.274	0.583
507	0.053	0.74	0.213	0.281	0.594
508	0.054	0.736	0.214	0.288	0.605
509	0.054	0.731	0.214	0.296	0.616
510	0.054	0.726	0.215	0.303	0.625
511	0.054	0.72	0.215	0.311	0.635
512	0.054	0.714	0.216	0.318	0.644
513	0.054	0.708	0.217	0.326	0.652
514	0.055	0.702	0.218	0.333	0.659
515	0.055	0.695	0.219	0.341	0.666
516	0.055	0.688	0.22	0.348	0.671
517	0.056	0.681	0.221	0.355	0.675
518	0.056	0.673	0.222	0.363	0.679
519	0.057	0.665	0.223	0.37	0.682
520	0.058	0.657	0.224	0.377	0.684
521	0.058	0.649	0.225	0.384	0.685
522	0.059	0.641	0.226	0.39	0.685
523	0.06	0.632	0.227	0.397	0.685
524	0.061	0.624	0.228	0.403	0.684
525	0.062	0.615	0.229	0.409	0.684
526	0.063	0.606	0.23	0.414	0.682
527	0.064	0.597	0.231	0.42	0.681
528	0.066	0.587	0.232	0.425	0.68
529	0.067	0.578	0.233	0.431	0.679
530	0.069	0.568	0.234	0.436	0.678
531	0.07	0.558	0.236	0.441	0.677
532	0.072	0.548	0.237	0.445	0.677
533	0.074	0.538	0.238	0.45	0.677
534	0.076	0.528	0.239	0.454	0.678
535	0.078	0.517	0.24	0.458	0.679
536	0.081	0.506	0.242	0.462	0.679
537	0.083	0.495	0.243	0.466	0.68
538	0.086	0.484	0.244	0.469	0.682
539	0.088	0.473	0.246	0.473	0.684
540	0.091	0.462	0.247	0.477	0.687
541	0.094	0.451	0.249	0.48	0.689
542	0.097	0.44	0.25	0.483	0.692
543	0.101	0.428	0.252	0.487	0.694
544	0.104	0.417	0.254	0.49	0.696
545	0.108	0.406	0.256	0.493	0.697
546	0.112	0.395	0.258	0.496	0.698
547	0.115	0.384	0.26	0.5	0.699
548	0.119	0.373	0.262	0.503	0.698
549	0.124	0.362	0.264	0.506	0.697
550	0.128	0.351	0.266	0.51	0.695
551	0.132	0.34	0.268	0.513	0.691
552	0.137	0.329	0.271	0.517	0.687
553	0.141	0.319	0.273	0.521	0.681
554	0.146	0.308	0.275	0.524	0.674
555	0.151	0.298	0.278	0.529	0.665
556	0.156	0.288	0.281	0.533	0.655
557	0.16	0.277	0.283	0.537	0.644
558	0.166	0.267	0.286	0.542	0.63
559	0.171	0.257	0.289	0.547	0.616
560	0.176	0.248	0.292	0.552	0.6

561	0.181	0.238	0.294	0.558	0.583
562	0.187	0.229	0.297	0.563	0.564
563	0.192	0.219	0.3	0.569	0.544
564	0.198	0.21	0.303	0.575	0.523
565	0.204	0.201	0.306	0.582	0.502
566	0.209	0.192	0.309	0.588	0.48
567	0.216	0.184	0.312	0.594	0.457
568	0.222	0.176	0.314	0.601	0.434
569	0.228	0.168	0.317	0.607	0.411
570	0.235	0.16	0.32	0.613	0.387
571	0.241	0.152	0.323	0.619	0.365
572	0.248	0.145	0.325	0.625	0.343
573	0.256	0.138	0.328	0.63	0.321
574	0.263	0.132	0.33	0.635	0.301
575	0.271	0.125	0.332	0.64	0.281
576	0.279	0.119	0.335	0.644	0.261
577	0.288	0.113	0.337	0.648	0.242
578	0.297	0.107	0.339	0.651	0.224
579	0.307	0.101	0.341	0.654	0.207
580	0.317	0.096	0.342	0.656	0.19
581	0.327	0.091	0.344	0.657	0.175
582	0.339	0.085	0.346	0.657	0.16
583	0.35	0.081	0.348	0.656	0.146
584	0.363	0.076	0.349	0.654	0.134
585	0.375	0.072	0.35	0.651	0.122
586	0.388	0.067	0.352	0.648	0.111
587	0.402	0.063	0.353	0.643	0.101
588	0.415	0.06	0.354	0.637	0.091
589	0.43	0.056	0.355	0.63	0.083
590	0.446	0.052	0.355	0.621	0.075
591	0.461	0.049	0.356	0.612	0.067
592	0.477	0.046	0.357	0.602	0.061
593	0.494	0.043	0.357	0.59	0.054
594	0.511	0.04	0.358	0.578	0.049
595	0.527	0.037	0.358	0.565	0.044
596	0.544	0.035	0.358	0.551	0.039
597	0.561	0.032	0.358	0.536	0.035
598	0.578	0.03	0.358	0.521	0.032
599	0.595	0.028	0.358	0.505	0.028
600	0.612	0.026	0.358	0.489	0.025
601	0.628	0.024	0.357	0.473	0.023
602	0.644	0.023	0.357	0.456	0.021
603	0.659	0.021	0.356	0.439	0.019
604	0.673	0.02	0.355	0.422	0.017
605	0.687	0.018	0.354	0.404	0.015
606	0.7	0.017	0.353	0.386	0.013
607	0.712	0.016	0.352	0.369	0.012
608	0.722	0.014	0.351	0.352	0.011
609	0.731	0.013	0.349	0.335	0.01
610	0.738	0.012	0.348	0.318	0.009
611	0.745	0.011	0.346	0.302	0.008
612	0.75	0.011	0.343	0.286	0.007
613	0.754	0.01	0.341	0.27	0.007
614	0.757	0.009	0.338	0.255	0.006
615	0.758	0.008	0.336	0.241	0.006
616	0.759	0.008	0.333	0.227	0.005
617	0.76	0.007	0.329	0.213	0.005
618	0.76	0.007	0.326	0.201	0.004
619	0.759	0.006	0.322	0.189	0.004
620	0.759	0.006	0.318	0.177	0.004
621	0.759	0.006	0.314	0.167	0.004
622	0.759	0.005	0.31	0.156	0.003
623	0.76	0.005	0.305	0.147	0.003
624	0.761	0.005	0.3	0.138	0.003
625	0.763	0.004	0.295	0.129	0.003
626	0.766	0.004	0.29	0.121	0.003
627	0.77	0.004	0.285	0.113	0.003
628	0.774	0.004	0.279	0.106	0.002
629	0.781	0.004	0.274	0.099	0.002
630	0.788	0.003	0.268	0.093	0.002
631	0.797	0.003	0.262	0.087	0.002
632	0.806	0.003	0.255	0.081	0.002
633	0.817	0.003	0.249	0.076	0.002
634	0.829	0.003	0.242	0.071	0.002
635	0.843	0.003	0.236	0.067	0.002
636	0.857	0.003	0.23	0.062	0.002

637	0.874	0.002	0.223	0.058	0.002
638	0.891	0.002	0.216	0.055	0.002
639	0.91	0.002	0.209	0.051	0.002
640	0.93	0.002	0.203	0.048	0.002
641	0.95	0.002	0.196	0.045	0.001
642	0.971	0.002	0.189	0.042	0.001
643	0.993	0.002	0.183	0.039	0.001
644	1.016	0.002	0.176	0.037	0.001
645	1.039	0.002	0.17	0.035	0.001
646	1.062	0.002	0.164	0.033	0.001
647	1.085	0.002	0.158	0.031	0.001
648	1.108	0.002	0.152	0.029	0.001
649	1.13	0.002	0.146	0.028	0.002
650	1.152	0.002	0.14	0.026	0.002
651	1.174	0.002	0.134	0.025	0.001
652	1.195	0.002	0.129	0.024	0.002
653	1.216	0.002	0.123	0.022	0.002
654	1.236	0.002	0.118	0.021	0.001
655	1.255	0.002	0.113	0.02	0.001
656	1.274	0.002	0.108	0.019	0.001
657	1.291	0.002	0.103	0.018	0.001
658	1.307	0.002	0.098	0.017	0.001
659	1.322	0.002	0.093	0.016	0.002
660	1.335	0.002	0.088	0.016	0.001
661	1.346	0.002	0.084	0.015	0.001
662	1.354	0.002	0.08	0.014	0.001
663	1.359	0.002	0.076	0.014	0.001
664	1.361	0.002	0.072	0.013	0.001
665	1.358	0.002	0.068	0.012	0.001
666	1.351	0.002	0.065	0.012	0.001
667	1.339	0.002	0.062	0.012	0.002
668	1.322	0.002	0.059	0.011	0.002
669	1.299	0.002	0.056	0.011	0.002
670	1.272	0.002	0.053	0.01	0.002
671	1.239	0.002	0.05	0.01	0.002
672	1.2	0.002	0.048	0.01	0.002
673	1.157	0.002	0.045	0.009	0.002
674	1.11	0.002	0.043	0.009	0.002
675	1.059	0.002	0.04	0.009	0.002
676	1.004	0.002	0.038	0.009	0.002
677	0.947	0.002	0.036	0.008	0.002
678	0.89	0.002	0.034	0.008	0.002
679	0.833	0.002	0.033	0.008	0.002
680	0.775	0.003	0.031	0.008	0.002
681	0.717	0.003	0.029	0.008	0.002
682	0.663	0.003	0.028	0.008	0.002
683	0.611	0.003	0.026	0.007	0.002
684	0.559	0.003	0.025	0.007	0.002
685	0.51	0.003	0.024	0.007	0.002
686	0.466	0.003	0.023	0.007	0.002
687	0.424	0.003	0.021	0.007	0.002
688	0.384	0.003	0.02	0.007	0.002
689	0.348	0.003	0.019	0.007	0.002
690	0.315	0.003	0.018	0.007	0.002
691	0.285	0.003	0.018	0.007	0.002
692	0.258	0.003	0.017	0.007	0.002
693	0.233	0.003	0.016	0.006	0.002
694	0.211	0.003	0.015	0.006	0.002
695	0.191	0.003	0.014	0.006	0.002
696	0.173	0.003	0.014	0.006	0.002
697	0.157	0.003	0.013	0.006	0.002
698	0.142	0.002	0.013	0.006	0.002
699	0.129	0.002	0.012	0.006	0.002
700	0.117	0.002	0.012	0.006	0.002
701	0.106	0.002	0.011	0.006	0.002
702	0.097	0.002	0.011	0.006	0.002
703	0.088	0.002	0.01	0.006	0.002
704	0.08	0.002	0.01	0.006	0.002
705	0.073	0.002	0.01	0.006	0.002
706	0.066	0.002	0.009	0.006	0.002
707	0.061	0.002	0.009	0.006	0.002
708	0.055	0.002	0.009	0.006	0.002
709	0.051	0.002	0.008	0.006	0.002
710	0.047	0.002	0.008	0.006	0.002
711	0.043	0.002	0.008	0.006	0.002
712	0.04	0.002	0.007	0.005	0.002

713	0.037	0.002	0.007	0.005	0.002
714	0.034	0.002	0.007	0.005	0.002
715	0.032	0.002	0.007	0.005	0.002
716	0.03	0.001	0.007	0.005	0.002
717	0.028	0.001	0.007	0.005	0.002
718	0.026	0.001	0.006	0.005	0.002
719	0.024	0.001	0.006	0.005	0.002
720	0.023	0.001	0.006	0.005	0.002
721	0.021	0.001	0.006	0.005	0.002
722	0.02	0.001	0.006	0.005	0.002
723	0.019	0.001	0.006	0.005	0.002
724	0.018	0.001	0.006	0.005	0.002
725	0.017	0.001	0.005	0.005	0.002
726	0.016	0.001	0.005	0.005	0.002
727	0.015	0.001	0.005	0.005	0.002
728	0.014	0.001	0.005	0.005	0.002
729	0.014	0.001	0.005	0.005	0.002
730	0.013	0.001	0.005	0.005	0.002
731	0.012	0.001	0.005	0.005	0.002
732	0.012	0.001	0.005	0.005	0.002
733	0.011	0.001	0.005	0.005	0.002
734	0.011	0.001	0.005	0.005	0.002
735	0.01	0.001	0.005	0.005	0.002
736	0.01	0.001	0.005	0.005	0.002
737	0.009	0.001	0.005	0.005	0.002
738	0.009	0.001	0.004	0.005	0.002
739	0.008	0.001	0.004	0.005	0.002
740	0.008	0	0.004	0.005	0.002
741	0.008	0	0.004	0.005	0.002
742	0.007	0	0.004	0.005	0.002
743	0.007	0	0.004	0.005	0.002
744	0.007	0	0.004	0.005	0.002
745	0.006	0	0.004	0.005	0.002
746	0.006	0	0.004	0.005	0.002
747	0.006	0	0.004	0.005	0.002
748	0.005	0	0.004	0.005	0.002
749	0.005	0	0.004	0.005	0.002
750	0.005	0	0.004	0.005	0.002
751	0.005	0	0.004	0.005	0.002
752	0.005	0	0.004	0.005	0.002
753	0.004	0	0.004	0.005	0.002
754	0.004	0	0.004	0.005	0.002
755	0.004	0	0.004	0.004	0.002
756	0.004	0	0.004	0.004	0.002
757	0.004	0	0.004	0.004	0.002
758	0.003	0	0.004	0.004	0.002
759	0.003	0	0.004	0.004	0.002
760	0.003	0	0.004	0.004	0.002
761	0.003	0	0.004	0.004	0.002
762	0.003	0	0.004	0.004	0.002
763	0.003	0	0.004	0.004	0.002
764	0.002	0	0.004	0.004	0.002
765	0.002	0	0.004	0.004	0.002
766	0.002	0	0.004	0.004	0.002
767	0.002	0	0.004	0.004	0.002
768	0.002	0	0.004	0.004	0.002
769	0.002	0	0.004	0.004	0.002
770	0.002	0	0.004	0.004	0.002
771	0.002	0	0.004	0.004	0.002
772	0.002	0	0.004	0.004	0.002
773	0.002	0	0.004	0.004	0.002
774	0.002	0	0.004	0.004	0.002
775	0.001	0	0.003	0.004	0.002
776	0.001	0	0.004	0.004	0.002
777	0.001	0	0.003	0.004	0.002
778	0.001	0	0.004	0.004	0.002
779	0.001	0	0.004	0.004	0.002
780	0.001	0	0.003	0.004	0.002
781	0.001	0	0.003	0.004	0.002
782	0.001	0	0.003	0.004	0.002
783	0.001	0	0.003	0.004	0.002
784	0.001	0	0.003	0.004	0.002
785	0.001	0	0.003	0.004	0.002
786	0.001	0	0.003	0.004	0.002
787	0.001	0	0.003	0.004	0.002
788	0.001	0	0.003	0.004	0.002

789	0.001	0	0.003	0.004	0.002
790	0.001	0	0.003	0.004	0.002
791	0.001	0	0.003	0.004	0.002
792	0.001	0	0.003	0.004	0.002
793	0	0	0.003	0.004	0.002
794	0	0	0.003	0.004	0.002
795	0	0	0.003	0.004	0.002
796	0	0	0.003	0.004	0.002
797	0	0	0.003	0.004	0.002
798	0	0	0.003	0.004	0.002
799	0	0	0.003	0.004	0.002
800	0	0	0.003	0.004	0.002
801	0	0	0.003	0.004	0.002
802	0	0	0.003	0.004	0.002
803	0	0	0.003	0.004	0.002
804	0	0	0.003	0.004	0.002
805	0	0	0.003	0.004	0.002
806	0	0	0.003	0.004	0.002
807	0	0	0.003	0.004	0.002
808	0	0	0.003	0.004	0.002
809	0	0	0.003	0.004	0.002
810	0	0	0.003	0.003	0.001
811	0	0	0.003	0.004	0.002
812	0	0	0.003	0.004	0.002
813	0	0	0.003	0.004	0.002
814	0	0	0.003	0.004	0.002
815	0	0	0.003	0.004	0.002
816	0	0	0.003	0.004	0.002
817	0	0	0.003	0.004	0.002
818	0	0	0.003	0.003	0.002
819	0	0	0.003	0.003	0.001
820	0	0	0.003	0.003	0.001
821	0	0	0.003	0.004	0.002
822	0	0	0.003	0.004	0.002
823	0	0	0.003	0.004	0.002
824	0	0	0.003	0.003	0.001
825	0	0	0.003	0.003	0.001
826	0	0	0.003	0.004	0.002
827	0	0	0.003	0.004	0.002
828	0	0	0.003	0.003	0.001
829	0	0	0.003	0.003	0.001
830	0	0	0.003	0.003	0.001
831	0	0	0.003	0.003	0.001
832	0	0	0.003	0.004	0.002
833	0	0	0.003	0.003	0.001
834	0	0	0.003	0.004	0.002
835	0	0	0.003	0.003	0.001
836	0	0	0.003	0.004	0.001
837	0	0	0.003	0.003	0.002
838	0	0	0.003	0.003	0.001
839	0	0	0.003	0.004	0.001
840	0	0	0.003	0.003	0.001
841	0	0	0.003	0.003	0.002
842	0	0	0.003	0.003	0.001
843	0	0	0.003	0.003	0.001
844	0	0	0.003	0.003	0.001
845	0	0	0.003	0.003	0.002
846	0	0	0.003	0.003	0.001
847	0	0	0.003	0.003	0.002
848	0	0	0.003	0.003	0.001
849	0	0	0.003	0.003	0.001
850	0	0	0.003	0.003	0.001
851	0	0	0.003	0.003	0.001
852	0	0	0.003	0.003	0.001
853	0	0	0.003	0.003	0.001
854	0	0	0.003	0.003	0.001
855	0	0	0.003	0.003	0.001
856	0	0	0.003	0.003	0.001
857	0	0	0.003	0.003	0.001
858	0	0	0.003	0.003	0.001
859	0	0	0.003	0.003	0.001
860	0	0	0.003	0.003	0.001
861	0	0	0.003	0.003	0.002
862	0	0	0.003	0.003	0.001
863	-0.001	0	0.003	0.003	0.001

APPENDIX B: CALIBRATION CURVE DATA

Concentration vs. absorbance values of selected dyes

Concentration gL^{-1}	**Absorbance**				
	Reactive Red	***Congo Red***	***Reactive Black B***	***Crystal Violet***	***Methylene Blue***
0.002	-	-	-	0.178	-
0.005	-	-	-	0.515	0.648
0.010	0.167	-	0.179	1.133	1.148
0.015	-	-	-	1.537	1.567
0.020	-	-	0.334	1.979	2.430
0.025	-	-	-	-	2.867
0.030	0.573	0.345	-	2.946	3.153
0.040	-	-	0.697	-	-
0.050	0.992	0.515	-	-	-
0.060	-	-	1.066	-	-
0.080	1.571	-	1.427	-	-
0.100	1.985	1.332	1.627	-	-
0.150	2.650	1.850	-	-	-
0.200	-	2.419	-	-	-
0.230	-	2.619	-	-	-

APPENDIX C: ABSORBANCE VALUES READINGS GIVEN BY UV-VIS SPECTROPHOTOMETER FOR ALL FIVE DYES

Absorbance values obtained

Test No	**Absorbance value**					
	S1	***S2***	***S3***	***S4***	***S5***	***S6***
T1	2.240	1.719	0.994	0.503	0.276	0.167
T2	1.808	1.515	0.932	0.459	0.336	0.191
T3	1.535	1.228	0.75	0.346	0.247	0.123
T4	0.877	0.681	0.409	0.193	0.128	0.068
T5	2.044	1.704	1.12	0.494	0.399	0.313
T6	1.624	1.440	0.873	0.44	0.344	0.237
T7	1.311	1.043	0.562	0.252	0.214	0.204
T8	0.532	0.406	0.245	0.141	0.116	0.087
T9	0.424	0.423	0.412	0.415	0.411	0.412
T10	0.549	0.527	0.464	0.343	0.253	0.079
T11	0.424	0.407	0.353	0.224	0.166	0.064
T12	0.356	0.342	0.297	0.21	0.144	0.068
T13	0.103	0.1	0.075	0.049	0.036	0.041
T14	0.542	0.531	0.520	0.523	0.535	0.492
T15	1.18	1.165	1.121	0.948	0.755	0.207

APPENDIX D: CONCENTRATION VALUES OBTAINED BY CONVERSION OF ABSORBANCE VALUE READINGS USING CALIBRATION CURVES

Concentrations obtained

Test No	**Concentration (mgL^{-1})**						
	Initial	***S1***	***S2***	***S3***	***S4***	***S5***	***S6***
T1	30.00	20.14	15.45	8.93	4.52	2.48	1.50
T2	25.00	16.25	13.62	8.38	4.13	3.02	1.72
T3	20.00	13.80	11.04	6.74	3.11	2.22	1.11
T4	10.00	7.88	6.12	3.68	1.73	1.15	0.61
T5	30.00	20.46	17.05	11.21	4.94	3.99	3.13
T6	25.00	16.25	14.41	8.74	4.40	3.44	2.37
T7	20.00	13.12	10.44	5.62	2.52	2.14	2.04
T8	10.00	5.32	4.06	2.45	1.41	1.16	0.87
T9	25.00	24.84	24.79	24.14	24.32	24.08	24.14
T10	50.00	46.13	44.28	38.99	28.82	21.26	6.64
T11	40.00	35.63	34.20	29.66	18.82	13.95	5.38
T12	30.00	29.91	28.74	24.96	17.65	12.10	5.71
T13	10.00	8.65	8.40	6.30	4.12	3.02	3.45
T14	30.00	29.09	28.49	27.90	28.07	28.71	26.40
T15	100.00	99.2	97.9	94.2	79.7	63.4	17.4